Genetic determinants of distinct CD8$^+$ α/β-TCR repertoires in the genus *Mus*

Moritz Peters[1*], Volker Soltys[1], Dingwen Su[1], Marek Kučka[1,2], Yingguang Frank Chan[1,3*]

1. Friedrich Miescher Laboratory of the Max Planck Society, 72076 Tübingen, Germany
2. Department of Translational Genomics, University of Cologne, 50931 Cologne, Germany
3. University of Groningen, Groningen Institute for Evolutionary Life Sciences, 9747 AG Groningen, Netherlands

*Corresponding authors: moritz.peters@tuebingen.mpg.de, frank.chan@rug.nl

Abstract

The adaptive immune system's efficacy relies on the diversity of T cell receptors and the ability to distinguish between self and foreign antigens. Analysis of the paired heterodimeric αβ-TCR chains of individual T cells requires single-cell resolution, but existing single-cell approaches offer limited coverage of the vast TCR repertoire diversity. Here we introduce CITR-seq, a novel, instrument-free, high-throughput method for single-cell TCR sequencing with >88% αβ-TCR pairing precision. We analyzed the TCR repertoires of CD8$^+$ T cells originated from 32 inbred mice using CITR-seq, comprising four evolutionary divergent sister species and their F1 hybrids. Overall, we identified more than 5 million confidently paired TCRs. We found that V(D)J gene usage patterns are highly specific to the genotype and that Vβ-gene usage is strongly impacted by thymic selection. Using F1 hybrids, we show that differences in gene segment usage across species are likely caused by *cis*-acting factors prior to thymic selection, which imposed strong allelic biases. At the greatest divergence, this led to increased rates of TCR depletion through rejection of particular Vβ-genes. TCR repertoire overlap analysis across all mice revealed that sharing of identical paired CDR3 amino acid motifs is four times more frequent than predicted by random pairing of TCRα and TCRβ chains, with significantly increased sharing rates among related individuals. Collectively, we show that beyond the stochastic nature of TCR repertoire generation, genetic factors contribute significantly to the shape of an individual's repertoire.

Introduction

Adaptive immunity relies on the recognition of antigens presented on the surface of virtually all nucleated cells through class I and II major histocompatibility complexes (MHC). These MHC-bound antigens are recognized by T cell receptors (TCRs) expressed on the surface of T cells, which collectively possess the remarkable ability to discriminate between antigens of “self” and “foreign” origin. This is critical for preserving self-tolerance, thereby preventing autoimmunity, while also enabling the identification of pathogen-infected or malignant cells to initiate an immune response [1]. The nature of an immune response depends largely on whether an antigen is presented via class I or class II MHC complexes, which are targeted by CD8$^+$ cytotoxic T cells [2] or CD4$^+$ helper T cells [3], respectively. The former can induce apoptosis in targeted cells while the latter can trigger secondary immune cascades involving B-lymphocytes and cells of the innate immune system. In both cases, TCRs are the key molecules that mediate signaling and enable a broad spectrum of immune responses.

TCRs are primarily composed of two heterodimeric chains, TCRα and TCRβ, both of which arise from somatic rearrangements of gene segments during T cell development. This rearrangement process, known as V(D)J-recombination, generates diversity through joining variable (V), diversity (D, exclusive to TCRβ) and joining (J) gene segments to a constant region, thereby generating a unique TCR receptor in each individual T cell [4]. Additional diversity is introduced through nucleotide insertions and deletions at each junction during V(D)J-recombination [5]. In the expressed TCRα and TCRβ chains, the resulting highly polymorphic junctional region is situated in closest proximity to antigens presented by MHCs to serve as a binding pocket [6] and is termed complementarity-determining region 3 (CDR3). The other CDRs, 1 and 2, constitute germline encoded regions within the V-segments of TCR chains and are believed to primarily facilitate TCR-MHC binding and are less relevant for antigen recognition [7, 8] (**Fig. 1A**).

The antigen specificity of each rearranged TCR as well as its affinity to MHCs is evaluated in a key multi-step process called thymic selection. It takes place during T cell maturation which is generally classified by the intra-thymic progression from the CD8/CD4 double negative (DN) stages of lymphoid precursors to the single positive stage (SP) of mature

T cells. The selection process is initiated at the so called β-checkpoint [9], at which the successful rearrangement of an in-frame TCRβ chain is controlled. Afterwards, the fully assembled αβ-TCR is tested for its affinity to MHCs during positive selection and its specificity to presented self-antigens during negative selection. Both processes are chronologically and spatially separated: Positive selection occurs in the cortex through interactions with cortical thymic epithelial cells (cTECs), whereas the subsequent negative selection occurs in the medulla through interactions with medullary thymic epithelial cells (mTECs) (reviewed here [10]). Overall, only about 5% of T cell precursors survive thymic selection of their TCRs by demonstrating adequate affinity to MHC complexes while simultaneously exhibiting tolerance towards the broad spectrum of presented self-antigens and thus thymic selection significantly decreases the diversity in the TCR repertoire (**Fig. 1B**).

In our current understanding, nucleotide insertions and deletions, V(D)J-segment usage and αβ-TCR pairing are mostly seen as stochastic events that give rise to highly unique and dynamic TCR repertoires within and across individuals [11]. However, recent work increasingly suggests that the diversity of TCR repertoires also relies on genetically encoded differences across individuals [12-15]. For example, V-segment usage in identical twins exhibits much greater similarity compared to unrelated individuals [16]. Notably, this provides evidence that genetics may operate at two different levels: V(D)J-recombination as well as thymic selection, as indicated by the fact that identical twins also share the same set of MHC class I and II (also known as human leukocyte antigen, or HLA) alleles. This observation, and the multi-level genetic determinants that collectively shape TCR diversity, are the focus of at least two debates: one concerning the existence of a co-evolutionary feedback process between TCR and MHC binding [17-21], and the other on whether HLA heterozygosity is evolutionarily optimal due to the presentation of a broader immunopeptidome [22, 23], or alternatively, deleterious due to a high frequency of presented self-peptides, leading to increased depletion of autoreactive TCRs [24, 25]. The extreme diversity of both binding partners, TCR and MHC, makes answering these questions extremely challenging. By contrast, panels of inbred mouse lines spanning within- and across-species diversity, along with their F1 hybrids, provide a tractable setup to address the question regarding the role of MHC/HLA alleles in shaping repertoire diversity during thymic selection.

Estimates on the theoretical αβ-TCR diversity vary greatly by species as well as methodology. Initial theoretical estimates on αβ-TCR diversity were approximately 10^{15} in mice [4] and 10^{18} [26] – 10^{20} [27] in humans. More recent calculations now greatly exceed those estimates and range up to 10^{61} [28]. However this needs context: the number of theoretical αβ-TCRs vastly outnumbers the actually realized TCRs in the repertoire of an individual, primarily because the number of present T cells of an individual (10^{12} [29] in humans and 10^{8} [30] in mice) is several orders of magnitude smaller at any given time.

Interestingly, despite the great difference in number of total T cells across different species (e.g. more than 1000x more T cells in humans than in mice), the diversity within the realized TCR repertoire has shown to be much more similar across species [30, 31]. This observation gave rise to the idea of a minimally required repertoire size defined as a functional unit of the “protecton” which is simply multiplied in species with larger numbers of total T cells [32]. Experimental validation of TCR repertoire diversity estimates still suffers from the limitations of current methodologies. While bulk assays can now feasibly analyze entire repertoires across many individuals [33-35], they leave out the critical pairing between TCRα and TCRβ chains within individual cells. Paired TCR analysis requires molecular barcoding of single cells, but existing methods often rely on pre-existing single-cell workflows, restricting analysis to thousands of T cells rather than entire repertoires [36-38]. These protocols typically utilize fluorescence-activated cell sorting (FACS), or microfluidic platforms to isolate individual cells and therefore require specialized equipment. The recent development of SPLiT-seq [39] has expanded the scope of single-cell whole transcriptome experiments to up to 10^{6} cells per experiment by using combinatorial indexing to molecularly barcode each individual cell. Despite this increase in throughput, the associated sequencing cost still substantially limits the feasibility of these methods for assessing large TCR repertoires, especially across multiple individuals.

Here, we investigate repertoires of paired αβ-TCRs from cytotoxic CD8^{+} T cells by developing a targeted TCR sequencing protocol called CITR-seq (**C**ombinatorial **I**ndexing **T** cell **R**eceptor sequencing) to analyze TCR repertoires at low cost and large scale. We apply CITR-seq to 32 individual mice from 4 distinct inbred sister species (C57BL/6J, CAST/EiJ, PWD/PhJ, SPRET/EiJ, abbreviated as BL6, CAST, PWD and SPRET, respectively) and their F1 hybrids with BL6, spanning an evolutionary divergence of approximately 3 million years [40-42] (**Fig. 1C**). The diverged but controlled genetic backgrounds provide a unique opportunity to determine the respective impact of TCR locus structure, the V, D and J gene segment usage frequency, TCR/MHC allele co-evolution via thymic selection and ultimately the joint effects on CDR3 diversity (**Fig. 1D**).

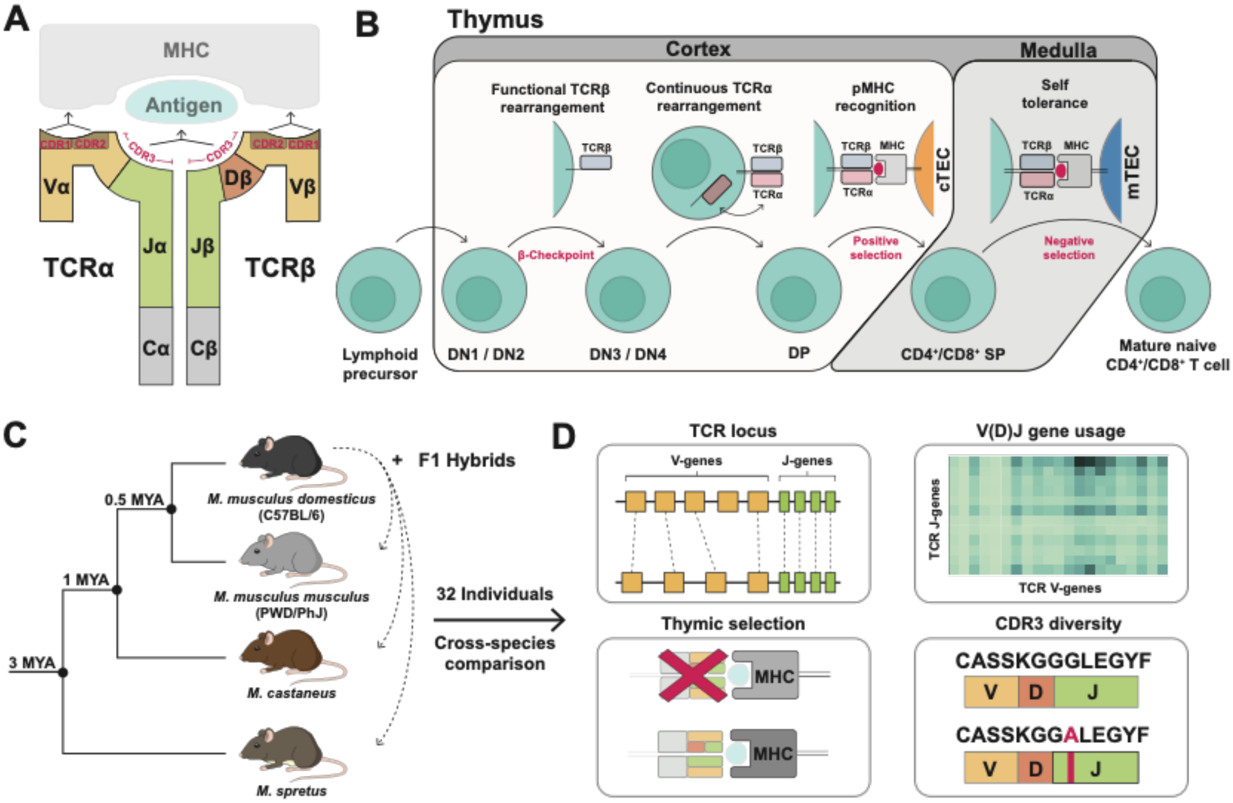

Figure 1: Introduction to T cell receptors and overview of the study design

- **(A)** Heterodimeric αβ-TCR consisting of a V-, D- (exclusive to TCRβ) and J-gene alongside the constant (C) region. The junctional region of V(D)J genes marks the CDR3 sequence that is in the closest proximity to the antigen in the TCR-MHC complex. CDR1 and CDR2 are germline-encoded sequences of V-genes that contribute to TCR-MHC binding.
- **(B)** T cell maturation in the thymus. Intra-thymic T cells are classified by the expression of the lineage-markers CD4 and CD8 (double negative: DN, double positive: DP and single positive: SP). T cells that successfully rearranged a functional TCRβ chain can pass the β-checkpoint. Subsequent continuous rearrangements of the TCRα chain leads to transition to the DP stage. T cells with a fully assembled αβ-TCR that is capable of binding self-MHCs on the surface of cTECs survive positive selection. Selected T cells migrate to the medulla and undergo negative selection, during which T cells that strongly bind self-MHCs on the surface of mTECs are rejected. T cells that survive both selection steps are released from the thymus.

(C) Phylogenetic tree showing the evolutionary divergence of inbred mouse species used in this study.
(D) The different aspects of TCR generation and selection analyzed in the course of this study.

Results

CITR-seq design and validation

To generate TCR repertoires we built on SPLiT-seq [39] to develop CITR-seq and modify the approach to generate RNA-based targeted paired αβ-TCR libraries (**Fig. 2A**). We first isolated CD8$^+$ T cells from spleens of 10-week-old mice by using anti-CD8 magnetic beads and subsequent purification by FACS (**Fig. S1A**). Purified CD8$^+$ T cells were either used directly or were transferred to anti-CD3 and anti-CD28 coated tissue culture plates for a 20-hour activation period before the library preparation (see **Suppl. Table 1** for detailed sample list; note that we limited the activation to 20 hours to avoid cell doubling). Primary or activated T cells were fixed and permeabilized and a set of barcoded TCRα and TCRβ constant-region primers was used to perform *in situ* reverse transcription (RT) inside individual cells (see **Suppl. Table 2** for a list of all primers and barcoding DNA-oligos). All RT-primers contain a unique molecular identifier (UMI) and a ligation overhang for single-cell barcoding. Here, cells are distributed in two split-and-pool cycles across two 96-well plates, such that the RT-primer overhangs are ligated to oligos carrying barcode segments. The split-and-pool approach allow all reactions to be performed in bulk, while giving each cell an effectively unique barcode (calculated barcode collision rate: 1.67%; **see methods**). Afterwards up to 10,000 cells are merged into sub-samples and reverse crosslinking is done to make the barcoded cDNA accessible for amplification. Second strand synthesis is done in a multiplex-PCR setup using 54 primers targeting the 5' ends of TCR V-segments. In a final index-PCR another DNA barcode is added to each sub-sample, which expands the total barcoding space to up to 28 million unique cellular barcodes. Subsamples can then be pooled to generate the final sequencing-ready library which is compatible with standard Illumina workflows and can be further multiplexed with other sequencing libraries (**Fig. 2B**). This process is cost efficient (**see methods**) and does not require specialized instrumentation.

Using CITR-seq, we profiled TCR repertoires from a total of 9,113,392 CD8$^+$ T cells (hereafter referred to as “T cells”) across all 32 individuals. Paired TCRα and TCRβ chains were successfully recovered in 75.8% of T cells, 55.4% of which carried exactly one α- and β-chain (**Fig. 2C**). To the best of our knowledge, this dataset of 5,049,334 singly α/β-paired T cells represents the largest set of paired TCRs analyzed in a single study to date (**Fig. 2D**). To assess pairing precision, we determined the rate of repeated observations of identical Vβ-Jβ-CDR3β and Vα-Jα-CDR3α mates (or “clonotypes”) in a sample of 150,000 T cells that underwent clonal expansion for 72h in tissue culture. Clonal expansion through prolonged tissue culture allowed us to enrich for cells carrying the same α/β-chain pairing, the recovery of which would have been unlikely under our standard protocol. TCRβ chains that were observed at least twice in this repertoire were seen with identical TCRα chains in 88% of cells, thus representing T cells with identical clonotypes. This rate marks the lower-bound pairing precision, since with 150,000 T cells, we expect a low, but non-negligible chance of recovering the same Vβ-Jβ-CDR3β chain from two non-clonal T cells which should therefore pair with a different TCRα chain. In agreement with this high pairing precision, we observed few cells with more than two TCRα (1.4%) or TCRβ (0.5%) chains across all 32 CITR-seq samples, which is biologically implausible because of the presence of just two alleles for each chain in each T cell (**Fig. S2A**).

We then compared transcripts (UMIs) per cell counts at saturating read coverage (mean reads/cell: 184.57; **Fig. S2B**) in activated and primary T cells in CITR-seq. Activated T cells had a significantly higher UMI/cell count (14.81) compared to primary T cells (5.9, pairwise t-test; $P < 0.01$; **Fig. 2E**). We compared these values to two publicly available human TCR sequencing datasets (Parse Bioscience; **see methods**), in which 72h activated T cells also showed significantly higher average UMI per cell count (18.44 UMIs/cell) than primary T cells (4.69 UMIs/cell). As a further benchmarking effort, we generated complementary datasets for each of the four inbred mouse species from primary T cells using the Chromium Next GEM Single Cell 5’ platform by 10x Genomics (**see methods**). For these, we recovered 10.1 UMIs/cell on average across samples (**Fig. 2E**).

We evaluated whether activation of T cells biases the recovered TCR repertoire by comparing V-J usage (discussed below) and clonal abundance in samples of primary and activated T cells, each down-sampled to 150,000 cells. To do so, we first compared the frequency of multiple observations of identical TCRα and TCRβ as well as full clonotypes (defined by identical V+J+CDR3 amino acid motif) across cells (**Fig. S2C**). In TCR repertoires of primary T cells and T cells that were activated for 20h, most αβ-TCR pairs were exclusive to a single cell (93% and 96.7% respectively). This is in contrast to αβ-TCR pairs in TCR repertoires of cells that were activated for 72 hours, in which less than half (48%) of pairs are exclusive to a single cell with all other pairs being observed multiple times. We therefore conclude, that in agreement with previous studies [79] the 20h activation protocol did exclude clonal expansion of T cells.

Validation of CITR-seq against 10x Genomics commercial platform

To validate complete coverage of all the functional V/J genes, we compared V-J gene usage frequencies from data generated using CITR-seq and 10x Genomics Immune Profiling. We find high correlation of V-J usage frequencies (Pearson: BL6 r = 0.91) across both methods (**Fig. S3C**). Additionally, the highly correlated V-J usage frequencies provide further evidence for the unbiased repertoire representation of 20h activated (CITR-seq) compared to primary (10x Genomics Immune Profiling) T cells.

To evaluate the coverage of cross-species repertoires, we analyzed CDR3 amino acid motif diversity in α- and β-chains both individually and jointly (**Fig. 2F**). In the 5,049,334 T cells from across all 32 samples, we detect 719,976 (14.26%) unique TCRα and 1,725,631 (34.18%) unique TCRβ chains. If analyzed jointly, 95.6% of these (4,826,991) represent unique αβ-TCR pairs. In contrast, in 9,445 paired T cells in our Chromium Next GEM Single Cell 5’ datasets, we found 85% and 94.9% unique TCRα and TCRβ chains, respectively (n = 8,021 and 8,963), and nearly all (98.6%, or 9,313 T cells) represent unique αβ-TCR pairs (**Fig. S2D**). Taken together, we interpret this data to show the remarkable diversity, especially across paired TCRs: even with the throughput of CITR-seq at 5 million cells, we were not close to sampling T cell clonotypes to saturation, let alone using much more limited platforms. This further emphasizes the need for high-throughput methods to gain reasonable insight into the diversity of TCR repertoires.

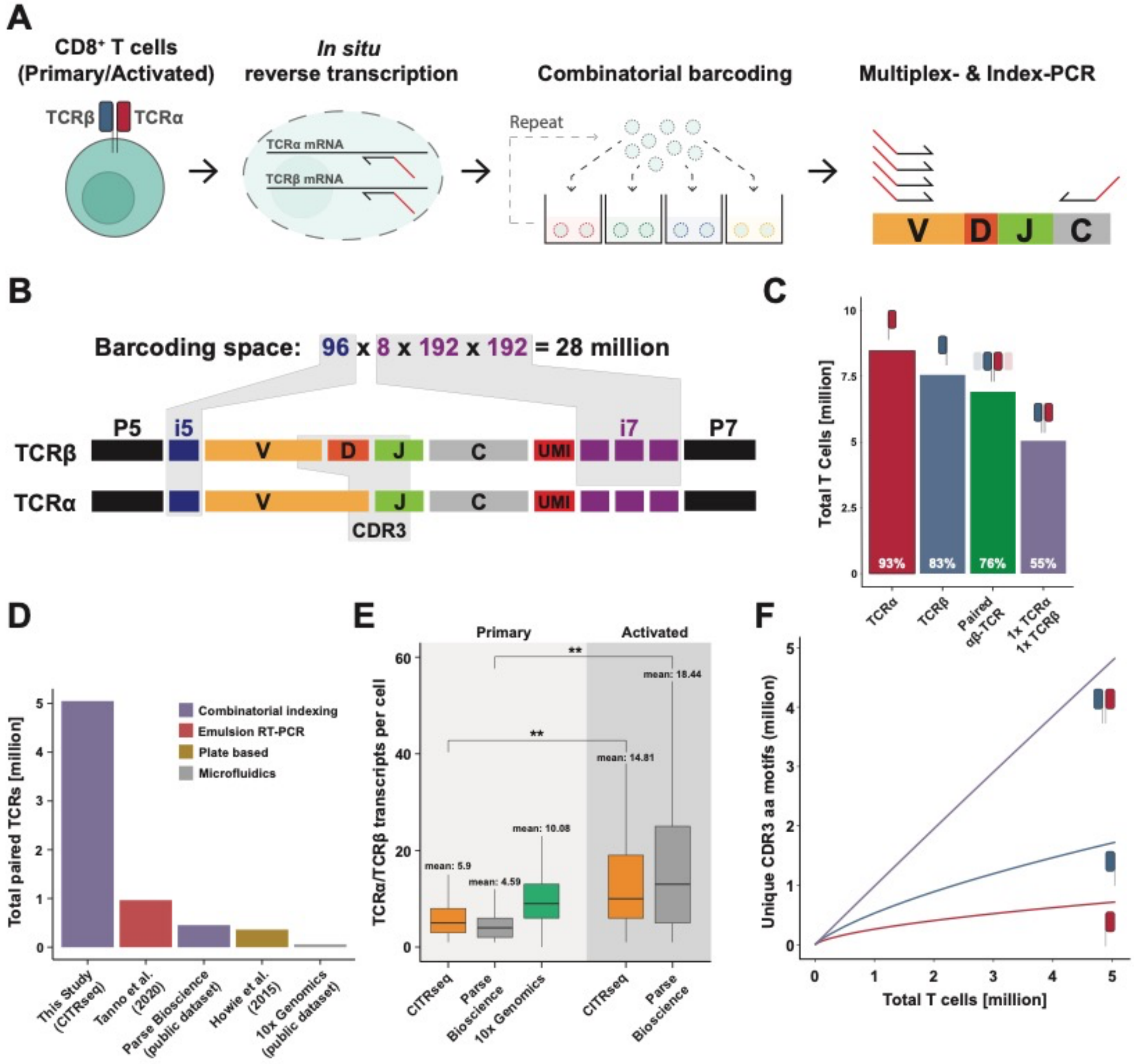

Figure 2: CITR-seq allows for the analysis of millions of confidently paired αβ-TCRs

(A) Workflow for generating paired αβ-TCR sequencing libraries using CITR-seq. Isolated T cells are fixed and permeabilized. TCRα and TCRβ are *in-situ* reverse transcribed using barcoded primers targeting both TCR constant regions. Afterwards, T cells are distributed across 96-well plates and well-specific barcodes are ligated to the cDNA. This process is repeated once by pooling all T cells and redistributing them to a second set of barcoding plates. T cells are then pooled again and split into sub-samples before reverse crosslinking. Second strand cDNA is generated in a multiplex-PCR with primers targeting the 5' region of Vα- and Vβ-genes. In a final Index-PCR a fourth barcode is added.

(B) Barcode and sequencing adapter structure in CITR-seq libraries. The different combinations of all four barcodes provide a barcoding space of more than 28 million possible barcodes. Sequencing reads fully cover CDR3α and CDR3β sequences.

(C) Pairing rate across all CITR-seq samples in this study. Fraction of the 9.113.392 total T cells that were assigned to a TCRα (93%, red), a TCRβ (83%, blue), at least one TCRα and TCRβ (76%, green) or exactly one TCRα and TCRβ chain (55%, violet).

(D) Total number of paired αβ-TCRs analyzed in different studies and publicly available datasets generated with different methods. Emulsion RT-PCT [14], PairSeq (plate-based) [43], two publicly available datasets generated with combinatorial indexing (Parse Bioscience) [44] and microfluidics (10x Genomics) [45].

(E) Mean number of TCRα and TCRβ transcripts (UMIs) per cell-barcode in primary and activated T cells in CITR-seq samples (primary and 20h activated mouse T cells), across all 10x Genomics Single-Cell Immune Profiling libraries (primary mouse T cells) and in two publicly available datasets from Parse Bioscience (primary and 72h activated human T cells) [44, 46].

(F) Total number of unique CDR3α, CDR3β or paired CDR3αβ amino acid motifs relative to the number of T cells across all 32 CITR-seq samples.

Distinct V-J usage patterns across mouse species

To compare V-J segment usage across the different mouse species, we first constructed species-specific V(D)J-segment references (**see methods**). Across all samples, mapping against the corresponding species-specific reference showed a slight increase in the total number of successfully aligned sequencing reads (PWD: +0.07%, CAST: +0.07% and SPRET: + 0.1% total reads; **Fig. S3A**) and per segment alignment scores (data not shown), relative to mapping against an mm10-based V(D)J reference provided in the MiXCR software [47]. Local alignment of TCR loci to the mm10 reference genome (GRCm38/mm10) revealed one-to-one orthology in Vβ-, Jβ- and Jα-segments. In contrast, we found extensive rearrangements, including inversions and gene-cluster triplications in the Vα cluster between the four mouse species (**Fig S3B**). For instance, the central region of the Vα cluster (Vα gene families 3-15) is expanded in BL6, PWD and SPRET relative to the CAST Vα cluster. This results in a Vα locus size reduction of ~0.6 Mb and approximately 70 fewer Vα genes in CAST. In a given species, sequence identity across Vα paralogues is extremely high (e.g., in BL6 *Trav11* and *Trav11D* are 100% identical on the nucleotide level; for details see [48]). For this reason, and to properly handle multiple Vα read mapping, we grouped Vα genes into their respective gene families for cross-species comparison.

We compared the mean of intra-species V/J gene segment usage across BL6, PWD, CAST and SPRET mice (**Fig. 3A**). Consistent with previous studies [33, 49], V/J segment usage within an individual typically spanned several orders of magnitude in both TCRα and TCRβ chains. For example, in BL6 TCR repertoires *Trbv12-1* and *Trbj2-7* were found in 2.37% of likely productive, in-frame, TCRβ chains, while the combination of *Trbv21* and

Trbj1-5 was only present in 0.0003% of in-frame TCRβ chains. Across species, segment usage frequencies are broadly similar, with some notable and extreme exceptions, mostly in Vβ-Segments (e.g. *Trbv13-2* is used in 7.75% of BL6 TCRβ chains compared to only 0.14% in SPRET). Consistent with previous studies [50] we observe decreased pairing of proximal Vα and distal Jα as well as distal Vα and proximal Jα segments. The only exception to this rule is CAST, where we observed significantly higher usage frequencies of the most distal Vα gene (*Trav1* and T*rav2*; chi-squared test; ** *P* < 0.01; **Fig S3D**). In laboratory mice, it has been shown that TCRα V-J recombination proceeds progressively from 3' (proximal) Vα genes towards more 5' (distal) Vα genes [51]. We therefore hypothesize, that the significantly higher usage of distal Vα genes in CAST is linked to its contracted Vα locus. As a general trend, we found that the average variance in V-segments usage frequency (var(Vβ) = 12.44, var(Vα) = 5.95) was higher compared to the average variance in J-segment usage frequency (var(Jβ) = 4.91, var(Jα) = 0.48) when compared across all species. This indicates that species-specific differences in V(D)J usage mostly arise from biases in V-segment usage rather than J-segment usage.

Further to the previous validation effort, we have also generated matching V(D)J usage profiles using the commercial 10x Genomics platform. Similar to BL6 mice, we observed excellent correlation of V-J gene usage frequencies in both approaches (Pearson correlation: PWD r = 0.89, CAST r = 0.88, SPRET r = 0.92) and only identified two V-gene segments that were not recovered in the CITR-seq dataset compared to the 10x Genomics dataset (*Trbv-31* in PWD, and *Trbv-24* in CAST/SPRET). The main difference between the platforms is that with CITR-seq we recovered on average ~160,000 T cells carrying a productive and paired TCR per experiment vs. 2,300 using the 10x Genomics platform.

Next, we performed principal component analysis (PCA) on combined TCRα and TCRβ V-J pairings across all CITR-seq replicates from each species alongside the 4 samples generated using 10x Genomics Immune Profiling, subsampling each sample to 5,000 TCRα and TCRβ chains each due to the lower throughput of the latter (**see methods**). Overall, samples are clustered strongly by species (PC1-PC3; **Fig. 3B**, **Fig S3E**) with only 6% of cross-sample variance explained by the technique (PC4, **Fig. S3E**). Mean intra-species V-J usage was highly correlated across samples for both TCRα and TCRβ

(Pearson: r = 0.987 +/- 0.052 stdev vs. r = 0.991 +/- 0.044 stdev) (**Fig. 3D**). Across samples the average V-J segment usages were more correlated for TCRα chains (r = 0.83 +/- 0.119 stdev) than TCRβ chains (r = 0.59 +/- 0.244 stdev) which is consistent with the difference in overall diversity across both chains described earlier (**Fig. 2E**). Therefore, we conclude that in the four different mouse species, V-J usage showed distinct genotype specific patterns primarily in Vβ-genes.

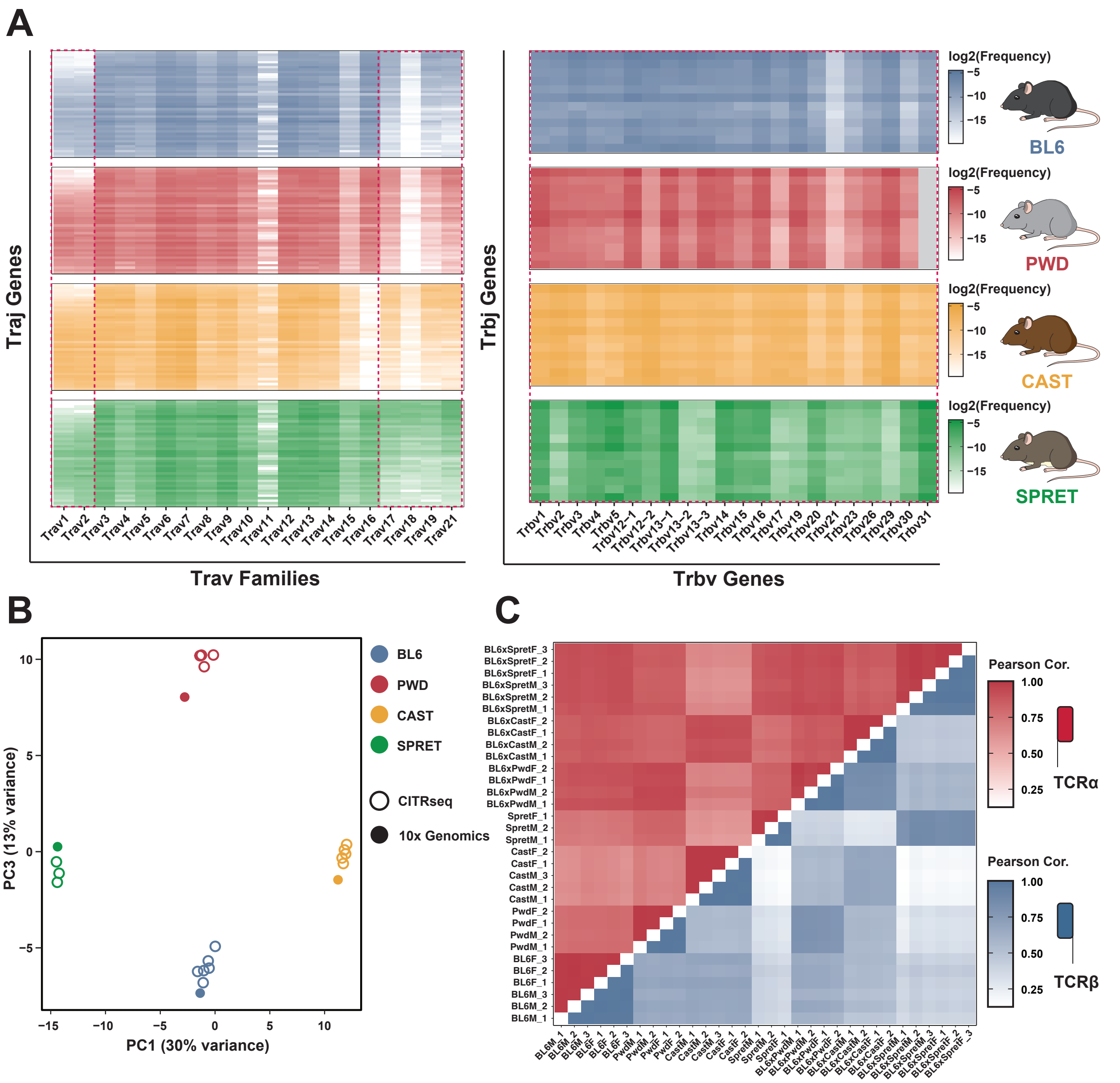

Figure 3: Species-specific V- and J-gene usage patterns in different mouse species

- **(A)** V-J usage frequency heatmaps. Heatmap shows the frequency ($\log_2$) of Vα-family + Jα-gene (left) and Vβ-gene + Jβ gene (right) usage of all functional TCRs in T cells across the four different mouse species (intra-species mean). Red boxes contain V-genes with one-to-one orthology in all four mouse species. J-genes are displayed in the order of their location within the locus (3' to 5'; see methods for full list). In PWD *Trbv31* is excluded due to failure of amplification during multiplex PCR.
- **(B)** Principal component analysis (PCA) of combined Vα-Jα and Vβ-Jβ usage across all four mouse species in different samples generated using CITR-seq (empty circles) or 10x Genomics Single Cell Immune Profiling (filled circles). Samples generated using both methods cluster by genotype.
- **(C)** Pearson correlation of inter-individual V-J gene usage in TCRα and TCRβ chains in all 32 individuals analyzed using CITR-seq in this study.

Thymic selection shapes TCR repertoire V-segment usage

Thymic selection ensures that T cells expressing TCRs with either too weak (positive selection) or to strong (negative selection) self-MHC binding properties fail to progress in the maturation process and are thus depleted from the repertoire. In effect, by collecting TCRs from peripheral (e.g., spleen-derived) T cell populations for CITR-seq, we report here the mature TCR repertoire after thymic selection. Here, we also emphasize a distinction between functional vs. non-functional TCR chains. This is because during V(D)J-recombination, random insertions and deletions of nucleotides at gene-segment junctions, often introduce frameshifts or premature stop-codons. These result in transcripts representing non-functional TCRs. However, mature T cells with an in-frame (IF) TCR often still retain active transcription of an out-of-frame (OOF) TCR from its second allele that is ultimately degraded, e.g., via non-sense mediated decay [52, 53]. This presented us with an opportunity to estimate the generative usage probability of gene segments, independent from the effects of positive or negative thymic selection (see also [54]). Crucially, our use of an inbred panel of species should result in an unchanged, homozygous MHC background resulting in a consistent thymic selection regime.

Across all 32 CITR-seq sample we found 4.58×10^6 (24.4% of total transcripts) transcripts that contain frameshifts or premature stop-codons with an average per transcript UMI count of 1.78 (compared to 4.87, two-sample t-test, $P < 0.001$). To evaluate the effect of thymic selection on TCR repertoires across the different species, we compared V- and J-gene usage in OOF (pre-selection) and IF (post-selection) TCRs (**Fig. 4A**). We observed that most V(D)J genes show similar frequencies in pre- and post-selection repertoires, summarized by normalized Shannon diversity index (nSDI, **see methods**), a measure of entropy (Vα (BL6 and PWD) as well as Jα (no significant changes) and Jβ (PWD and SPRET; **Fig. S4B**)). Again, the strong exceptions reside mostly within Vβ-genes: we observed significant differences in Vβ gene usage frequencies in all four species (**Fig. 4B**, paired t-test $P < 0.05$). The strongest absolute reduction of nSDI was observed in SPRET (-0.15) and PWD (-0.06), indicating significantly biased Vβ-segment usage in post-selection repertoires. For specific Vβ-segments, we found striking differences between pre- and post-selection repertoires, e.g., an average ~60-fold reduction in *Trbv13-2* usage frequency in SPRET post-selection repertoires (**Fig. 4C**). Notably, these extreme fold changes were mostly present in Vβ genes that showed strong cross-species frequency difference (e.g. *Trbv-2*, *Trbv12-2*, *Trbv13-2*, *Trbv17*, *Trbv21*) as shown before (**Fig. 3A**). We interpret the striking reduction in usage for these Vβ segments to be strongly suggestive of segment rejection during thymic selection.

While the most extreme differences in Vβ-segment usage tend to be species specific, we also observed common trends shared across all four species. For instance, we observed *Trbv-2* frequencies to be consistently lower in post-selection than pre-selection repertoires across all species (log2 FC IF/OOF; BL6: -1.2, PWD -1.3, CAST -0.5, SPRET -4.4). While thymic selection acts only to remove T cells from maturation, such that the absolute number of TCRs containing a particular gene segment only decrease from pre- to post-selection repertoires, in relative terms, a given segment can be overrepresented in the final, mature repertoire through thymic selection. One such example was *Trbv-14* whose relative contribution to the TCR repertoire was higher in all post-selection repertoires across species (log2 FC IF/OOF; BL6: 1.3, PWD 1.8, CAST 1.24, SPRET 1.38).

In summary, we show that thymic selection exerts an effect on the composition of the TCR repertoire by distorting usage frequencies in all segments across all four species, but its effect is most notable in Vβ-genes, in particular in the reduction of particular Vβ-genes (e.g. *Trbv13-2*, *Trbv2*, *Trbv12-2* etc.) in PWD and SPRET, likely due to strong rejection during positive thymic selection.

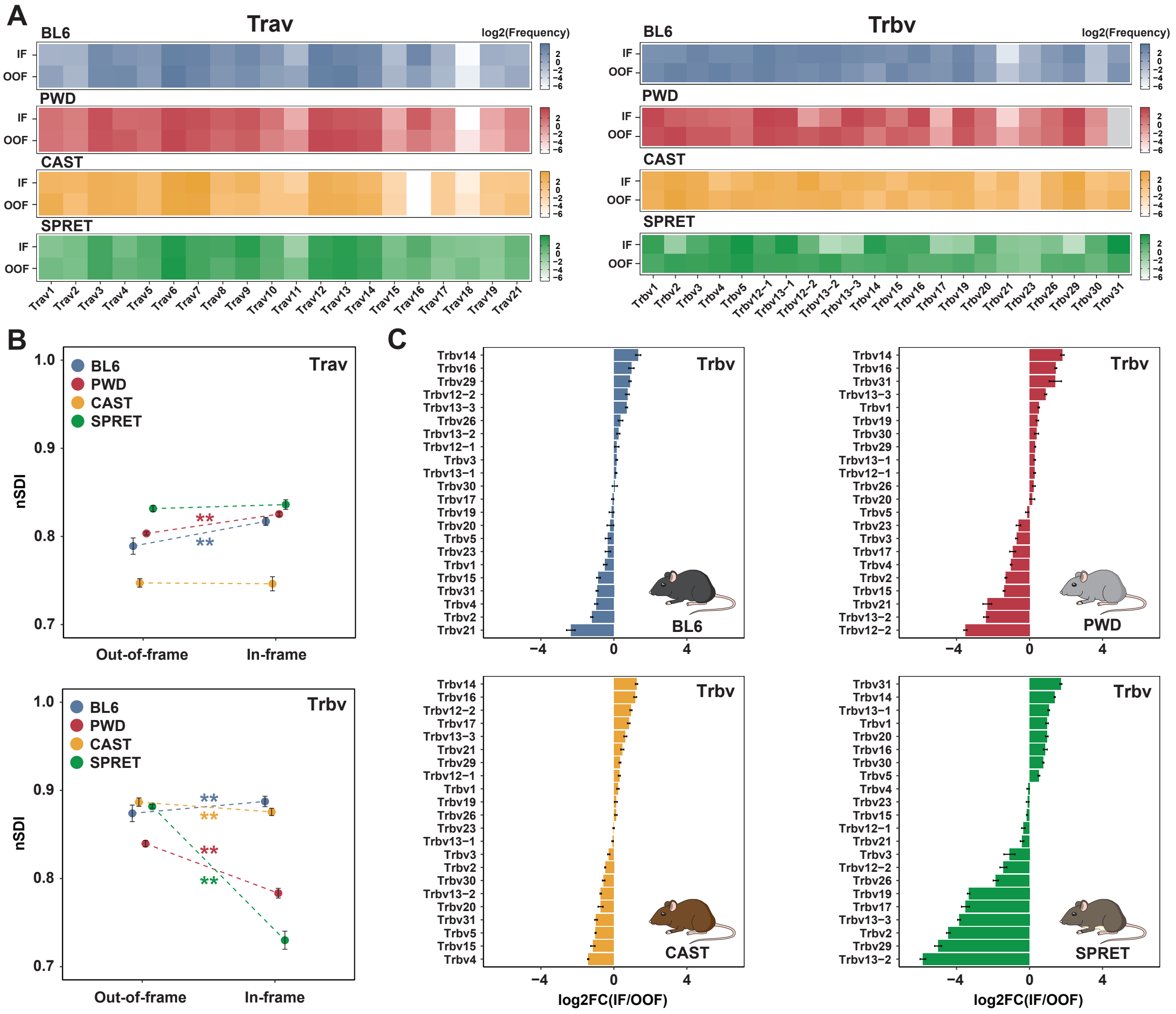

Figure 4: Thymic selection shapes V-gene usage

(A) Vα family (left) and Vβ gene (right) usage frequency ($\log_2$) heatmaps. Heatmaps show the mean intra-species V-usage in in-frame (IF) and out-of-frame (OOF) TCRs across all T cells.

(B) Mean intra-species entropy in Vα-usage (top) and Vβ-usage (bottom) distributions calculated using the normalized Shannon diversity index (nSDI) for OOF and IF TCRs (error bars indicate the standard deviation in species replicates, significance calculated using a paired t-test, * *P-value* < 0.05).

(C) Log_2 fold-changes (log2FC) in Vβ gene usage frequencies between IF and OOF TCRs across the different mouse species (error bars indicate the standard deviation in species replicates).

Allele-specific V/J segment usage in F1 Hybrids revealed by patterns of thymic selection

In contrast to outbred individuals, assaying V(D)J gene usage in inbred mouse strains benefits from consistent thymic selection, thanks to the homozygous MHC-allele background. If so, the observed OOF-IF profile should shift in individuals carrying alternative MHC-haplotypes (see also [55, 56]). This raises further the tantalizing possibility that, depending on the actual MHC-haplotype, there may be different outcomes associated with positive vs. negative thymic selection. To test our hypothesis, we generated F1 hybrids from crosses of BL6 with each of the three other mouse species (BL6xPWD, BL6xCAST, BL6xSPRET). This gave us a powerful tool to track how the two otherwise distinct sets of species-specific V(D)J gene repertoires may be shaped by thymic selection in the respective heterozygous MHC allele state.

We first compared V(D)J usage frequencies in F1 hybrids with the respective frequencies in the parental species (**Fig. 5A** for V-genes and **Fig. S5A** for J-genes). Similar to our previous analysis, we see the most differences across Vβ-genes, in both directions: Vβ-genes can be significantly more abundant (e.g., *Trbv1*) or less abundant in F1 hybrids than in either parent (e.g., *Trbv12-1* and *Trbv12-2*; Wald-test; $P < 0.01$; **Fig. S6A-D**). To analyze the general trends across Vα, Jα, Vβ and Jβ frequencies between parental lines and their F1 hybrids, we classified their relative V(D)J gene usage frequencies into five broad categories: conserved, additive, dominant, over- and under-dominant (**Fig. 5B, see methods**). In Vα and Jα genes, 78.6% of genes only show modest frequency changes (<1%) relative to both parents. Over- and underdominance (>1% higher/lower frequency than both parents, respectively) are only seen in genes in the TCRβ chain and mostly in Vβ-genes. Notably, we observe overlaps in the identity of over-dominant (e.g., *Trbv1*) and under-dominant (e.g., *Trbv12-1*) Vβ-genes across all three hybrids. Collectively, V(D)J gene frequency changes between F1 hybrids and the parental lines are predominantly observed in the TCRβ chain.

We then calculated the nSDI for pre- and post-selection repertoires in the F1 hybrids and compared them to the previously calculated nSDI values in the parental species (Trav and Trbv **Fig. 5C** Traj and Trbj **Fig. S5B**). Across all F1 hybrids, we see significantly reduced nSDI values for Vβ-gene frequencies ($P < 0.05$; paired t-test). The increase in unevenness between pre- and post-selection repertoires are consistently greater in F1 hybrids compared to their parental species, suggesting that thymic selection introduces stronger biases on Vβ-gene usage in F1 hybrids relative to their respective parental species. Interestingly, we observed a constant increase of nSDI values in post-selection compared to pre-selection Vα gene frequencies in F1 hybrids (*P* < 0.05 in BL6xCAST and BL6xSPRET).

Next, we took advantage of our ability to assign V(D)J genes in F1 hybrids in an allele-specific manner to identify potential biases towards usage of one parental allele. We compared the allelic ratios of V(D)J genes in pre- and post-selection repertoires (V genes: **Fig 5D, Fig S5D** and J genes: **Fig S5C**). We found significant allelic biases in Vβ-genes in post-selection repertoires that were not observed in the pre-selection repertoire. For example, in pre-selection repertoires of BL6xSPRET hybrids, ~60% of *Trbv13-2* usage was assigned to the SPRET allele, whereas in post-selection repertoires this rate dropped to ~1%. Therefore, while in BL6xSPRET hybrids the *Trbv13-2* allele was frequently recombined during V(D)J recombination, it was almost completely rejected during thymic selection. The almost exclusive selection of one parental allele in a heterozygous MHC haplotype and a common *trans*-environment, provides strong evidence that this selection process is primarily determined by genetically encoded polymorphisms in the underlying Vβ gene. Similarly, we saw that while Traj35 pre-selection frequencies are balanced between parental alleles (Percent of BL6 alleles: PWD 49%, CAST 44%, SPRET 50%), the BL6 allele was substantially less frequent in post-selection repertoires (Percent of BL6 alleles: PWD 25%, CAST 26%, SPRET 25%; **Fig S5C**).

Apart from these strong exceptions, allelic bias is strongly correlated in pre- and post-selection repertoires for most V(D)J genes (see Pearson correlation in **Fig. 5D** and **S5C**). Genes that show strong frequency differences between both parental species (*Trav16* and *Trbv21* in BL6/CAST, *Trav18* in BL6/SPRET or *Trbv17* in BL6/PWD) often show strong F1 allelic bias towards usage of the respective parental allele that had a higher frequency in the pure contrast (**Fig. 5D**). We therefore conclude that the (generative) pre-selection biases observed between species are primarily controlled by linked factors acting in *cis*, e.g., polymorphisms in the RSS sequences that influence the recombination likelihood of a particular gene during V(D)J recombination.

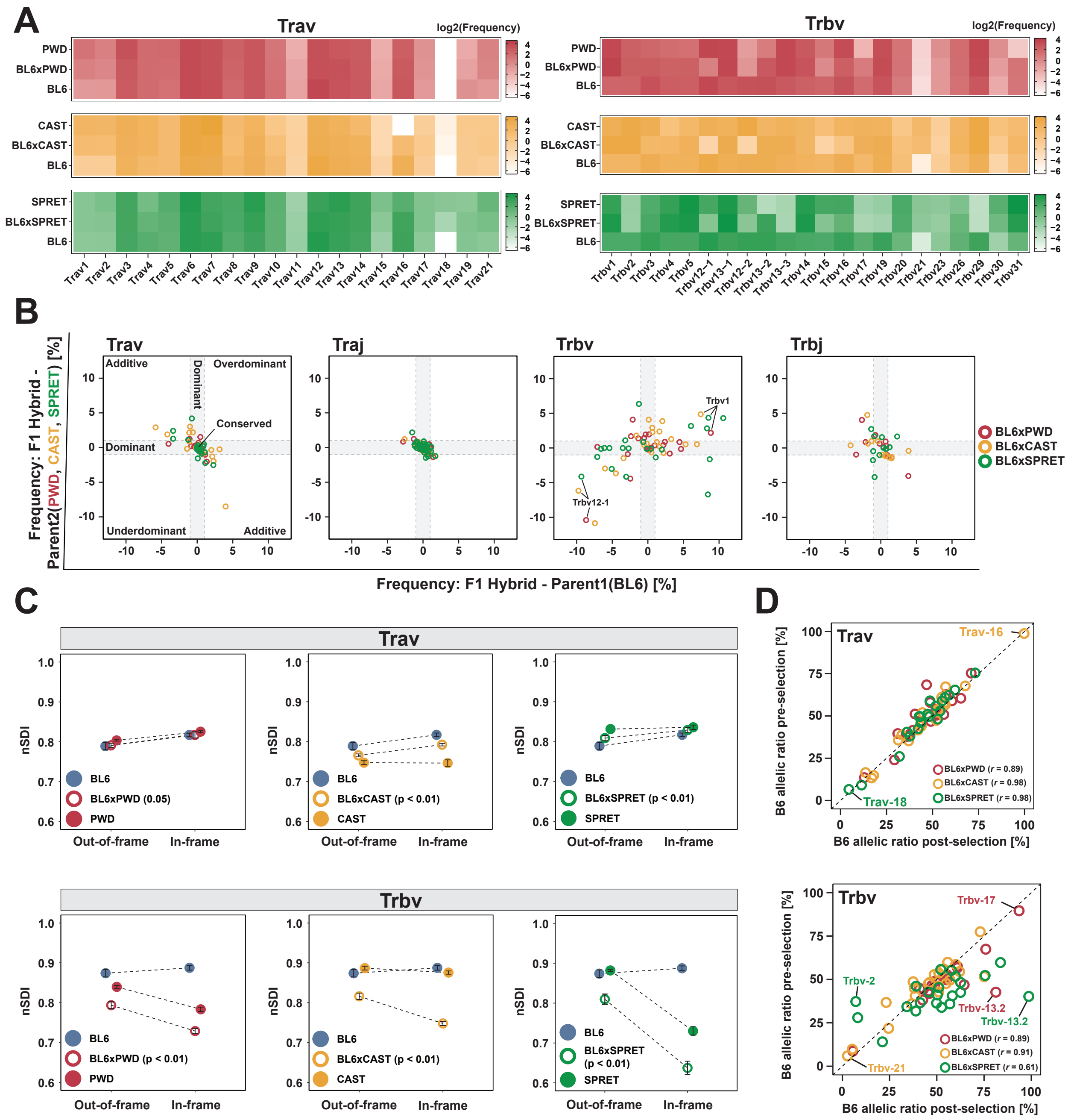

Figure 5: V-gene usage is more restricted in F1 hybrids and shows allele specific usage biases

(A) Vα family (left) and Vβ gene (right) usage frequency ($\log_2$) heatmaps of in-frame TCRs in F1 hybrids and their respective parental species.

(B) Relative frequency changes of V(D)J gene usage in F1 hybrids and the respective parental species (x-axis: F1 hybrid – BL6 and y-axis: F1 hybrid – PWD, CAST or SPRET) categorized into mode of inheritance. Conserved (center), dominant (grey area), additive (top left and bottom right quadrant), under-dominant (bottom left quadrant) and over-dominant (top right quadrant; see methods). Each circle represents a Vα-family, Jα-gene, Vβ-gene or Jβ-gene.

(C) Comparison of entropy of V-usage distribution in F1 hybrids and the respective parental species calculated using the normalized Shannon diversity index (nSDI) for OOF (left) and IF (right) TCRs (error bars indicate the standard deviation in species replicates, significance tested for F1 hybrid IF vs OOF contrast using paired t-tests, *P-value* < 0.05).

(D) Analysis of biased V gene allele usage in F1 hybrids. Plots show the percentage of BL6 Vα family alleles and Vβ gene alleles in post- (x-axis) and pre-selection (y-axis) TCRs. Each circle represents a Vα-family (top) or Vβ-gene (bottom). Pearson-correlation was calculated for post- and pre-selection V gene usage.

Composition and diversity of the paired CDR3αβ repertoire depends on an individual's genotype

Next, we addressed CDR3 diversity 32 samples, representing seven different genotypes. We reasoned that given the cumulative bias in gene segment usage, availability, as well as genetic differences, we should observe distinct CDR3 amino acid motif repertoires. To test this hypothesis, we first compared the CDR3α, CDR3β and CDR3αβ diversity in a set of 100,000 T cells sampled randomly from each individual (**Fig. 6A**). We found that, across all comparisons, F1 hybrids show an increased number of unique CDR3 sequences relative to their respective parental species. In single CDR3α motifs, we see significant differences in diversity within the parental species, which is in line with the observed differences in locus structure of the TCRα loci across these mice (e.g., ~50 fewer Vα segments in CAST compared to all other species; pairwise t-test; ** = *P* < 0.01; * = *P* < 0.05). These parental diversity differences are not recapitulated in the F1 hybrids. Instead, the absolute diversity increases with the increasing evolutionary divergence of the parental species.

A strikingly different picture emerged for the CDR3β motifs. Importantly, V(D)J segments in the TCRβ locus follow a strict one-to-one orthology across all parental species. Accordingly, single-chain CDR3β diversity showed little variation across the parental species. In contrast, F1 hybrids showed much greater variation and generally display greater TCR diversity than observed in the repertoire of either parent (pairwise t-test; ** = *P* < 0.01; * = *P* < 0.05). A possible explanation for this is the strictly restricted selection of Vβ segments during thymic selection in the TCRβ chain. We observe remarkable diversity of paired CDR3αβ across all genotypes, with an average of 98.2% of all motifs being observed only once in each set of 100,000 motifs. Notably, among F1 hybrids, the lowest diversity is observed in BL6xSpret hybrids despite the highest evolutionary divergence in the respective parental species.

Due to random insertions and deletions at the segment junction sides, the highest amino acid diversity within CDR3 motifs is observed in the central region of the peptide chains (**Fig**. **S7A**). It has been shown that this central region overlaps the region of highest antigen proximity in TCR-MHC complexes (position 107-115 according to IMGT nomenclature [57]) and therefore contributes most to the antigen specificity of the underlying TCR [6]. Further, the same study also provided evidence that antigen-specificity is defined by specificity-groups of similar amino acid motifs within TCRs. With this in mind, we analyzed germline-encoded differences in the central motifs across all mice. Because the same antigen might be recognized by several similar TCRs rather than just one CDR3αβ motif we first generated amino acid 4mers from both CDR3 motifs of TCRs of individual cells (**Fig 6B**). We then identified a list of 1,201,646 common 4mers across all genotypes (**see methods**). Next, we performed PCA analysis based on the abundance of all 4mer pairs across all 32 individuals. We see that 4mer pairs are strictly clustered according to the underlying genotype of each sample (**Fig. 6B**). This pattern was also observed in the corresponding analysis on single-chain derived unpaired 4mers (**Fig S7B**).

Comparison of TCR repertoires often involves the analysis of shared “public” CDR3 motifs. Typically, this type of analysis addresses motif sharing within single chains across repertoires. While these comparisons might provide information on the generative probability of distinct single-chain CDR3 motifs across individuals, the missing CDR3 motif in the second chain makes it challenging to identify potential shared TCR responses to antigens. Here, we utilized CITR-seq’s large set of more than 5 million paired CDR3 motifs to analyze motif sharing across all individuals. In total, we identified 25,894 (~0.5% of all motifs) paired motifs with identical amino acid sequence, observed in different individuals. Across single chains, sharing of identical amino acid sequences was more common with 264,088 shared CDR3α (~36.7% of all unique motifs) and 469,827 shared CDR3β (~ 27.2% of all unique motifs) motifs observed in at least two individuals. Notably, we found 1696 CDR3α and 644 CDR3β amino acid motifs that were observed in all 32 individuals, while identical CDR3αβ pairs were at most observed in 12 individuals (**Fig. S7C**)

To test whether the extent of paired CDR3αβ motif sharing was higher than expected by chance, we shuffled the α- and β-chains within each individual and then re-calculated the count of shared motifs. We saw that the observed sharing count is about 4-fold higher than the mean across 100 permutations of αβ-chains shuffled samples (mean: 6182 shared CDR3αβ motifs across shuffled pairs, permutation test *P-value* < 0.01). Next, we analyzed whether the extent of sharing in CDR3αβ motifs is dependent on the underlying genotype of each sample. To account for the variance in sample size across all samples, we calculated the Jaccard Index of repertoire sharing using paired CDR3αβ motifs (**Fig. 6C, see methods**). We observed that motif sharing is significantly higher across samples of identical genotypes (56.7% of all shared motifs), compared to individuals with partially shared genotypes (F1 hybrid samples, 32.0% of all shared motifs) and especially in contrast to completely unrelated individuals (11.3% of all shared motifs; Wilcoxon rank sum test *p-value* < 0.01) (**Fig. 6D**). While we caution here that our use of inbred individuals may differ from the usual comparison contexts with CDR3 motifs, nevertheless, the extent of sharing across fully unrelated individuals led us to conclude that an individual's genotype contributes significantly to the final TCR repertoire. Additionally, public TCR responses are far more likely to be observed across related individuals than unrelated individuals.

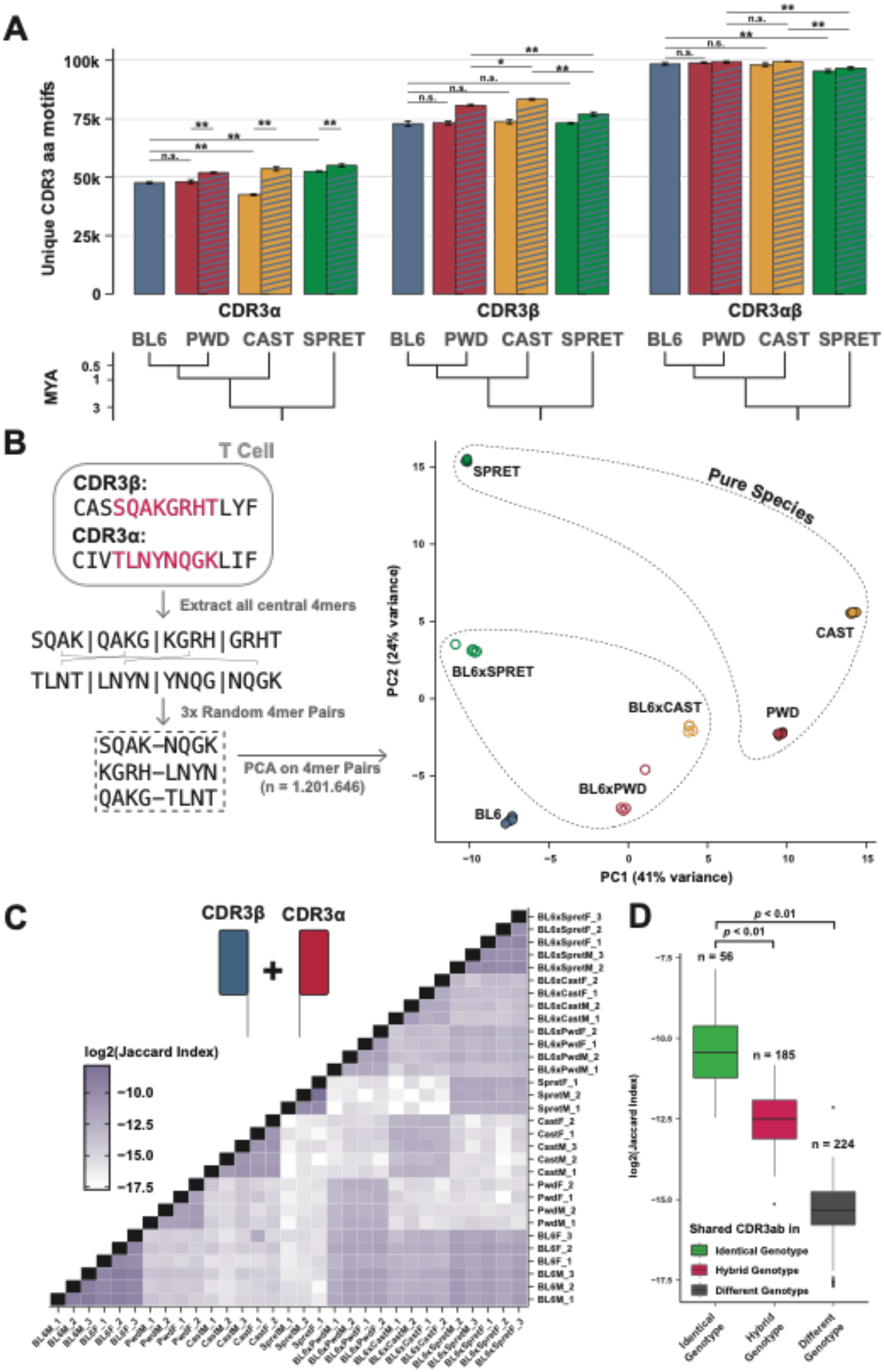
A
Unique CDR3 aa motifs
100k
75k
50k
25k
0
n.s.
**
*
n.s.
CDR3α
CDR3β
CDR3αβ
BL6
PWD
CAST
SPRET
MYA
0.5
1
3
B
T Cell
CDR3β:
CASSQAKGRHTLYF
CDR3α:
CIVTLNYNQGKLIF
Extract all central 4mers
SQAK | QAKG | KGRH | GRHT
TLNT | LNYN | YNQG | NQGK
3x Random 4mer Pairs
SQAK–NQGK
KGRH–LNYN
QAKG–TLNT
PCA on 4mer Pairs
(n = 1.201.646)
Pure Species
SPRET
CAST
PWD
BL6xSPRET
BL6xCAST
BL6xPWD
BL6
PC2 (24% variance)
PC1 (41% variance)
15
10
5
0
−5
−10
C
CDR3β
CDR3α
+
log2(Jaccard Index)
−10.0
−12.5
−15.0
−17.5
BL6xSpretF_3
BL6xSpretF_2
BL6xSpretF_1
BL6xSpretM_3
BL6xSpretM_2
BL6xCastF_2
BL6xCastF_1
BL6xCastM_2
BL6xCastM_1
BL6xPwdF_2
BL6xPwdF_1
BL6xPwdM_2
BL6xPwdM_1
SpretF_1
SpretM_2
SpretM_1
CastF_2
CastF_1
CastM_3
CastM_2
CastM_1
PwdF_2
PwdF_1
PwdM_2
PwdM_1
BL6F_3
BL6F_2
BL6F_1
BL6M_3
BL6M_2
BL6M_1
D
p < 0.01
p < 0.01
n = 56
n = 185
n = 224
log2(Jaccard Index)
−7.5
−10.0
−12.5
−15.0
−17.5
Shared CDR3ab in
Identical Genotype
Hybrid Genotype
Different Genotype
Identical Genotype
Hybrid Genotype
Different Genotype

Figure 6: CDR3 motif diversity and sharing depends on an individual's genotype

(A) Mean count of unique CDR3α (left) CDR3β (middle) and paired CDR3αβ (right) amino acid motifs in a set of 100,000 randomly sampled TCRs from each individual grouped by genotype (error bars indicate the standard deviation in species replicates, significance calculated by pairwise t-tests with * *P-value* < 0.05 and ** *P-value* <0.01). Single-color bars represent the parental species, diagonally striped bars represent the respective F1 hybrids. The phylogenetic tree (bottom) shows the evolutionary divergence of parental species.

(B) Analysis of paired 4mers extracted CDR3αβ motifs. For each paired CDR3αβ amino acids sequence all possible 4mers were extracted and subsequently, 3 random 4mer pairs (one from the CDR3α and one from the CDR3β sequence) were generated (left panel). The combined filtered (see methods) count matrix of 4mer pairs from all 32 individuals was then used for PCA analysis. Samples cluster based on the sample genotype.

(C) Overlap of paired CDR3αβ amino acid motifs between all 32 CITR-seq samples calculated using the Jaccard index ($\log_2$; see methods)

(D) Based on overlap of genotypes all samples were grouped into identical genotype (within species, e.g., BL6F_1 and BL6M_1), hybrid genotype (50 % identical genotype, e.g., CAST and BL6xCAST) and different genotype (completely unrelated individuals, e.g. PWD and SPRET). Boxplot shows the calculated Jaccard index values ($\log_2$) in each respective group (significance tested using Wilcoxon rank-sum test, *P-value* < 0.01).

Discussion

Production and maintenance of large and diverse repertoire of TCRs is crucial for a functioning adaptive immune system. For decades researchers have now accumulated insights into the generative process, the size and overlap, as well as associations to disease states of TCR repertoires. High-throughput sequencing technologies have reached sufficient sensitivity and throughput to capture reasonable portions of an individual's TCR repertoire. Yet they still suffer from severe limitations in the face of the extreme diversity of TCR repertoires. To date, arguably the most limiting of these factors is the requirement for single-cell resolution to link both TCR chains of the heterodimeric αβ receptor to the T cell of origin. With few (mostly non-commercial) exceptions, single-cell TCR sequencing methods suffer from low-throughput (10^3-10^5 T cells) and high cost (reviewed here [58]). Pit against the vast TCR repertoire diversity, especially in naïve repertoires, those technologies often capture only a tiny fraction of an individual's repertoire.

In this study we present CITR-seq, a high-throughput low-cost single-cell TCR sequencing method that overcomes many of these limitations. We use CITR-seq to generate TCR repertoires of four evolutionary divergent inbred mouse species and t their respective F1 hybrids, covering more than 9 million T cells with 76% successful αβ-pairing rate.

We first identified large differences in V(D)J gene usage across the different mouse species, with very high within-species consistency for both TCR chains. While the arrangement and number of genes in the TCRβ locus are conserved across all species, the TCRα locus has undergone complex rearrangements leading to triplications and inversions of Vα gene clusters. As a result, the number as well as their relative distance to Jα genes varies substantially between Vα genes of the different mouse species. We observed that at the TCRα locus in CAST, in which the Vα locus was contracted by 0.6 Mb, the distal Vα genes showed significantly higher segment usage compared to the other species. Considering the progressive 3' to 5' recombination of V-J segments [59], we interpret this as evidence for a direct relation of gene segment locus size and chromosomal position dependent usage frequency.

Due to the very conserved arrangement of TCRβ genes, the tightly enforced allelic exclusion as well as prevention of continuous rearrangements, the relative position of genes should contribute less to biases in the TCRβ gene usage across species. Nevertheless, we see that the relative fold-changes in gene usage of Vβ genes can be extreme, with up to 60-fold difference between different mouse species.

We show that many of those extreme gene usage differences are introduced during thymic selection by comparing pre- vs post-selection repertoires. We use the nSDI of segment usage to demonstrate that thymic selection primarily acts on Vβ segments and show that their generative frequency immediately after V(D)J recombination is more similar across different mouse species than the actual usage frequencies observed in mature and selected TCR repertoires. Critically, we observed that many of the Vβ genes that are rejected during thymic selection, contribute identical amino acids to CDR3 motifs compared to other Vβ genes that do not significantly change in frequency in pre- vs. post-selection repertoires. Thus, we hypothesize, that the rejection of those Vβ genes is unlikely to be enforced during negative selection as a consequence of strong affinity to a self-MHC complex. Rather, it is reflective of their particular germline-encoded ability to bind MHCs evaluated during positive selection. This hypothesis is further supported by the fact that we did not observe categorical rejection of J-segments, that are though to mostly contribute to the antigen specificity of a TCR rather than its ability to bind to MHCs.

Further experiments, where both Vβ and MHC components can be experimentally controlled, may be able to shed light on the mechanism underlying our observation.

We also used F1 hybrids of inbred mouse species, as a powerful tool to evaluate the thymic selection of TCRs in a defined heterozygous MHC haplotype. In those hybrids, two sets of V(D)J genes are exposed to a common *trans*-environment that subject both to a common pre- and post-selection repertoires regime. As a general trend, we see that most V(D)J genes show conserved usage frequencies relative to the parental species, or alternatively, in the case of substantial differences between the parental species, exhibit intermediate (*additive*) gene usage frequencies. These general patterns are far less pronounced for Vβ gene usage frequencies of F1 hybrids. We see that the selection against particular Vβ genes mostly resembles the patterns seen in the parents, with additional rejections of particular genes that were frequent in both parents. By utilizing our species-specific V(D)J references, we were able to disentangle the usage frequencies of particular alleles in F1 hybrids. We provide examples of Vβ-genes with balanced allelic ratios in pre-selection repertoires and striking allelic biases in post-selection repertoires. The nearly mono-allelic usage of particular Vβ-genes as a consequence of thymic selection in a defined heterozygous MHC allele state in F1 hybrids, provides strong evidence that the rejection of particular Vβ-gene alleles is based on genetically encoded polymorphisms. To the best of our knowledge, such extreme cases of allele-specific Vβ-genes selection have not been described before. This finding has important implications for the ongoing debate about whether binding to MHCs is an inherent and germline-encoded feature of TCRs that progressively co-evolves, or alternatively, MHC restriction of TCRs is enforced by TCR co-receptor signaling involved in TCR-MHC complex formation. Due to the common *trans*-environment during thymic selection of TCRs, the strong allelic biases of particular Vβ genes can hardly be explained by co-receptor signaling and thus should reflect the inherent ability of particular Vβ gene alleles to bind MHCs originated from heterozygous alleles in the F1 hybrids. Consequently, we hypothesize that TCR-MHC binding is a co-evolutionary process mediated by changes in amino acid sequences of V gene regions and MHC alleles that facilitate complex formation. In this context, the highly variable germline-encoded CDR1 and CDR2 regions of TCR V-genes have been shown to be crucial for altering TCR-MHC binding strength.

A secondary consequence of the co-evolution of TCR-MHC binding would likely be the increased rate of TCRs that exhibit insufficient or overly strong affinity to MHCs in hybrids between highly divergent parents. Indeed, as shown in this study, thymic selection had the strongest effect on Vβ genes in BL6xSPRET individuals in which the respective parental individuals had the highest degree of evolutionary divergence.

We further show that biases that are consistent in pre- and post-selection repertoires mostly reflect selection independent gene usage frequency differences observed in the parents. For instance, TCR consisting of *Trbv21* are extremely rare in BL6 (0.03% of TCRs) but much more frequent in CAST (3.0% TCRs) with minor differences in pre- and post-selection frequency. In BL6xCAST F1 hybrids, 2.2% of all TCRs consist of *Trbv21* with an allelic ratio of 97.3% of CAST alleles and only 2.7% BL6 alleles. Therefore, gene segment frequency biases are mediated through *cis*-effects in the absence of any additional biases introduced by thymic selection. For instance, polymorphisms in the RSS in between V(D)J genes could bias the recombination efficiency of particular gene segments.

What are the consequences of the observed frequency and selection biases across the different mouse species for the total diversity within the TCR repertoires? To answer this question, we evaluated CDR3 motif diversity in single chains as well as paired TCRs. CDR3α diversity varies most across the pure species, which is likely caused by the severe rearrangements and consequently different number of functional gene segments in the Vα cluster. We generally observe minor frequency changes of Vα families in pre- and post-selection repertoires, indicating that those gene segments are subject to less stringent thymic selection. As a consequence, F1 hybrids can make full use of both parental sets of V(D)J genes, which likely leads to the correlation of increased CDR3α diversity with increased evolutionary divergence of parental species. Here, we note that grouping of Vα genes by their respective families might mask the rejection of particular genes during thymic selection. While this potentially impacts the gene usage frequency differences across the species, it does not bias the comparison of total CDR3α diversity.

The single-chain CDR3β motif diversity is extremely similar across pure species, which is in line with the one-to-one orthology of V(D)J genes in the TCRβ locus. In contrast to this, we see substantial differences in CDR3β diversity in the hybrids. Based on the observed impact of thymic selection on Vβ genes, we hypothesize that the observed differences in CDR3β diversity in F1 hybrids result from a trade-off between the diversity of parental V(D)J gene sets and the increased likelihood of gene segment rejection during thymic selection, which should correlate with the increasing evolutionary divergence of parental species. While in this study, thymic selection is evaluated in a fixed and genotype-specific MHC-haplotype set-up, it has been shown that increased intra-individual MHC diversity is associated with increased rates of T cell depletion during thymic selection [60, 61]. Given that HLA allele frequencies vary substantially across human populations [62], we assume that the general trends observed in this study would therefore also apply in the context of CDR3 diversity evaluation in evolutionary divergent outbreed populations exhibiting diverse MHC haplotypes.

To the best of our knowledge, the present study analyzes the largest set of paired αβ-TCR to date. Especially in the context of TCR repertoire analysis of antigen in-experienced naïve T cells we benefit greatly from the scale of our dataset. Sharing of identical CDR3αβ motifs is rare but about 4-fold higher than expect by chance. Additionally, shared motifs are found at significantly higher rates in related individuals compared to unrelated individuals. Importantly, the increased sharing rate of paired CDR3αβ motifs analyzed in this study is not limited to the comparison of 100% identical motifs. Because similar CDR3αβ motifs might recognize identical antigens and similar antigens might be recognized by a range of similar CDR3αβ motifs we used a kmer-based approach to emphasize the similarity of paired CDR3αβ motifs in species of identical genotypes. We showed that 4mers originated from the central region of paired CDR3αβ motifs exhibit remarkably similar frequencies in species with identical genotypes relative to unrelated individuals. We therefore conclude that the combined effects of differences in TCR locus structure, V(D)J recombination frequencies and biases introduced by thymic selection, collectively shape the TCR repertoire in a genotype-specific manner.

This also has important implications for our understanding of public TCR motifs with potential disease associations. The number of shared CDR3 motifs in individuals with diverse MHC haplotypes is representative of those TCRs, that are selected by the specific set of MHCs in the sampled individuals. Public CDR3 motifs should therefore always be cataloged in the specific MHC haplotype context they have been observed in to allow for the comparison of such public motifs across different studies. Additionally, public TCR responses are often evaluated in common disease context, such as cytomegalovirus (CMV) and Epstein-Barr virus (EBV) [63-65]. Since large parts of human populations are persistently infected by those pathogens, a broad range of MHC haplotypes should have evolved to effectively present EBV- and CMV-derived peptides. Consequently, EBV- and CMV-associated CDR3 motifs might be more public compared to CDR3 motifs that specifically recognize less frequent pathogenic peptides.

Immune receptor diversity is one of the most characteristic and important features of adaptive immunity. While the generation of diversity is in large parts driven by stochastic events, the present study highlights important genetic contributions to TCR diversity. We show that the number of functional V(D)J segments, their *cis*-regulated recombination frequency as well as MHC haplotype dependent thymic selection, collectively generates TCR repertoires that are significantly more similar within than across genotypes.

Methods

Mice

All mice were housed in the animal facility of the Friedrich-Miescher Laboratory of the Max-Planck Society. Experiments were performed under license issued by the local competent authority (EB 01/21 M). Spleens were collected from mice aged 9-11 weeks. The following mouse strains were used in the experiments: C57BL/6J (The Jackson Laboratory, Strain #: 000664), CAST/EiJ (The Jackson Laboratory, Strain #: 000928), SPRET/EiJ (The Jackson Laboratory, Strain #: 001146), PWD/PhJ (The Jackson Laboratory, Strain #: 004660) as well as their respective F1 hybrids (C57BL/6J x SPRET/EiJ/CAST/EiJ/ PWD/PhJ). Male and female mice of all strains were used.

Isolation of CD8a$^+$ T-cells

Spleens of euthanized mice were collected and placed on a 40µm cell-strainer. Spleens were then pressed through the strainer using the backside of a syringe plunger. After thorough rising of the cell-strainer using ice-cold PBS, the flow-through was centrifuged at 400xg 4°C for 10 minutes in a swing-bucket centrifuge. Afterwards, supernatant was carefully discarded, and the cell pellet was resuspended in 1ml ice-cold PBS + 2% FBS. Isolation of CD8a$^+$ T-cells was then done using the “Dynabeads™ FlowComp™ Mouse CD8 Kit” (Invitrogen, 11462D) according to the manufacturer’s instructions. Pre-enriched cells were then stained using anti-CD4 BV510 (Bio Legend, 100553) and anti-CD8 PerCP-Cy5.5 (Bio Legend, 155013) in 500µl PBS + 2% FBS for 15 minutes on ice. Afterwards, cells were centrifuged at 400xg 4°C for 5 minutes. Supernatant was discarded and cell pellet was resuspended in 500µl ice-cold PBS + 2% FBS. This washing step was repeated once before final resuspension in 1 ml ice-cold PBS + 2% FBS. Cells were then further purified by fluorescence activated cell sorting (Fig. S1A). Depending on the size of the spleen (approx. 20mg in SPRET and up to 100mg in BL6) between 1x10^6 and 5x10^6 CD8+ T-cells were isolated from each spleen. Isolated T-cells were immediately transferred to prepared tissue culture dishes or used as primary cells for CITR-seq experiments.

Tissue Culture

Tissue culture of isolated CD8$^+$ T-cells was done as described by Lewis et al. [66]. Briefly, 6-well plates were coated with 0.5µg/ml anti-CD3 and 5µg/ml anti-CD28 in 3ml PBS at 4°C overnight. Before seeding the isolated CD8$^+$ T-cells, plates were washed twice with PBS. Cells were cultured in RPMI 1640 medium (ThermoFisher, 11875093) supplemented with 10% FBS, 1% GlutaMAX (ThermoFisher, 35050061), 1% penicillin/streptomycin (ThermoFisher, 15140122), 0.1% 2-mercaptoethanol (ThermoFisher, 21985023) and 0.1% human recombinant insulin (ThermoFisher, 12585014) at 37°C, 5% CO_2. After 20 hours cells were washed once with culture medium and then carefully detached from plate by repeatedly flushing the plates with a P1000 pipette. The cell suspension was then centrifuged at 400xg, RT for 5 minutes. Afterwards cell pellet was resuspended in 1ml PBS.

CITR-seq protocol

Oligonucleotides for barcoding

Two rounds of barcoding, each with 192 unique DNA barcodes are performed in CITR-seq. To prepare the barcoding plates in each well of two 96-well plates one unique round 1 top-stand oligo and one corresponding round 1 bottom-strand oligo were diluted in 10µl annealing buffer (10mM Tris pH 8, 50mM NaCl and 1mM EDTA). Top-strand round 1 oligos are partially complementary to the 5` overhang of the RT primers and anneal to the complementary sequence of the round 1 bottom-strand including the 7bp barcode sequence. Round 1 bottom-strand oligos contain a common 3bp 5` phosphorylated linker overhangs (“TCT”). The same procedure was repeated for two 96-well round 2 barcoding plates. Round 2 top-strand oligos contain a 3`-linker sequence (“AGA”) complementary to the 5’ linker sequence of round 1 oligos. Further, it contains another unique 7bp DNA barcode and the standard Illumina TrueSeq i7 sequencing adapter (Illumina, see document: 1000000002694). Round 2 bottom-strand oligo is complementary to its respective round 2 top-strand mate but lacks the 3bp linker sequence.

Oligos are used at the following concentrations: For each well of round 1 plates: µM of round 1 bottom-strand and µM of round 1 top-strand. For round 2 plates: µM of round 2 bottom-strand and µM of round 2 top-strand. Prior to each experiment round 1 and round 2 oligo plates are annealed in a PCR machine by heating plates to 90°C and then decreasing the temperature by 1°C every 30 seconds until room temperature is reached.

Oligonucleotides for reverse transcription

To increase the barcoding space further, barcoded RT-primers are used. Eight pairs of RT-primers targeting the constant region of the TCR alpha and TCR beta locus were designed with a 4bp barcode and a 10bp UMI as well as a phosphorylated 5’ overhang complementary to the overhang of the round 1 top-strand barcoding oligo.

TCR-V-segment primer pool for multiplex PCR

Primers were initially designed by alignment of annotated C57BL/6J cDNA sequence (IMGT database) belonging to the same TCR-V-segment family. For each family 1-5 primers (depending on number and sequence similarity of TCR-V-segment families) with similar annealing temperature (+/- 1°C), length and G/C content were designed (see supplementary table X). Subsequently, C57BL/6J TCRα and TCRβ loci were aligned to the corresponding genomic sequence in the genomes of CAST/Ei, PWK/PhJ (evolutionarily closest publicly available genome compared to the used PWD/PhJ mouse strain) and SPRET/EiJ (genome data available as part of the Mouse Genome Project from Sanger Institute). Candidate primers were then BLAT searched against the aligned genomes to rule out the presence of SNPs in the primer binding region across all strains. All candidate primers were individually tested to exclusively amplify the corresponding V-segment(s) in reverse transcription reactions using RNA isolated from C57BL/6J CD8a$^+$ T cells.

The final set of TCR-V-Segment primers consists of 58 individual primers (19 Vβ and 39Vα primers). Additional to the V-segment specific 3\` end of the primer, each primer also contains a common 5\` sequence used as target in the index-PCR. All V-segment primers were pooled at an equimolar ratio with a final concentration of 100 µM (1.72 µM of each primer). The primer pool was prepared once, and aliquots were frozen until used in an experiment to prevent biases introduced by varying primer pools across all experiments.

Cell fixation

After cell collection from tissue culture plates, 1ml of cell-suspension in PBS was added to 2.8ml of ice-cold PBS with 200µl of 16% PFA (ThermoFisher, 28908), for a final concentration of 0.8% PFA. After 10 minutes of incubation on ice 150µl 10% Triton-X was added to permeabilize cells and incubation on ice was continued for another 3 minutes. Cells were then centrifuged at 400xg 4°C for 5 minutes. Supernatant was discarded and the cell pellet was resuspended in 500µl 0.6M Tris-HCL pH8. Afterwards, 500µl of wash-buffer (PBS + 2% FBS and 0.4U/µl RNAseInhibitor (JenaBioscience, PCR-392L)) was added and cells were centrifuged at 400xg 4°C for 5 minutes. Washing was repeated once with 1ml wash-buffer before cells were counted and the concentration was adjusted to 50.000 cells/ml with wash-buffer.

Reverse transcription

10µl of fixed cells (~50.000 cells) were added to each of 8 tubes of a prepared PCR-strip containing 1µl 10µM barcoded TCRalpha constant region RT-primer, 1µl 10µM barcoded TCRbeta constant region RT-primer, 7.5µl NEB TS Buffer (NEB, B0466SVIAL) and 2µl 10mM dNTPs (ThermoFisher, R0181). TCRalpha and TCRbeta RT-primers within each tube share the same tube-specific 4bp barcode. The number of reverse transcription reactions can be scaled up easily by increasing the number of prepared PCR strips. Typically, two PCRs strips for a total of 16 reverse transcription reactions were prepared resulting in a final cell count of ~600.000 after barcoding (during the barcoding procedure about 25% of cells are lost due to repeated transferring and pooling of cells). Cells were then heated to 55°C for 5 minutes and rapidly cooled down to 4°C to allow pre-annealing of the RT-oligos to their target mRNAs. Afterwards, 6.3µl water, 1.5µl Maxima H Minus Reverse Transcriptase (ThermoFisher, EP0751) and 1ml RNAseInhibitor (JenaBioscience, PCR-392L) was added to each reaction for a final reaction volume of 30µl. Reverse transcription was carried out under the following conditions: 50°C for 10 minutes followed by 3 cycles of (8°C for 12 s, 15°C for 45 s, 20°C for 45 s, 30°C for 30 s 42°C for 2 minutes and 50°C for 3 minutes) and a final incubation at 50°C for 10 minutes. After reverse transcription cells were centrifuged at 400xg 4°C for 5 minutes. Supernatant was carefully discarded without disturbing the cell pellet. Cells were then resuspended in 50µl wash-buffer per tube and pooled in one 5ml tube and washing was repeated once.

Barcode ligation

All tubes used for pooling and washing of cells were coated with PBS +2% FBS to prevent cells from sticking to the plastic. Cells were resuspended in 2ml ligation buffer 1 (1460 µl water, 400 µl 10x T4 DNA ligase reaction buffer (NEB, B0202SVIAL), 100 µl T4 DNA ligase (NEB, M0202LVIAL), and 40 µl 10% Tween-20). 10µl of cell suspension was pipetted to each well of the two 96-well round 1 barcoding plates, taking care to not touch the liquid at the bottom of the plate. Plates were sealed with adhesive seals (ThermoFisher, AB0558) and incubated on a shaker for 40 minutes at room temperature. Afterwards, 3.5µl blocking oligo solution (20µM blocking oligo in water) was added to each well of both round 1 barcoding plates and incubation was continued for additional 20 minutes. The blocking oligo anneals to un-ligated round 1 top-strand oligos to prevent undesired ligations during the first cell pooling. Using a multichannel pipette, cells from both round 1 barcoding plates were pooled into a reservoir and then transferred to a 5 ml tube. Afterwards cells were centrifuged at 750xg 4°C for 3 minutes, supernatant was discarded, and cells were resuspended in 5ml of ligation buffer 2 (2260 µl water, 700 µl T4 DNA ligase reaction buffer, 100 µl T4 DNA ligase, 1900 µl annealing buffer and 40 µl 10% Tween-20). 25µl of cell suspension was pipetted into each well of the two 96-well round 2 barcoding plates, again without touching the liquid at the bottom of the wells. Plates were sealed and incubated for 40 minutes on a shaker at room temperature. Cells were then pooled as described before, centrifuged at 750xg 4°C for 3 minutes and resuspend in 200µl wash buffer. 1x DAPI (ThermoFisher, D1306) was added, and cells were counted on the Evos Countess II. The concentration of cells was adjusted to 2x10^6 cells/ml and 5 µl of cell suspension was transferred to separate tubes of PCR-strips for the generation of sub-libraries. The number of cells in each sub-library determines the expected number of barcode collisions in each sub-library. The number of collisions can be calculated with the formular used in the birthday problem. Here the total number of barcodes B is 294.912 (8 reverse transcription barcodes * 192 round 1 * 192 round 2 ligation barcodes) with a cell count of N = 10.000 cells per sub-library. The number of expected barcode collisions therefore is:

$$10000 - 294912 + 294912\left(\frac{294912 - 1}{294912}\right)^{10000} = 167$$

With 167 barcode collisions the expected collision rate is ~1.67% in each sub-library.

Reverse Crosslinking

8 µl reverse crosslinking buffer (1% SDS, 100mM Tris-HCl pH8 and 100mM NaCl), 2 µl Proteinase K (Qiagen, RP107B-1) and 5 µl water was added to each tube with 5 µl sub-library for a final volume of 20 µl per reaction. Reverse crosslinking was done at 62°C for 2 hours on a shaker followed by a final incubation at 95°C for 15 minutes to inactivate Proteinase K. Afterwards, 12µl 10% Tween-20 was added to each sub-library to quench SDS before PCR.

cDNA library preparation

After reverse crosslinking and SDS quenching 48µl multiplex-PCR mix (23 µl water, 16 µl 5x Q5 reaction buffer, 3.2 µl TrueSeq-i7-long primer, 3 µl 10mM dNTPs, 2 µl 100 µM TCR-V-Segment primer pool and 0.8 µl Q5 DNA polymerase) was directly added to each sub-library for a final PCR reaction volume of 80µl. PCR was done using the following parameters: 98°C 2min, then 10 cycles of (98°C 20 s, 63°C 30 s, 72°C 2 minutes) and a final incubation at 72°C for 5 minutes. After PCR amplified cDNA was purified by bead clean-up using custom size-selection beads at a ratio of 1.2x beads to PCR reaction (100 µl beads) to get rid of excess primers from the multiplex PCR. During this clean-up it is important to not cross-contaminate different sub-libraries as they have not yet received their sub-library specific index.

14.5 µl index-PCR mix (10 µl 5x Q5 reaction buffer, 2 µl TrueSeq-i7-long primer, 2 µl 10mM dNTPs and 0.5 µl Q5 DNA polymerase) was added to each sub-library. Afterwards, 2.5µl of a unique 10µM Nextera N5xx primer was added to each sub-library for a final reaction volume of 50 µl. Index PCR was done using the following parameters: 98°C 2min, then 12 cycles of (98°C 20 s, 63°C 30 s, 72°C 2 minutes) and a final incubation at 72°C for 5 minutes. After index PCR sub-libraries were purified using 1.2x size-selection beads as described above. cDNA concentration of each sub-library was measured, and sub-libraries were then pooled at an equimolar ratio. Before freezing the pooled libraries until sequencing they were quantified using the Qubit HS dsDNA Quantification Kit and run on the Agilent 2100 bioanalyzer with a High Sensitivity DNA kit.

DNA size selection with custom beads

To prepare custom DNA size-selection beads, 750 µl of SPRIselect (Beckman Coulter, B23318) were transferred to a 1.5 ml tube and placed on a magnetic stand. Supernatant was discarded and beads were washed once with 1 ml Tris-HCl pH 8. Beads were then resuspended in 50 ml bead buffer (22 mM PEG-8000, 2.5 M NaCl, 10mM Tris HCl pH 8, 1 mM EDTA in water).

In general, size selection beads are added to the solution containing DNA at a defined ratio to bind DNA of a specific length (e.g., 1.2x beads will bind dsDNA >200bp). After binding DNA for 5 minutes, tubes are placed on a magnetic stand and supernatant is discarded (or transferred to a different tube in case of upper cut-off size selection). Beads are then washed twice with 80% EtOH before DNA is eluted from the beads by adding the desired volume of water or 10mM Tris HCl pH 8.

Sequencing

All TCR cDNA libraries have been sequenced on the Nova-seq 6000 platform by Illumina using S4 2x150bp v1.5 kits with the following sequencing-cycle set-up: Read1: 150 cycles, Index1: 17 cycles, Read2: 150 cycles and Index2: 8 cycles.

Cost of CITR-seq experiments

In CITR-seq all molecular reactions are carried out in bulk for ~5.000-50.000 cells depending on the protocol step. This offers significant cost advantages, especially in contrast to plate-based single-cell protocols in which all molecular reactions are done separately for each cell. Enzymes needed for one experiment (using 500.000 input cells) in our hands cost about 350$ (ligase, reverse-transcriptase, polymerase, RNAse inhibitor etc.). The required barcoding oligos can be bought in high quantities and are then sufficient for many CITR-seq runs bringing down the oligo costs to less than 50$ per experiment. Collectively, the cost for library preparation in each experiment is therefore roughly 400$.

Analysis

CITR-seq sequencing data pre-processing

Demultiplexing of fastq-files was done using a custom script, allowing one nucleotide mismatch in the cellular barcode sequence (relative to the barcode whitelist). Afterwards, adapter sequences were trimmed from the sequencing reads using *cutadapt* [67]. We then used *UMItools* [68] to extract the 4bp in-line barcode sequence from each sequencing read. For each read the in-line barcode and the barcode sequence extracted from the corresponding index reads were combined. The combined barcode sequences were then added to the 5' end of read1. Afterwards, the full barcode information is present at the beginning of read 1 (16bp) followed by the UMI (10bp) and the 150bp sequencing read. Read 2 contains just the 150bp sequencing read. This pre-processing of sequencing reads modifies the fastq-files to be easily integrated into the subsequent MiXCR-pipeline.

Species-specific V(D)J reference libraries

To construct individual V(D)J reference libraries for PWD/PhJ, CAST and SPRET we built on the strategy used in the *findAlleles* function implemented in the MiXCR [47] software. First, we used full-length TCR sequencing data of each species generated using the 10x Genomics Immune Profiling Kit (see below), to assemble gene-segment candidate-alleles: Raw sequencing fastq files were processed using *Cellranger VDJ* supplying the built-in mm10 based VDJ-reference (GRCm38-ensemble-7.0.0). In this pipeline fragmented reads are combined into full length contigs based on sequence overlap in reads and matching cellular barcodes. We used the generated "filtered_contig.fastq" output and passed it directly to the MiXCR alignment step ("*align*", --species mmu, --preset generic-amplicon --floating-left-alignment-boundary --floating-right-alignment-boundary C --rna) to generate binary vdjca-files. We then used *mixcr exportAlignments* (--dont-impute-germline-on-export -allNFeatures UTR5Begin FR3End) to extract gene-features so that SNPs in candidate-alleles are not modified to match the provided reference. For each candidate V(D)J-allele we then used the extremely unique combination of associated UMI and CDR3 sequences to distinguish low-frequency alleles from alleles generated by sequencing or PCR errors by requiring each allele to be identified with at least two unique CDR3/UMI combinations. The list of identified V,D and J segment alleles was then used to generate a MiXCR compatible reference libraries for each species using the *buildLibrary* function implemented in MiXCR. Since the underlying RNA-based input libraries are generated using template-switching rather than multiplex-PCR, they allow for the discovery of *de novo* V(D)J-segments since template-switch based cDNA libraries do not require previous knowledge of the entire set of gene-segments for amplification.

Full list of V(D)J genes/families analyzed in cross-species comparisons

All names of V(D)J genes/families correspond to the official IMGT nomenclature [57]. Pseudogenes as well as extremely low-expressed genes (< 200 transcripts across all ~5x10^6 T cells of all species) are excluded from the analysis. *Trbv24* (all species) and *Trbv31* (PWD) were excluded from the analysis due to failure of amplification during the multiplex PCR. The remaining list contains the following V(D)J genes/families:

1) **Trav-families:**
   Trav1, Trav2, Trav3, Trav4, Trav5, Trav6, Trav7, Trav8, Trav9, Trav10, Trav11, Trav12, Trav13, Trav14, Trav15, Trav16, Trav17, Trav18, Trav19, Trav21

2) **Trbv-genes:**
   Trbv1, Trbv2, Trbv3, Trbv4, Trbv5, Trbv12-1, Trbv12-2, Trbv13-1, Trbv13-2, Trbv13-3, Trbv14, Trbv15, Trbv16, Trbv17, Trbv19, Trbv20, Trbv21, Trbv23, Trbv26, Trbv29, Trbv30, Trbv31

3) **Traj-genes:**
   Traj2, Traj4, Traj5, Traj6, Traj7, Traj9, Traj11, Traj12, Traj13, Traj15, Traj16, Traj17, Traj18, Traj21, Traj22, Traj23, Traj24, Traj26, Traj27, Traj28, Traj30, Traj31, Traj32, Traj33, Traj34, Traj35, Traj37, Traj38, Traj39, Traj40, Traj42, Traj43, Traj44, Traj45, Traj47, Traj48, Traj49, Traj50, Traj52, Traj53, Traj54, Traj56, Traj57, Traj58

4) **Trbj-genes:**
   Trbj1-1, Trbj1-2, Trbj1-3, Trbj1-4, Trbj1-5, Trbj1-6, Trbj2-1, Trbj2-2, Trbj2-3, Trbj2-4, Trbj2-5, Trbj2-16, Trbj2-7

All gene names in the generated species-specific V(D)J reference files correspond to the closest relative (by sequence identity) in mm10 based MiXCR reference library.

Alignment of sequencing reads using MiXCR

Sequencing reads in pre-processed fastq-format were integrated into a custom MiXCR pipeline (MiXCR version 4.5.0) using the following steps:

1) *mixcr align*
   ```
   -- preset generic-ht-single-cell-amplicon-with-umi
   -- library Species Specific custom library (see above)
   -- tag-pattern ^(CELL:N(16))(UMI:N(10))(R1:*)\^(R2:*)
   -- floating-left-alignment-boundary
   ```

```
-- floating-right-alignment-boundary C
-  OvParameters.geneFeatureToAlign=VRegionWithP
-  OminSumScore=100
```

2) *mixcr refineTagsAndSort*

3) *mixcr assemble*

```
-- assemble-clonotypes-by CDR3
-- cell-level
```

We then used *mixcr exportClones* to extract the required information for all downstream analysis (e.g., cellular barcodes, transcript counts, V(D)J segments, CDR3 amino acid and nucleotide sequence etc.).

Construction of 10x Genomics Single Cell Immune Profiling sequencing libraries

We generated four sequencing libraries (from 10-week-old male mice, primary CD8$^+$ T cells of one of each: BL6, PWD, CAST, SPRET, see cell isolation described above) using the 10x Genomics Immune Profiling platform (Chromium Next GEM Single Cell 5' Kit v2) according to the manufacturer's instructions. T cells from each mouse were used in two separate reactions, each with 2.500 input cells (eight total reactions). V(D)J sequencing libraries were sequenced at 5.000 reads/cell. Raw sequencing data was pre-processed as described above and then aligned to species-specific V(D)J references using the outlined MiXCR pipeline.

Assignment of parental alleles in F1 hybrids

Pre-processed fastq-files of all F1 hybrid samples were aligned using MiXCR as described above. Importantly, the F1 hybrid samples were aligned to both parental V(D)J references and the alignment scores for V- and J-genes were extracted (*mixcr exportAlignments -vHitScore* and *-jHitScore*). We then compared the alignment scores for V- and J-genes from both alignments for each sequencing read. Each gene segment was then assigned to one parental species based on the higher alignment score in both alignments. Absence of SNPs in a gene-segment lead to identical alignment scores and therefore the respective reads were only assigned to a parental allele if the second gene segment in the same read was assigned to one parental allele. Reads in which both V- and J-segments had identical alignment scores in both alignments (e.g. no parental SNPs in both gene segments) as well as reads in which V- and J-parental assignment disagreed were discarded from the analysis together with all other reads sharing the respective identical cellular barcode.

Comparison of CITR-seq data with publicly available datasets from Parse Bioscience and 10x Genomics

Absolute counts of paired αβ-TCRs shown in **Fig. 2D** were taken from the following datasets:

1) **Parse Bioscience [44]:**
   TCR Sequencing of 1 Million Primary Human T Cells in a Single Experiment (primary human Pan T cells, sequencing depth: 5000 reads/cell).

2) **10x Genomics Single Cell Immune Profiling [45]:**
   CD8+ T cells of Healthy Donor 2 (v1, 150x91), Single Cell Immune Profiling Dataset by Cell Ranger v3.0.2, 10x Genomics, (2019, May, 9)

The UMI/cell recovery rates in CITR-seq were compared to the UMI/cell recovery rates in two publicly available datasets provided by Parse Bioscience:

1) **Parse Bioscience [44]:**
   TCR Sequencing of 1 Million Primary Human T Cells in a Single Experiment
   (primary human Pan T cells, sequencing depth: 5000 reads/cell)

2) **Parse Bioscience [46]:**
   Performance of Evercode TCR in Activated Human T cells
   (Pan T cells after 72h activation using CD3/CD28 beads + IL-2 supplementation, sequencing depth: 5000 reads/cell)

Datasets are available from their website (https://www.parsebiosciences.com) and the specific UMI/cell rates were extracted from the "TCR:Barcode Report (TSV)" tables (column: "transcript_count")

PCA of VJ-pairing and central CDR3 4mer abundance

We conducted Principal Component Analysis (PCA) on two different datasets.

1) **V-J pairing**

The first PCA was done to compare total counts of observed V-J pairs across all sample down-sampled to a common cell count of 5.000 T cells (each with one associated TCRα and TCRβ chain). The count-tables were analyzed using DESeq2's[69] *varianceStabilizingTransformation* (*vst*, blind=FALSE, nsub=300) and PCA was conducted on the top 300 most variable V-J pairs (*plotPCA* , ntop=300). Using this parameters PC1-4 explain approximately 67% of variance in V-J usage across samples.

2) **CDR3 4mers**

The second PCA analysis was done on a set of amino acid 4mers (or 4mer pairs) extracted from the central region of CDR3 amino acid motifs (the three most 3' and 5' amino acids were trimmed from the motif). Initially three randomly chosen 4mers were extracted from each trimmed CDR3 motif. For paired CDR3αβ motifs we extracted 3 random 4mer pairs of the respective CDR3α and CDR3β motifs associated with a cellular barcode. Subsequently, we generated count-matrices with the total counts of each 4mer across the 32 individuals. We filtered the matrices to only contain 4mer/pairs that were observed at least once across three individuals of a specific genotype (final 4mer counts: 39.843 CDR3α, 56.538 CDR3β and 1.201.646 CDR3αβ 4mers). The filtered count matrices were then analyzed following the standard DESeq2 [69] workflow for un-normalized count-matrix inputs. Afterwards, PCA was done on the top 5000 most variable 4mers using the *plotPCA* function.

Diversity and overlap indices used for repertoire comparison in CITR-seq data

Many of the commonly used indices from the analysis of TCR repertoires within and across different samples, were originally developed to quantify the diversity of species in an ecosystem. For this reason, they are often classified as either *alpha-diversity* indices that measure species richness and/or evenness within a particular population or alternatively as *beta-diversity* indices, which evaluate differences or overlaps between different populations. Similar to species diversity studies in ecology, TCR repertoire diversity estimates suffer from inherent incompleteness of the sampled diversity, a problem first described as the unseen species problem [70]. The use of diversity indices for adaptive immune receptor analysis is reviewed here [71]. The following indices were used in this study:

1) **Shannon diversity index** [72] (for proportions)

   The Shannon diversity index considers both, species richness and species evenness to evaluate the entropy within a distribution of species:

$$H = -\sum_{i=1}^{k} p_i \log(p_i)$$

   With p_i = the proportion (frequency) in the group k (e.g. gene segments). The index can be normalized by dividing it by the maximum diversity. Which then is the normalized Shannon diversity index (nSDI) used in this study:

$$E_H = \frac{H}{\log(k)}$$

   In the context of gene segment usage in nSDI of 1 would indicate that all gene segments are used at identical frequencies in a TCR repertoire.

2) **Jaccard index**

The Jaccard index was developed by Paul Jaccard in 1901 and is commonly used to calculate the overlap (of CDR3 motifs) between two samples of TCRs:

$$J(A,B) = \frac{A \cap B}{A \cup B}$$

The Jaccard index calculates the intersection size divided by union size of two samples (A and B).

Classification of relative V(D)J gene usage in parental lines and their F1 hybrids

In classical F1 hybrid experiments, genes are often categorized into additive, dominant, over- and under-dominant, based on their expression in F1 hybrids relative to the parental individuals [73]. When adopted to V(D)J-gene usage in F1 hybrids and their parental lines it is important to note, that the frequency of a particular gene does not only depend on differences in gene expression regulation but is also influenced by biases during V(D)J recombination and thymic selection. We see that thymic selection introduces significant changes to V(D)J gene usage and therefore amplifies gene usage differences across species relative to the differences emerging from differential gene regulation alone. This effect is especially strong in F1 hybrids were almost all V(D)J genes show significantly different frequencies relative to the parental species (**Fig S5A**). Instead of using a *p*-value based classification, we therefore decided to rather compare the relative frequencies of V(D)J gene usage across F1 hybrids and the parental species. Accordingly, V(D)J gene frequencies are classified using the following criteria:

1) **Conserved:** Gene frequency in the F1 hybrid is within 1% of the frequency in both parents

2) **Dominant:** Gene frequency in the F1 hybrid is within 1% of the frequency in one parent and more than 1% larger or smaller than the frequency in the other parent.

3) **Additive:** Gene frequency in the F1 hybrid is more than 1% smaller than the frequency in one parent and more than 1% larger than the frequency in the other parent.

4) **Over-dominant:** Gene frequency in the F1 hybrid is more than 1% larger than the frequency in bother parents.

5) **Under-dominant:** Gene frequency in the F1 hybrid is more than 1% smaller than the frequency in bother parents.

Acknowledgements

We thank all past and present members of the Chan and Jones laboratory for input into experimental design, helpful discussion and improving the manuscript. We especially thank Felicity Jones for her scientific input throughout the entire study. We thank Sinja Mattes and the remaining team of animal caretakers at the Friedrich-Miescher Laboratory led by Cemal Yilmaz. We thank Aurora Panzera and Christian Feldhaus from the Bio Optics core facility of the Max Planck Institute for Biology for their support with all FACS experiments. We thank Insa Hirschberg for supporting tissue culture experiments. We also thank the Genome Center of the Max Planck Institute for Biology for providing support with CITR-seq library sequencing. M.P. and D.S. are supported by an International Max Planck Research School fellowship. M.K. and Y.F.C are supported by the European Research Council Starting Grant 639096 “HybridMix” and Proof-of-Concept Grant 101069216 “Haplotagging”. The research done in this study is supported by the Max Planck Society.

Author Contributions

M.P. and Y.F.C. designed the experiments. M.P. and V.S. developed the barcoding framework for CITR-seq. M.P. developed the rest of the protocol and performed all experiments. M.P. performed the computational analysis advised by Y.F.C. M.P. wrote the manuscript. V.S., D.S., M.K. and Y.F.C. provided support for the experiments and the computational analysis. All authors reviewed the manuscript. Y.F.C. direct the study.

Declaration of Interest

The authors declare no competing interests.

Literature

1. von Boehmer, H. and P. Kisielow, *Self-nonself discrimination by T cells.* Science, 1990. **248**(4961): p. 1369-73.
2. Raskov, H., et al., *Cytotoxic CD8(+) T cells in cancer and cancer immunotherapy.* Br J Cancer, 2021. **124**(2): p. 359-367.
3. Luckheeram, R.V., et al., *CD4(+)T cells: differentiation and functions.* Clin Dev Immunol, 2012. **2012**: p. 925135.
4. Davis, M.M. and P.J. Bjorkman, *T-cell antigen receptor genes and T-cell recognition.* Nature, 1988. **334**(6181): p. 395-402.
5. Nadel, B. and A.J. Feeney, *Nucleotide deletion and P addition in V(D)J recombination: a determinant role of the coding-end sequence.* Mol Cell Biol, 1997. **17**(7): p. 3768-78.
6. Glanville, J., et al., *Identifying specificity groups in the T cell receptor repertoire.* Nature, 2017. **547**(7661): p. 94-98.
7. Garcia, K.C., et al., *Structural basis of plasticity in T cell receptor recognition of a self peptide-MHC antigen.* Science, 1998. **279**(5354): p. 1166-72.
8. Wu, L.C., et al., *Two-step binding mechanism for T-cell receptor recognition of peptide MHC.* Nature, 2002. **418**(6897): p. 552-6.
9. Dutta, A., B. Zhao, and P.E. Love, *New insights into TCR β-selection.* Trends in Immunology, 2021. **42**(8): p. 735-750.
10. Klein, L., et al., *Positive and negative selection of the T cell repertoire: what thymocytes see (and don't see).* Nat Rev Immunol, 2014. **14**(6): p. 377-91.
11. Sethna, Z., et al., *Population variability in the generation and selection of T-cell repertoires.* PLoS Comput Biol, 2020. **16**(12): p. e1008394.
12. Krishna, C., et al., *Genetic and environmental determinants of human TCR repertoire diversity.* Immun Ageing, 2020. **17**: p. 26.
13. Dewitt, W.S., et al., *Human T cell receptor occurrence patterns encode immune history, genetic background, an receptor specificity.* Elife, 2018. **7**.
14. Tanno, H., et al., *Determinants governing T cell receptor α/β-chain pairing in repertoire formation of identical twins.* Proceedings of the National Academy of Sciences of the United States of America, 2020. **117**(1): p. 532-540.
15. Glanville, J., et al., *Naive antibody gene-segment frequencies are heritable and unaltered by chronic lymphocyte ablation.* Proc Natl Acad Sci U S A, 2011. **108**(50): p. 20066-71.
16. Zvyagin, I.V., et al., *Distinctive properties of identical twins' TCR repertoires revealed by high-throughput sequencing.* Proc Natl Acad Sci U S A, 2014. **111**(16): p. 5980-5.
17. Garcia, K.C., *Reconciling views on T cell receptor germline bias for MHC.* Trends Immunol, 2012. **33**(9): p. 429-36.

18. Rangarajan, S. and R.A. Mariuzza, *T cell receptor bias for MHC: co-evolution or co-receptors?* Cell Mol Life Sci, 2014. **71**(16): p. 3059-68.
19. Van Laethem, F., et al., *Deletion of CD4 and CD8 coreceptors permits generation of alphabetaT cells that recognize antigens independently of the MHC.* Immunity, 2007. **27**(5): p. 735-50.
20. La Gruta, N.L., et al., *Understanding the drivers of MHC restriction of T cell receptors.* Nat Rev Immunol, 2018. **18**(7): p. 467-478.
21. Feng, D., et al., *Structural evidence for a germline-encoded T cell receptor-major histocompatibility complex interaction 'codon'.* Nat Immunol, 2007. **8**(9): p. 975-83.
22. Pierini, F. and T.L. Lenz, *Divergent Allele Advantage at Human MHC Genes: Signatures of Past and Ongoing Selection.* Molecular Biology and Evolution, 2018. **35**(9): p. 2145-2158.
23. Penn, D.J., K. Damjanovich, and W.K. Potts, *MHC heterozygosity confers a selective advantage against multiple-strain infections.* Proc Natl Acad Sci U S A, 2002. **99**(17): p. 11260-4.
24. Migalska, M., A. Sebastian, and J. Radwan, *Major histocompatibility complex class I diversity limits the repertoire of T cell receptors.* Proc Natl Acad Sci U S A, 2019. **116**(11): p. 5021-5026.
25. Woelfing, B., et al., *Does intra-individual major histocompatibility complex diversity keep a golden mean?* Philos Trans R Soc Lond B Biol Sci, 2009. **364**(1513): p. 117-28.
26. Janeway, C. and C. Janeway, *Immunobiology : the immune system in health and disease*. 5th ed. 2001, New York: Garland Pub. xviii, 732 pages : illustrations.
27. Zarnitsyna, V.I., et al., *Estimating the diversity, completeness, and cross-reactivity of the T cell repertoire.* Front Immunol, 2013. **4**: p. 485.
28. Thierry Mora, A.W., *Quantifying lymphocyte receptor diversity.* Systems Immunology, (ed. J. Das, C. Jayaprakash), 2019.
29. Arstila, T.P., et al., *A direct estimate of the human alphabeta T cell receptor diversity.* Science, 1999. **286**(5441): p. 958-61.
30. Casrouge, A., et al., *Size estimate of the alpha beta TCR repertoire of naive mouse splenocytes.* J Immunol, 2000. **164**(11): p. 5782-7.
31. Wiegel, F.W. and A.S. Perelson, *Some scaling principles for the immune system.* Immunology and Cell Biology, 2004. **82**(2): p. 127-131.
32. Langman, R.E. and M. Cohn, *The E-T (elephant-tadpole) paradox necessitates the concept of a unit of B-cell function: the protection.* Mol Immunol, 1987. **24**(7): p. 675-97.
33. Freeman, J.D., et al., *Profiling the T-cell receptor beta-chain repertoire by massively parallel sequencing.* Genome Res, 2009. **19**(10): p. 1817-24.
34. Robins, H.S., et al., *Comprehensive assessment of T-cell receptor beta-chain diversity in alphabeta T cells.* Blood, 2009. **114**(19): p. 4099-107.
35. Wang, C., et al., *High throughput sequencing reveals a complex pattern of dynamic interrelationships among human T cell subsets.* Proc Natl Acad Sci U S A, 2010. **107**(4): p. 1518-23.
36. Han, A., et al., *Corrigendum: Linking T-cell receptor sequence to functional phenotype at the single-cell level.* Nat Biotechnol, 2015. **33**(2): p. 210.
37. Neal, J.T., et al., *Organoid Modeling of the Tumor Immune Microenvironment.* Cell, 2018. **175**(7): p. 1972-1988 e16.
38. Tu, A.A., et al., *TCR sequencing paired with massively parallel 3' RNA-seq reveals clonotypic T cell signatures.* Nat Immunol, 2019. **20**(12): p. 1692-1699.
39. Rosenberg, A.B., et al., *Single-cell profiling of the developing mouse brain and spinal cord with split-pool barcoding.* Science, 2018. **360**(6385): p. 176-182.
40. Goios, A., et al., *mtDNA phylogeny and evolution of laboratory mouse strains.* Genome Res, 2007. **17**(3): p. 293-8.
41. Morgan, A.P., et al., *Population structure and inbreeding in wild house mice (Mus musculus) at different geographic scales.* Heredity (Edinb), 2022. **129**(3): p. 183-194.
42. Yang, H., et al., *Subspecific origin and haplotype diversity in the laboratory mouse.* Nat Genet, 2011. **43**(7): p. 648-55.
43. Howie, B., et al., *High-throughput pairing of T cell receptor alpha and beta sequences.* Sci Transl Med, 2015. **7**(301): p. 301ra131.
44. Bioscience, P., *TCR Sequencing of 1 Million Primary Human T Cells in a Single Experiment*, P. Bioscience, Editor.

45. Genomics, x., *CD8+ T cells of Healthy Donor 2, (v1, 150x91), Single Cell Immune Profiling Dataset*, x. Genomics, Editor. 2019.
46. Bioscience, P., *Performance of Evercode TCR in Activated Human T Cells*.
47. Bolotin, D.A., et al., *MiXCR: software for comprehensive adaptive immunity profiling.* Nat Methods, 2015. **12**(5): p. 380-1.
48. Bosc, N. and M.P. Lefranc, *The mouse (Mus musculus) T cell receptor alpha (TRA) and delta (TRD) variable genes.* Dev Comp Immunol, 2003. **27**(6-7): p. 465-97.
49. Hou, X.L., et al., *High Throughput Sequencing of T Cell Antigen Receptors Reveals a Conserved TCR Repertoire.* Medicine, 2016. **95**(10).
50. Kitaura, K., et al., *A new high-throughput sequencing method for determining diversity and similarity of T cell receptor (TCR) alpha and beta repertoires and identifying potential new invariant TCR alpha chains.* BMC Immunol, 2016. **17**(1): p. 38.
51. Thompson, S.D., J. Pelkonen, and J.L. Hurwitz, *First T cell receptor alpha gene rearrangements during T cell ontogeny skew to the 5' region of the J alpha locus.* J Immunol, 1990. **145**(7): p. 2347-52.
52. Mahowald, G.K., et al., *Out-of-Frame T Cell Receptor Beta Transcripts Are Eliminated by Multiple Pathways.* Plos One, 2011. **6**(7).
53. Weischenfeldt, J., et al., *NMD is essential for hematopoietic stem and progenitor cells and for eliminating by-products of programmed DNA rearrangements.* Genes & Development, 2008. **22**(10): p. 1381-1396.
54. Murugan, A., et al., *Statistical inference of the generation probability of T-cell receptors from sequence repertoires.* Proc Natl Acad Sci U S A, 2012. **109**(40): p. 16161-6.
55. Sharon, E., et al., *Genetic variation in MHC proteins is associated with T cell receptor expression biases.* Nature Genetics, 2016. **48**(9): p. 995-+.
56. Logunova, N.N., et al., *MHC-II alleles shape the CDR3 repertoires of conventional and regulatory naive CD4*
T cells. Proceedings of the National Academy of Sciences of the United States of America, 2020. **117**(24): p. 13659-13669.
57. Lefranc, M.P., et al., *IMGT®, the international ImMunoGeneTics information system®.* Nucleic Acids Research, 2009. **37**: p. D1006-D1012.
58. Pai, J.A. and A.T. Satpathy, *High-throughput and single-cell T cell receptor sequencing technologies.* Nat Methods, 2021. **18**(8): p. 881-892.
59. Huang, C.Y. and O. Kanagawa, *Ordered and coordinated rearrangement of the T cell receptor α locus:: role of secondary rearrangement in thymic selection.* Faseb Journal, 2001. **15**(5): p. A1023-A1023.
60. Lawlor, D.A., et al., *Evolution of Class-I Mhc Genes and Proteins - from Natural-Selection to Thymic Selection.* Annual Review of Immunology, 1990. **8**: p. 23-63.
61. Vidovic, D. and P. Matzinger, *Unresponsiveness to a Foreign Antigen Can Be Caused by Self-Tolerance.* Nature, 1988. **336**(6196): p. 222-225.
62. Arrieta-Bolanos, E., D.I. Hernandez-Zaragoza, and R. Barquera, *An HLA map of the world: A comparison of HLA frequencies in 200 worldwide populations reveals diverse patterns for class I and class II.* Front Genet, 2023. **14**: p. 866407.
63. Argaet, V.P., et al., *Dominant Selection of an Invariant T-Cell Antigen Receptor in Response to Persistent Infection by Epstein-Barr-Virus.* Journal of Experimental Medicine, 1994. **180**(6): p. 2335-2340.
64. Day, E.K., et al., *Rapid CD8*
T cell repertoire focusing and selection of high-affinity clones into memory following primary infection with a persistent human virus:: Human Cytomegalovirus. Journal of Immunology, 2007. **179**(5): p. 3203-3213.
65. Trautmann, L., et al., *Selection of T cell clones expressing high-affinity public TCRs within human cytomegalovirus-specific CD8 T cell responses.* Journal of Immunology, 2005. **175**(9): p. 6123-6132.
66. Lewis, M.D., et al., *A reproducible method for the expansion of mouse CD8+ T lymphocytes.* J Immunol Methods, 2015. **417**: p. 134-138.
67. Martin, M., *Cutadapt removes adapter sequences from high-throughput sequencing reads.* EMBnet.journal, 2011. **17(1)**: p. pp. 10-12.

68. Smith, T., A. Heger, and I. Sudbery, *UMI-tools: modeling sequencing errors in Unique Molecular Identifiers to improve quantification accuracy.* Genome Res, 2017. **27**(3): p. 491-499.
69. Love, M.I., W. Huber, and S. Anders, *Moderated estimation of fold change and dispersion for RNA-seq data with DESeq2.* Genome Biology, 2014. **15**(12).
70. Fisher, R.A., A.S. Corbet, and C.B. Williams, *The relation between the number of species and the number of individuals in a random sample of an animal population.* Journal of Animal Ecology, 1943. **12**: p. 42-58.
71. Chiffelle, J., et al., *T-cell repertoire analysis and metrics of diversity and clonality.* Curr Opin Biotechnol, 2020. **65**: p. 284-295.
72. Shannon, C.E., *A Mathematical Theory of Communication.* Bell System Technical Journal, 1948. **27**(3): p. 379-423.
73. Metzger, B.P.H., P.J. Wittkopp, and J.D. Coolon, *Evolutionary Dynamics of Regulatory Changes Underlying Gene Expression Divergence among Species.* Genome Biology and Evolution, 2017. **9**(4): p. 843-854.

Supplement

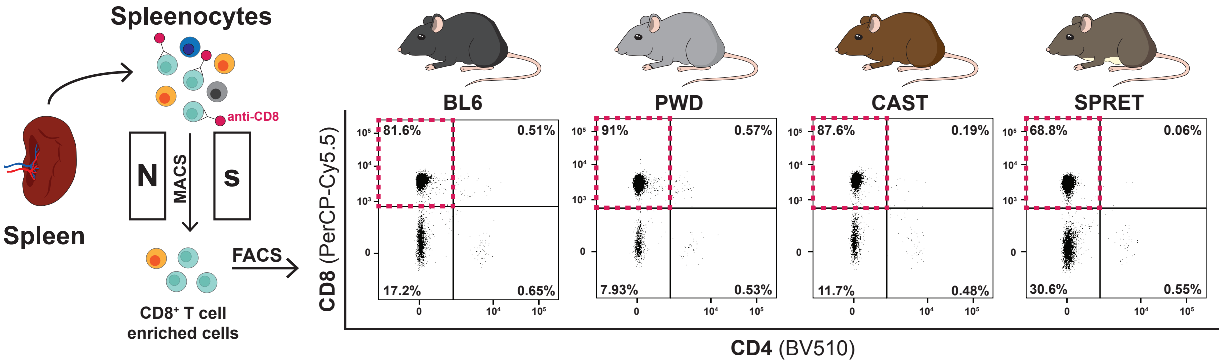

Supplementary Figure 1: CD8$^+$ T cells isolation strategy for all CITR-seq samples

(A) Spleenocyte cell-suspensions were pre-enriched for CD8$^+$ T cells by magnetic extraction of anti-CD8 labeled cells (magnetic-activated cell sorting, MACS using Dynabeads™ FlowComp™ Mouse CD8 Kit). Afterwards pre-enriched cell-suspension was further purified using fluorescence activated cell sorting (FACS). Percentages in each quadrant of the FACS plots represent the mean frequencies of the respective cell population in the pre-enriched cell-suspension. CD8$^+$ T cells in the top left quadrant (red box) were sorted and used for CITR-seq experiments.

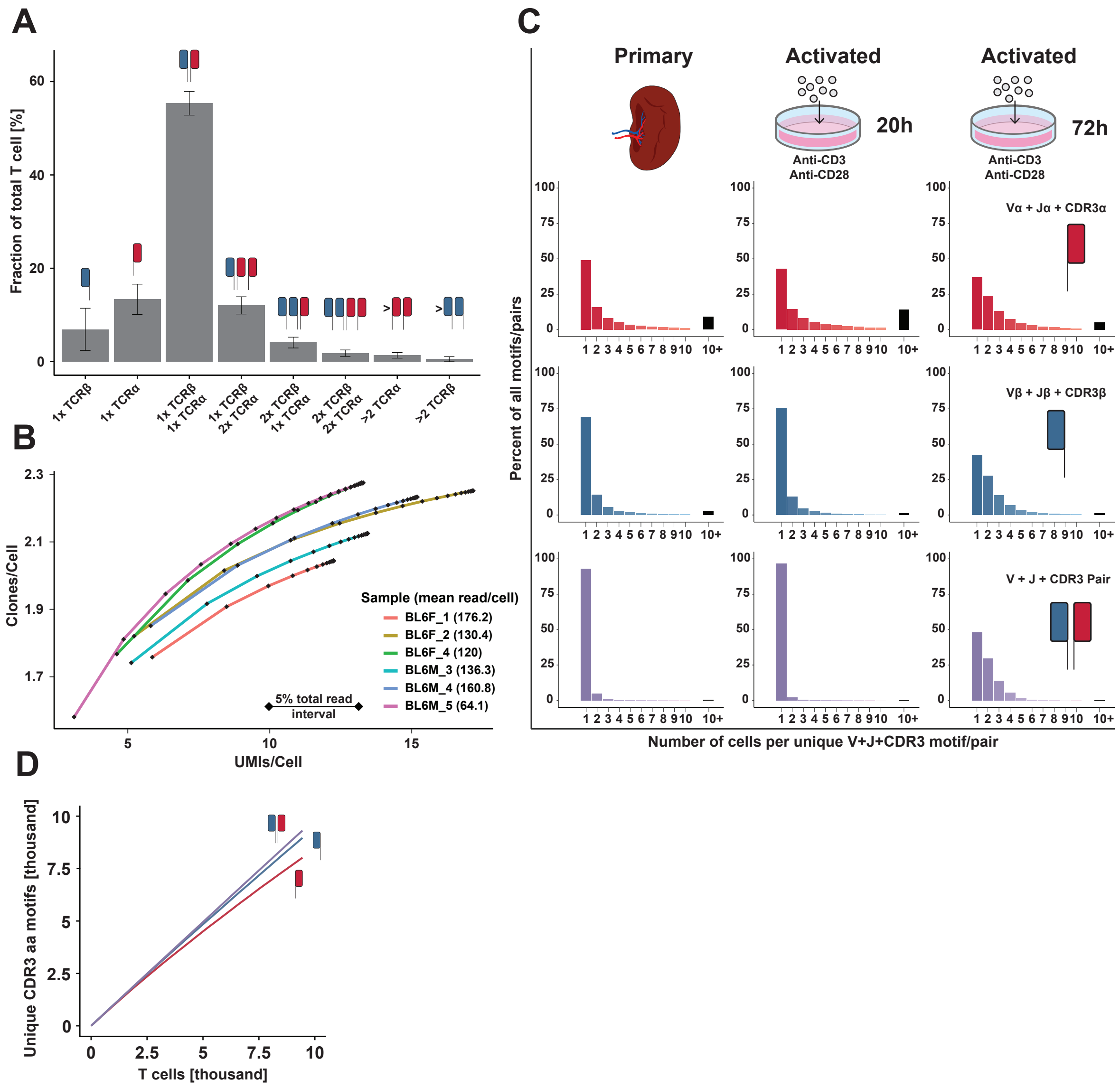

Supplementary Figure 2: Additional analysis for CITR-seq validation

(A) Mean fraction of T cells assigned to different numbers of distinct TCRα and TCRβ chains (error bars represent the standard deviation across all 32 CITR-seq samples). Most T cells (~55%) are associated with a single TCRα and a single TCRβ chain. Few T cells are associated with more than two TCRα (~1.4%) or TCRβ (~0.5%) chains, likely representing cell doublets or barcode collisions.

(B) Saturation curve showing UMI/cell and clone/cell counts relative to the fraction of total sequencing reads. Diamonds represent the respective UMI/cell and clone/cell counts at intervals of 5% of sequencing reads (5% - 100% of reads) for six representative CITR-seq samples (all BL6 samples). The mean reads per cell are shown for the representative samples.

(C) Clone size distributions (number of cells observed with a unique V+J+CDR3 TCR) in samples from primary T cells (left), 20h activated T cells (middle) and 72h activated T cells (right). The respective clone size distributions are shown for Vα+Jα+CDR3α TCRs (top), Vβ+Jβ+CDR3β TCRs (middle) or V+J+CDR3 paired αβ-TCRs (bottom). In contrast to primary and 20h activated T cells, 72h activated T cells show an increased clone size distribution caused by the onset of clonal expansion by prolonged T cell activation.

(D) Total number of unique CDR3α, CDR3β or paired CDR3αβ amino acid motifs relative to the number of T cells across all 4 samples generated using the 10x Genomics Single Cell Immune Profiling Kit.

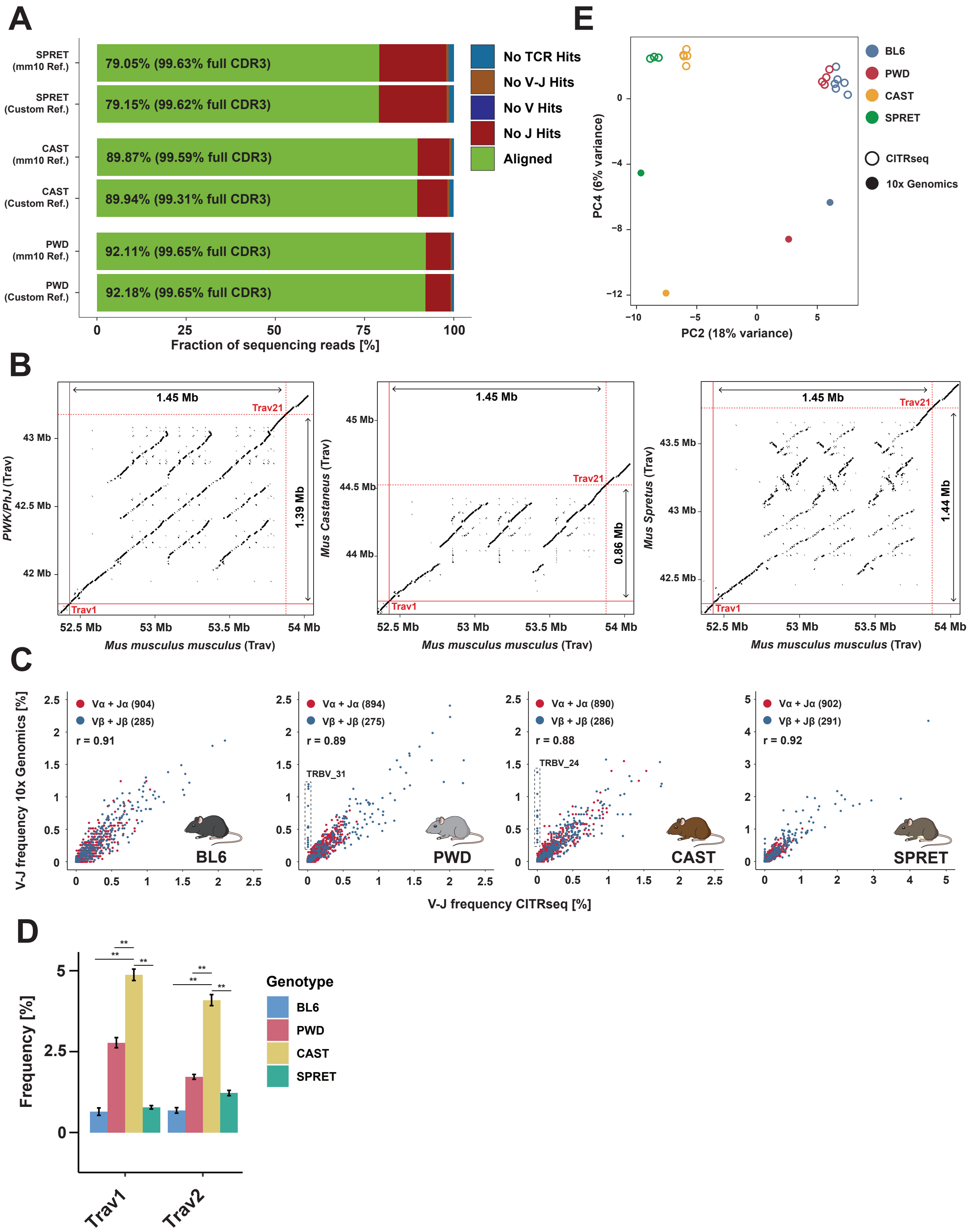
A
SPRET (mm10 Ref.)
SPRET (Custom Ref.)
CAST (mm10 Ref.)
CAST (Custom Ref.)
PWD (mm10 Ref.)
PWD (Custom Ref.)
79.05% (99.63% full CDR3)
79.15% (99.62% full CDR3)
89.87% (99.59% full CDR3)
89.94% (99.31% full CDR3)
92.11% (99.65% full CDR3)
92.18% (99.65% full CDR3)
No TCR Hits
No V-J Hits
No V Hits
No J Hits
Aligned
0
25
50
75
100
Fraction of sequencing reads [%]
E
PC4 (6% variance)
PC2 (18% variance)
0
−4
−8
−12
−10
−5
0
5
BL6
PWD
CAST
SPRET
CITRseq
10x Genomics
B
1.45 Mb
Trav21
Trav1
1.39 Mb
PWK/PhJ (Trav)
43 Mb
42.5 Mb
42 Mb
52.5 Mb
53 Mb
53.5 Mb
54 Mb
Mus musculus musculus (Trav)
1.45 Mb
Trav21
Trav1
0.86 Mb
Mus Castaneus (Trav)
45 Mb
44.5 Mb
44 Mb
52.5 Mb
53 Mb
53.5 Mb
54 Mb
Mus musculus musculus (Trav)
1.45 Mb
Trav21
Trav1
1.44 Mb
Mus Spretus (Trav)
43.5 Mb
43 Mb
42.5 Mb
52.5 Mb
53 Mb
53.5 Mb
54 Mb
Mus musculus musculus (Trav)
C
V-J frequency 10x Genomics [%]
Vα + Jα (904)
Vβ + Jβ (285)
r = 0.91
BL6
Vα + Jα (894)
Vβ + Jβ (275)
r = 0.89
TRBV_31
PWD
Vα + Jα (890)
Vβ + Jβ (286)
r = 0.88
TRBV_24
CAST
Vα + Jα (902)
Vβ + Jβ (291)
r = 0.92
SPRET
0
0.5
1
1.5
2
2.5
3
4
5
V-J frequency CITRseq [%]
D
Frequency [%]
**
**
**
**
**
**
5
2.5
0
Trav1
Trav2
Genotype
BL6
PWD
CAST
SPRET

Supplementary Figure 3: Different structure of TCRα loci across inbred species and comparison of observed V-J usage frequencies in different methods

(A) Fraction of sequencing reads that were successfully aligned to V(D)J genes using different reference libraries (green bars; full CDR3 coverage in brackets). Each stacked bar shows the mapping percentage for a representative sample from SPRET, CAST and PWD when aligned to the in-build mm10 based MiXCR V(D)J reference (top) and the species-specific custom V(D)J reference (see methods). All other colors in the stacked bar represent the reason for the failure of alignment. In all cases, the total fraction of successfully aligned reads is higher when using the species-specific custom library.

(B) Dot plots of local alignment of genomic sequence from the GRCm38/mm10 TCR Vα locus to the PWK/PhJ (closest available genomic sequence to PWD, left), CAST (middle) and SPRET (right) genomic sequence of the TCR Vα locus. Intersections of the red lines indicate the location of the most distal (*Trav1*) and proximal (*Trav21*, dashed line) Vα genes. The genomic distances between these two Vα genes are shown. The central region of the Vα cluster is triplicated in BL6, PWK and SPRET relative to CAST.

(C) Dot plots showing the mean frequency of single-chain V-J pairing in TCRα (red) and TCRβ (blue) chains observed in samples generated with -seq and 10x Genomics Single Cell Immune Profiling. The respective frequencies are shown for BL6, PWD, CAST and SPRET samples. Pearson-correlation and the total number of detected Vα-Jα and Vβ-Jβ are shown. Boxes highlight Vβ genes that are almost exclusively observed in 10x Genomics samples indicating failure of amplification for these Vβ genes by the multiple PCR primer pool used in CITR-seq. The respective Vβ genes were excluded from the analysis.

(D) Usage frequencies of distal (5') Vα genes (*Trav1*, *Trav2)* with one-to-one orthology across all four species. CAST mice have significantly higher frequencies of both genes compared to all other species (chi-squared test, ** *P-value* < 0.01).

(E) PCA of combined Vα-Jα and Vβ-Jβ gene segment usage frequencies across all species as observed in samples generated with CITR-seq (empty circle) or 10x Genomics Single Cell Immune Profiling (filled circles). PC2 and PC4 are shown. PC4 contains 6% of the total variance across samples and separates samples by the respective methods used to generate the data.

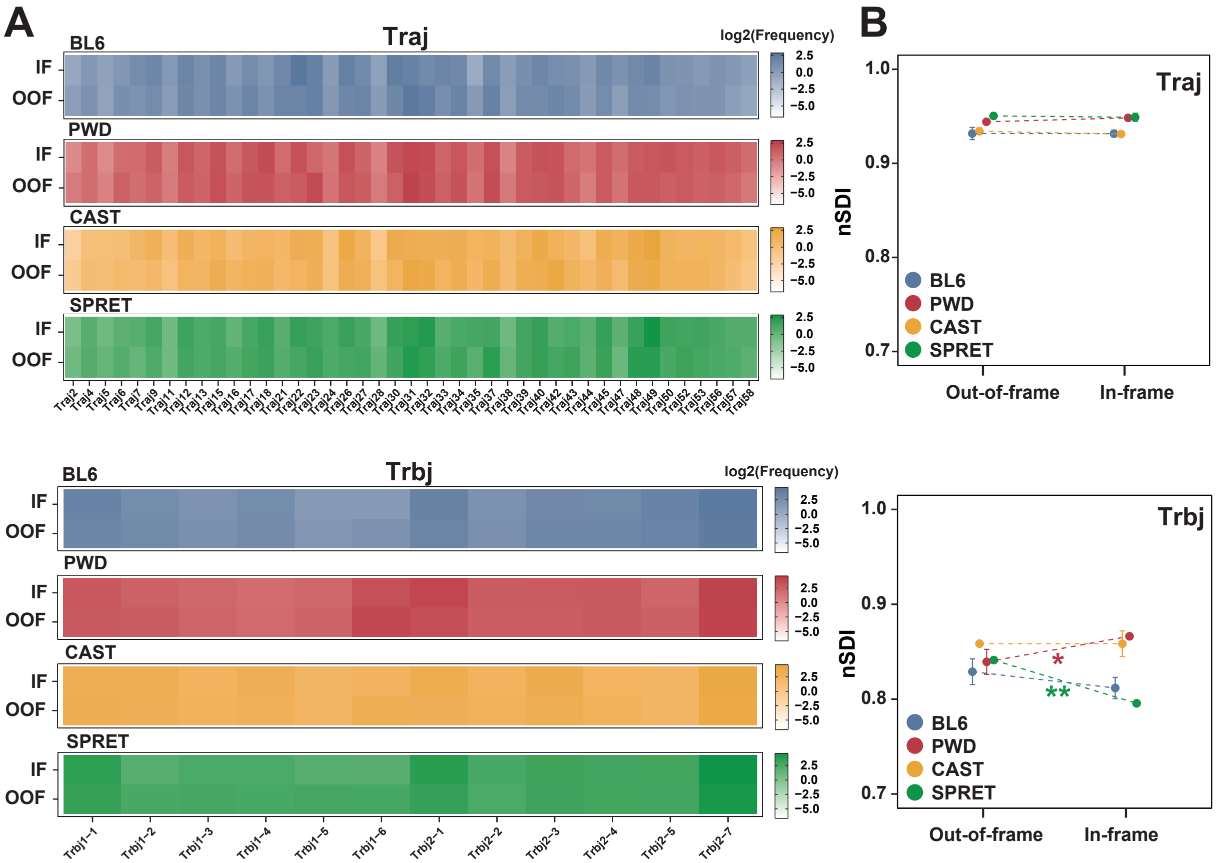

Supplementary Figure 4: Comparison of Jα and Jβ gene usage in in-frame and out-of-frame TCRs

- **(A)** Jα family (top) and Jβ gene (bottom) usage frequency ($\log_2$) heatmaps. Heatmaps show the mean intra-species J-usage in in-frame (IF) and out-of-frame (OOF) TCRs across all T cells.
- **(B)** Mean intra-species entropy in Jα-usage (top) and Jβ-usage (bottom) distributions calculated using the normalized Shannon diversity index (nSDI) for OOF and IF TCRs (error bars indicate the standard deviation in species replicates, significance calculated using paired t-test, * *P-value* < 0.05, ** *P-value* < 0.01).

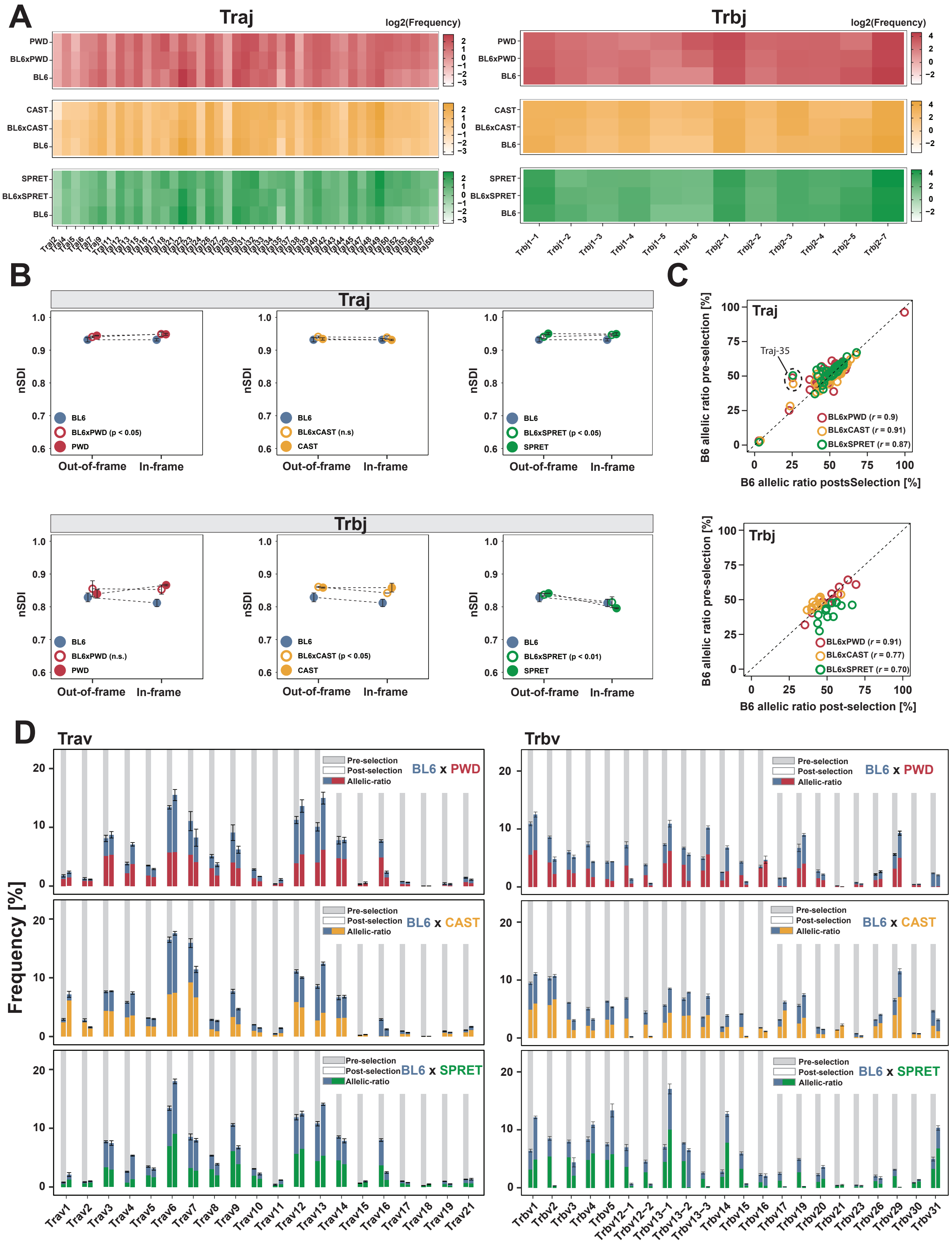
A
Traj
log2(Frequency)
PWD
BL6xPWD
BL6
CAST
BL6xCAST
BL6
SPRET
BL6xSPRET
BL6
2
1
0
−1
−2
−3
Traj2 Traj4 Traj5 Traj6 Traj7 Traj9 Traj11 Traj12 Traj13 Traj15 Traj16 Traj17 Traj18 Traj21 Traj22 Traj23 Traj24 Traj26 Traj27 Traj28 Traj30 Traj31 Traj32 Traj33 Traj34 Traj35 Traj37 Traj38 Traj39 Traj40 Traj42 Traj43 Traj44 Traj45 Traj47 Traj48 Traj49 Traj50 Traj52 Traj53 Traj56 Traj57 Traj58
Trbj
log2(Frequency)
4
2
0
−2
Trbj1−1 Trbj1−2 Trbj1−3 Trbj1−4 Trbj1−5 Trbj1−6 Trbj2−1 Trbj2−2 Trbj2−3 Trbj2−4 Trbj2−5 Trbj2−7
B
Traj
nSDI
1.0
0.9
0.8
0.7
0.6
BL6
BL6xPWD (p < 0.05)
PWD
BL6xCAST (n.s)
CAST
BL6xSPRET (p < 0.05)
SPRET
Out-of-frame
In-frame
Trbj
BL6xPWD (n.s.)
BL6xCAST (p < 0.05)
BL6xSPRET (p < 0.01)
C
Traj
Traj-35
B6 allelic ratio pre-selection [%]
B6 allelic ratio postsSelection [%]
0
25
50
75
100
BL6xPWD (r = 0.9)
BL6xCAST (r = 0.91)
BL6xSPRET (r = 0.87)
Trbj
B6 allelic ratio post-selection [%]
BL6xPWD (r = 0.91)
BL6xCAST (r = 0.77)
BL6xSPRET (r = 0.70)
D
Trav
Trbv
Frequency [%]
0
10
20
Pre-selection
Post-selection
Allelic-ratio
BL6 x PWD
BL6 x CAST
BL6 x SPRET
Trav1 Trav2 Trav3 Trav4 Trav5 Trav6 Trav7 Trav8 Trav9 Trav10 Trav11 Trav12 Trav13 Trav14 Trav15 Trav16 Trav17 Trav18 Trav19 Trav21
Trbv1 Trbv2 Trbv3 Trbv4 Trbv5 Trbv12−1 Trbv12−2 Trbv13−1 Trbv13−2 Trbv13−3 Trbv14 Trbv15 Trbv16 Trbv17 Trbv19 Trbv20 Trbv21 Trbv23 Trbv26 Trbv29 Trbv30 Trbv31

Supplementary Figure 5: Usage frequencies of Jα and Jβ genes in F1 hybrids and the impact of thymic selection on their abundance

- **(A)** Jα gene (left) and Jβ gene (right) usage frequency ($\log_2$) heatmaps of in-frame TCRs in F1 hybrids and their respective parental species.
- **(B)** Comparison of entropy of J-usage distribution in F1 hybrids and the respective parental species calculated using the normalized Shannon diversity index (nSDI) for OOF (left) and IF (right) TCRs (error bars indicate the standard deviation in species replicates, significance tested for F1 hybrid IF vs OOF contrast using paired t-tests).
- **(C)** Analysis of biased J gene allele usage in F1 hybrids. Plots show the percentage of BL6 Jα gene alleles and Jβ gene alleles in post- (x-axis) and pre-selection (y-axis) TCRs. Each circle represents a Jα-gene (top) or Jβ-gene (bottom). Pearson-correlation was calculated for post- and pre-selection J gene usage. Genes with substantial changes in allelic ratios in pre- and post-selection repertoires are highlighted (*Traj35*).
- **(D)** Detailed representation of the mean Vα-family and Vβ-gene usage frequencies in F1 hybrids in pre-selection (grey background) and post-selection (white background) TCRs. Stacked bars show the allelic ratio in the respective V-gene/family (error bars indicate the standard deviation in species replicates).

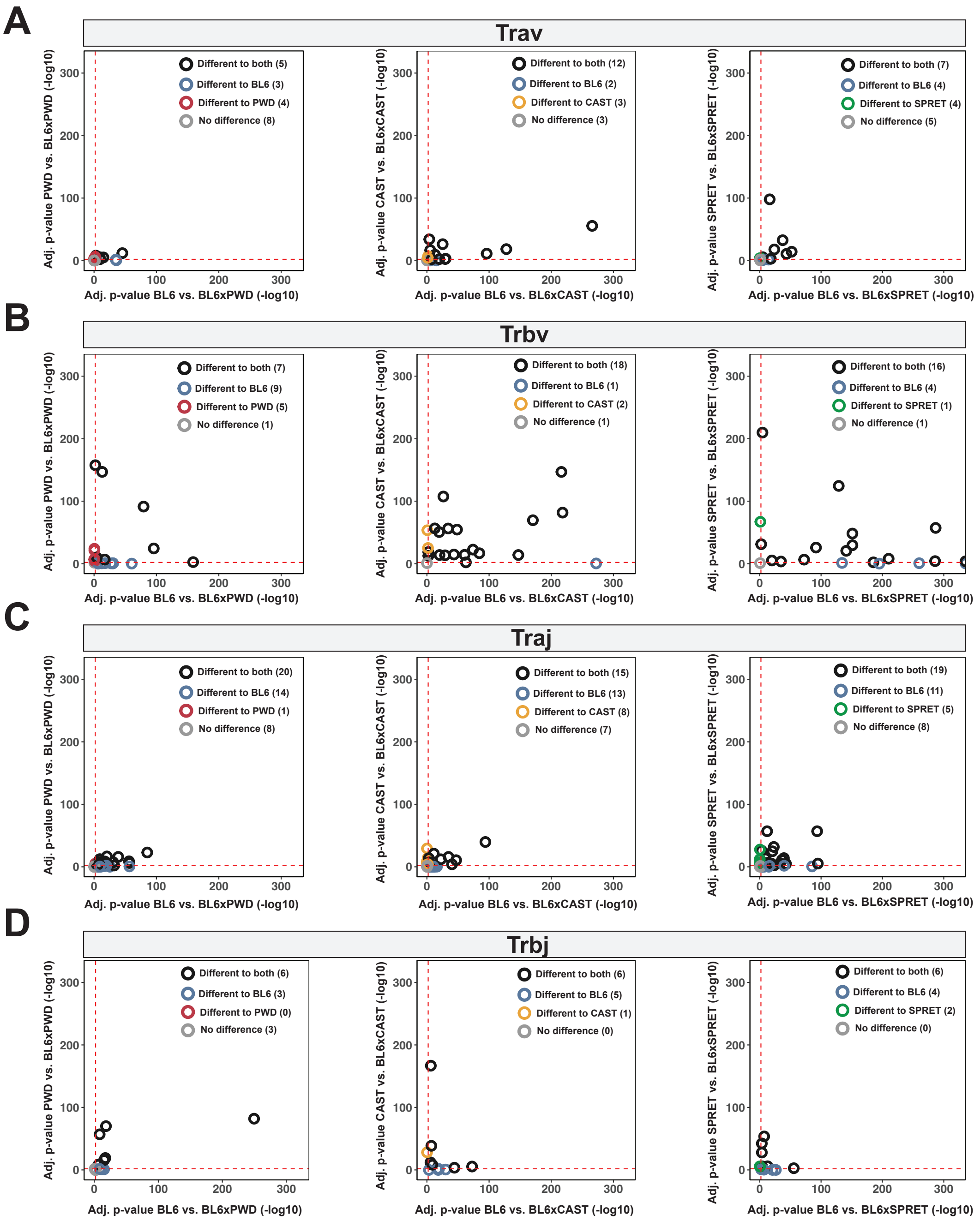

Supplementary Figure 6: *P-values* (-log$_{10}$) of V/J gene usage frequency changes in F1 hybrids relative to both parents

Adjusted *P-values* for V and J gene frequency changes in F1 hybrids relative to their parents. Plots show *P-values* for BL6xPWD (left), BL6xCAST (middle) and BL6xSPRET (right) for Vα-families **(A)**, Vβ-genes **(B)**, Jα-genes **(C)** and Jβ-genes **(D)**. *P-values* have been calculated for differences in absolute count of TCRs with the respective V/J genes using Wald-test. Dashed red lines show that *P-value* cut-off of $P < 0.01$. Genes with significant ($P < 0.01$) changes relative to both parents (empty black circles), to the BL6 parent (empty blue circles), the respective other parent (PWD, CAST, SPRET, empty red, yellow, green circles) as well as genes with no differences to both parents (empty grey circles) are shown with the respective total counts of genes in each category.

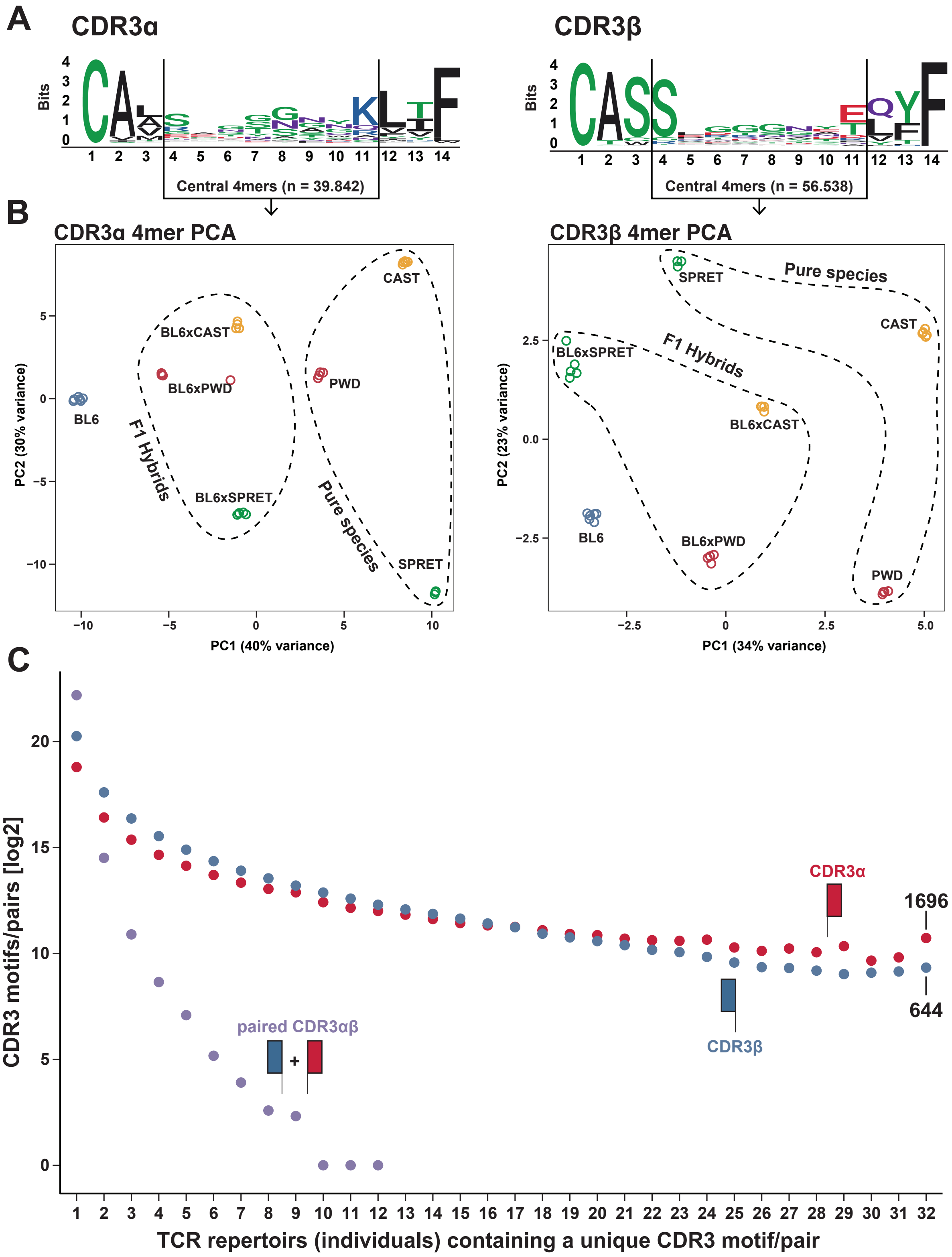
A
CDR3α
Bits
4
3
2
1
0
1 2 3 4 5 6 7 8 9 10 11 12 13 14
Central 4mers (n = 39.842)
CDR3β
Bits
4
3
2
1
0
1 2 3 4 5 6 7 8 9 10 11 12 13 14
Central 4mers (n = 56.538)
B
CDR3α 4mer PCA
CAST
BL6xCAST
BL6xPWD
PWD
BL6
F1 Hybrids
BL6xSPRET
Pure species
SPRET
PC2 (30% variance)
5
0
−5
−10
−10 −5 0 5 10
PC1 (40% variance)
CDR3β 4mer PCA
SPRET
Pure species
CAST
BL6xSPRET
F1 Hybrids
BL6xCAST
BL6
BL6xPWD
PWD
PC2 (23% variance)
2.5
0.0
−2.5
−2.5 0 2.5 5.0
PC1 (34% variance)
C
CDR3 motifs/pairs [log2]
20
15
10
5
0
CDR3α
1696
644
CDR3β
paired CDR3αβ
+
1 2 3 4 5 6 7 8 9 10 11 12 13 14 15 16 17 18 19 20 21 22 23 24 25 26 27 28 29 30 31 32
TCR repertoirs (individuals) containing a unique CDR3 motif/pair

Supplementary Figure 7: Comparison of single-chain CDR3α and CDR3β amino acid motifs in all 32 CITR-seq samples

- **(A)** Positional diversity of amino acids in 10,000 randomly chosen CDR3α (left) and CDR3β (right) single-chain motifs from all 32 CITRs-eq samples. Black lines mark the central region of CDR3 motifs. Three 4mers were randomly selected from this central region of all CDR3 sequences across the 32 individuals. The filtered count-matrix of 4mers (see methods) contained 39,842 unique CDR3α and 56,538 unique CDR3β 4mers.
- **(B)** PCA analysis done using the 4mer count-matrices of CDR3α 4mers (left) and CDR3β 4mers (right). PC1 and PC2 are shown. 4mer samples cluster by genotype of the underlying sample.
- **(C)** Number of TCR repertoires (of individuals) in which each unique CDR3α (red), CDR3β (blue) or paired CDR3αβ (purple) motif is observed. 1,696 CDR3α motifs and 644 CDR3β motifs have been observed in TCR repertoires of every single individual analyzed in this study. Identical CDR3αβ motifs have not been observed in more than 12 individuals.

Supplementary Table 1: Detailed sample list of all 32 CITR-seq samples analyzed in the present study.

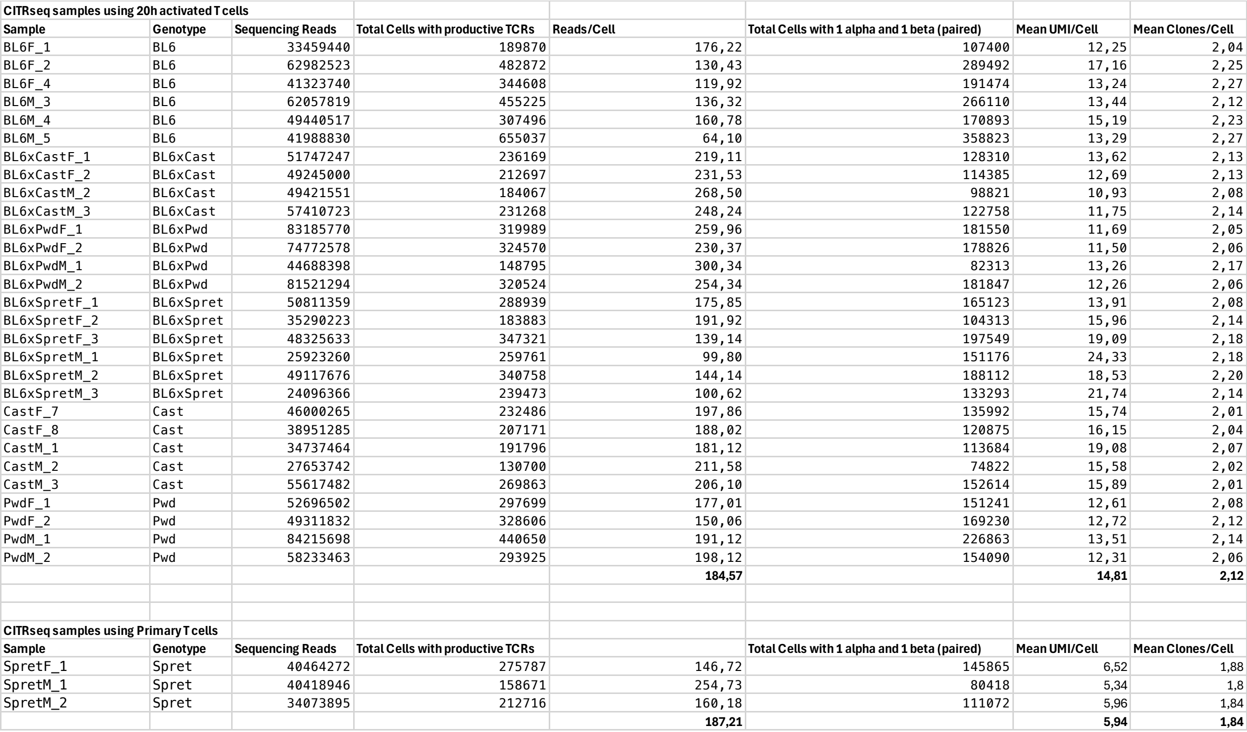

CITRseq samples using 20h activated T cells							
Sample	**Genotype**	**Sequencing Reads**	**Total Cells with productive TCRs**	**Reads/Cell**	**Total Cells with 1 alpha and 1 beta (paired)**	**Mean UMI/Cell**	**Mean Clones/Cell**
BL6F_1	BL6	33459440	189870	176,22	107400	12,25	2,04
BL6F_2	BL6	62982523	482872	130,43	289492	17,16	2,25
BL6F_4	BL6	41323740	344608	119,92	191474	13,24	2,27
BL6M_3	BL6	62057819	455225	136,32	266110	13,44	2,12
BL6M_4	BL6	49440517	307496	160,78	170893	15,19	2,23
BL6M_5	BL6	41988830	655037	64,10	358823	13,29	2,27
BL6xCastF_1	BL6xCast	51747247	236169	219,11	128310	13,62	2,13
BL6xCastF_2	BL6xCast	49245000	212697	231,53	114385	12,69	2,13
BL6xCastM_2	BL6xCast	49421551	184067	268,50	98821	10,93	2,08
BL6xCastM_3	BL6xCast	57410723	231268	248,24	122758	11,75	2,14
BL6xPwdF_1	BL6xPwd	83185770	319989	259,96	181550	11,69	2,05
BL6xPwdF_2	BL6xPwd	74772578	324570	230,37	178826	11,50	2,06
BL6xPwdM_1	BL6xPwd	44688398	148795	300,34	82313	13,26	2,17
BL6xPwdM_2	BL6xPwd	81521294	320524	254,34	181847	12,26	2,06
BL6xSpretF_1	BL6xSpret	50811359	288939	175,85	165123	13,91	2,08
BL6xSpretF_2	BL6xSpret	35290223	183883	191,92	104313	15,96	2,14
BL6xSpretF_3	BL6xSpret	48325633	347321	139,14	197549	19,09	2,18
BL6xSpretM_1	BL6xSpret	25923260	259761	99,80	151176	24,33	2,18
BL6xSpretM_2	BL6xSpret	49117676	340758	144,14	188112	18,53	2,20
BL6xSpretM_3	BL6xSpret	24096366	239473	100,62	133293	21,74	2,14
CastF_7	Cast	46000265	232486	197,86	135992	15,74	2,01
CastF_8	Cast	38951285	207171	188,02	120875	16,15	2,04
CastM_1	Cast	34737464	191796	181,12	113684	19,08	2,07
CastM_2	Cast	27653742	130700	211,58	74822	15,58	2,02
CastM_3	Cast	55617482	269863	206,10	152614	15,89	2,01
PwdF_1	Pwd	52696502	297699	177,01	151241	12,61	2,08
PwdF_2	Pwd	49311832	328606	150,06	169230	12,72	2,12
PwdM_1	Pwd	84215698	440650	191,12	226863	13,51	2,14
PwdM_2	Pwd	58233463	293925	198,12	154090	12,31	2,06
				184,57		**14,81**	**2,12**
CITRseq samples using Primary T cells							
Sample	**Genotype**	**Sequencing Reads**	**Total Cells with productive TCRs**		**Total Cells with 1 alpha and 1 beta (paired)**	**Mean UMI/Cell**	**Mean Clones/Cell**
SpretF_1	Spret	40464272	275787	146,72	145865	6,52	1,88
SpretM_1	Spret	40418946	158671	254,73	80418	5,34	1,8
SpretM_2	Spret	34073895	212716	160,18	111072	5,96	1,84
				187,21		**5,94**	**1,84**

Supplementary Table 2: List of all DNA oligos and PCR primers used in the present study

T cell receptor alpha V-segment primers		
Target	**Protocol Step**	**Sequence**
Trav1	Multiplex-PCR	TCGTCGGCAGCGTCAGATGTGTATAAGAGACAGGGTTATCCTGGTACCAGCAAC
Trav2	Multiplex-PCR	TCGTCGGCAGCGTCAGATGTGTATAAGAGACAGCCAGGGACCACAGTTTATCATTC
Trav3.1	Multiplex-PCR	TCGTCGGCAGCGTCAGATGTGTATAAGAGACAGTTATCATCTGCACCTACACAGAC
Trav3.2	Multiplex-PCR	TCGTCGGCAGCGTCAGATGTGTATAAGAGACAGCTCCTCACCTGAGTGTCC
Trav4.1	Multiplex-PCR	TCGTCGGCAGCGTCAGATGTGTATAAGAGACAGTCAAGGAACAAAGGAGAATGGAAG
Trav4.2	Multiplex-PCR	TCGTCGGCAGCGTCAGATGTGTATAAGAGACAGATTCTGTGGGTGCAGATTTGC
Trav4.3	Multiplex-PCR	TCGTCGGCAGCGTCAGATGTGTATAAGAGACAGCAGGAACAAAGGAGAATGGGAG
Trav5.1	Multiplex-PCR	TCGTCGGCAGCGTCAGATGTGTATAAGAGACAGGGAGAGAATCCTAAGCTCATCATTG
Trav5.2	Multiplex-PCR	TCGTCGGCAGCGTCAGATGTGTATAAGAGACAGGAAGCGTCTTCAGTTCATCATAGAC
Trav6.1	Multiplex-PCR	TCGTCGGCAGCGTCAGATGTGTATAAGAGACAGAGCAGAGGTTTTGAAGCTACATATG
Trav6.2	Multiplex-PCR	TCGTCGGCAGCGTCAGATGTGTATAAGAGACAGCCCTCTCAGAAGAGGACTTTC
Trav6.3	Multiplex-PCR	TCGTCGGCAGCGTCAGATGTGTATAAGAGACAGGGAGATTCCGTGACTCAAACAG
Trav6.4	Multiplex-PCR	TCGTCGGCAGCGTCAGATGTGTATAAGAGACAGCAGAAAGCCTCAGTGCAGG
Trav6.5	Multiplex-PCR	TCGTCGGCAGCGTCAGATGTGTATAAGAGACAGCAAAGGCCAACGAGAAGGG
Trav7	Multiplex-PCR	TCGTCGGCAGCGTCAGATGTGTATAAGAGACAGAGCAGAGCCCAGAATCCC
Trav8.1	Multiplex-PCR	TCGTCGGCAGCGTCAGATGTGTATAAGAGACAGGGGTGAAAGTGTCACGGTG
Trav8.1	Multiplex-PCR	TCGTCGGCAGCGTCAGATGTGTATAAGAGACAGGGGAGAAGAGAATCTTCAGGC
Trav9.1	Multiplex-PCR	TCGTCGGCAGCGTCAGATGTGTATAAGAGACAGCTCCAGTTTCTCCTCAAGTACTATTC
Trav9.2	Multiplex-PCR	TCGTCGGCAGCGTCAGATGTGTATAAGAGACAGCAGTGCTGGGGATACACTTT
Trav9.3	Multiplex-PCR	TCGTCGGCAGCGTCAGATGTGTATAAGAGACAGACCTTATCTGTTCTGGTATGTCCA
Trav10	Multiplex-PCR	TCGTCGGCAGCGTCAGATGTGTATAAGAGACAGCAACTGCACTTACACAGATACTGC
Trav11	Multiplex-PCR	TCGTCGGCAGCGTCAGATGTGTATAAGAGACAGAAGATGCTAAGCACAGCACG
Trav12.1	Multiplex-PCR	TCGTCGGCAGCGTCAGATGTGTATAAGAGACAGCAGACAGAAGGCCTGGTC
Trav12.2	Multiplex-PCR	TCGTCGGCAGCGTCAGATGTGTATAAGAGACAGCAGAAGGAAGGCCTGGTC
Trav12.3	Multiplex-PCR	TCGTCGGCAGCGTCAGATGTGTATAAGAGACAGCTGAACTGCACCTATCAGACT
Trav13.1	Multiplex-PCR	TCGTCGGCAGCGTCAGATGTGTATAAGAGACAGCAGCTCTTTGCACATTTCCTC
Trav13.2	Multiplex-PCR	TCGTCGGCAGCGTCAGATGTGTATAAGAGACAGCTCTTTGCACATTTCCTCCTCC
Trav13.3	Multiplex-PCR	TCGTCGGCAGCGTCAGATGTGTATAAGAGACAGGAGAACGCAGAGCTGCA
Trav13.4	Multiplex-PCR	TCGTCGGCAGCGTCAGATGTGTATAAGAGACAGGGAGAATGCAGAGCTGCAG
Trav14.1	Multiplex-PCR	TCGTCGGCAGCGTCAGATGTGTATAAGAGACAGTCTCTGACAGTCTGGGAAGG
Trav14.2	Multiplex-PCR	TCGTCGGCAGCGTCAGATGTGTATAAGAGACAGAAGGAAGATGGACGATTCACAA
Trav15	Multiplex-PCR	TCGTCGGCAGCGTCAGATGTGTATAAGAGACAGGTGGCCTTGGCTTTCTCT
Trav16.1	Multiplex-PCR	TCGTCGGCAGCGTCAGATGTGTATAAGAGACAGTTCCTTATTCGTCAGGACTCTTACA
Trav16.2	Multiplex-PCR	TCGTCGGCAGCGTCAGATGTGTATAAGAGACAGGCTGATTCTAAGCCTGTTGGG
Trav17	Multiplex-PCR	TCGTCGGCAGCGTCAGATGTGTATAAGAGACAGCCTGGAGCTCAGATGCAG
Trav18	Multiplex-PCR	TCGTCGGCAGCGTCAGATGTGTATAAGAGACAGGTTTCTGAGTATCCAGGAGGG
Trav19	Multiplex-PCR	TCGTCGGCAGCGTCAGATGTGTATAAGAGACAGCATCGCTGACTGTTCAAGAGG
Trav21	Multiplex-PCR	TCGTCGGCAGCGTCAGATGTGTATAAGAGACAGCCAATAGTATGGCTTTCCTGGC
Trav23	Multiplex-PCR	TCGTCGGCAGCGTCAGATGTGTATAAGAGACAGGCTCTGGTATAGACAAGATCTGG

T cell receptor beta V-segment primers		
Target	**Protocol Step**	**Sequence**
Trb1	Multiplex-PCR	TCGTCGGCAGCGTCAGATGTGTATAAGAGACAGCAGTATCCCTGGATGAGCTG
Trb2	Multiplex-PCR	TCGTCGGCAGCGTCAGATGTGTATAAGAGACAGTATGGACAATCAGACTGCCTC
Trb3	Multiplex-PCR	TCGTCGGCAGCGTCAGATGTGTATAAGAGACAGGATATGGGGCAGATGGTGAC
Trb4	Multiplex-PCR	TCGTCGGCAGCGTCAGATGTGTATAAGAGACAGGACGGCTGTTTTCCAGACTC
Trb5	Multiplex-PCR	TCGTCGGCAGCGTCAGATGTGTATAAGAGACAGGCCAGAGCTCATGTTTCTCT
Trb12	Multiplex-PCR	TCGTCGGCAGCGTCAGATGTGTATAAGAGACAGCCAGCAGATTCTCAGTCCAAC
Trb13	Multiplex-PCR	TCGTCGGCAGCGTCAGATGTGTATAAGAGACAGATGTACTGGTATCGGCAGGAC
Trb14	Multiplex-PCR	TCGTCGGCAGCGTCAGATGTGTATAAGAGACAGCTCCCAGATATGCAGTCCTAC
Trb15	Multiplex-PCR	TCGTCGGCAGCGTCAGATGTGTATAAGAGACAGAGTGTGAGCCAGTTTCAGG
Trb16	Multiplex-PCR	TCGTCGGCAGCGTCAGATGTGTATAAGAGACAGCAACAAATGCTGGTGTCATCC
Trb17	Multiplex-PCR	TCGTCGGCAGCGTCAGATGTGTATAAGAGACAGTTGAACAGGGAAGCTGACAC
Trb19	Multiplex-PCR	TCGTCGGCAGCGTCAGATGTGTATAAGAGACAGCTGGTACCGACAGGATTCAG
Trb20	Multiplex-PCR	TCGTCGGCAGCGTCAGATGTGTATAAGAGACAGAGCTTGGTATCGTCAATCGC
Trb21	Multiplex-PCR	TCGTCGGCAGCGTCAGATGTGTATAAGAGACAGCAAGAAACCGGGAGAAGAACTC
Trb23	Multiplex-PCR	TCGTCGGCAGCGTCAGATGTGTATAAGAGACAGTCAACAGCCTCTTGATCAAATAGAC
Trb26	Multiplex-PCR	TCGTCGGCAGCGTCAGATGTGTATAAGAGACAGGATGAGGTGTATCCCTGAAAAGG
Trb29	Multiplex-PCR	TCGTCGGCAGCGTCAGATGTGTATAAGAGACAGGTACTGGTATCGACAAGACCC
Trb30	Multiplex-PCR	TCGTCGGCAGCGTCAGATGTGTATAAGAGACAGGGGACATCTGTCAAAGTGGC
Trb31	Multiplex-PCR	TCGTCGGCAGCGTCAGATGTGTATAAGAGACAGCTAACCTCTACTGGTACTGGC

T cell receptor constant region primers		
Target	**Protocol Step**	**Sequence**
TCR Constant Alpha	Reverse Transcription	/5Phos/GGGCTCGGAGATGTGTATAAGAGACAGNNNNNNNNNN**AACC**CACAGCAGGTTCTGGGTTCTG
TCR Constant Beta	Reverse Transcription	/5Phos/GGGCTCGGAGATGTGTATAAGAGACAGNNNNNNNNNN**AACC**TTGGGTGGAGTCACATTTCTCAGATC
TCR Constant Alpha	Reverse Transcription	/5Phos/GGGCTCGGAGATGTGTATAAGAGACAGNNNNNNNNNN**GTCA**CACAGCAGGTTCTGGGTTCTG
TCR Constant Beta	Reverse Transcription	/5Phos/GGGCTCGGAGATGTGTATAAGAGACAGNNNNNNNNNN**GTCA**TTGGGTGGAGTCACATTTCTCAGATC
TCR Constant Alpha	Reverse Transcription	/5Phos/GGGCTCGGAGATGTGTATAAGAGACAGNNNNNNNNNN**TGCT**CACAGCAGGTTCTGGGTTCTG
TCR Constant Beta	Reverse Transcription	/5Phos/GGGCTCGGAGATGTGTATAAGAGACAGNNNNNNNNNN**TGCT**TTGGGTGGAGTCACATTTCTCAGATC
TCR Constant Alpha	Reverse Transcription	/5Phos/GGGCTCGGAGATGTGTATAAGAGACAGNNNNNNNNNN**CGAA**CACAGCAGGTTCTGGGTTCTG
TCR Constant Beta	Reverse Transcription	/5Phos/GGGCTCGGAGATGTGTATAAGAGACAGNNNNNNNNNN**CGAA**TTGGGTGGAGTCACATTTCTCAGATC
TCR Constant Alpha	Reverse Transcription	/5Phos/GGGCTCGGAGATGTGTATAAGAGACAGNNNNNNNNNN**ACGA**CACAGCAGGTTCTGGGTTCTG
TCR Constant Beta	Reverse Transcription	/5Phos/GGGCTCGGAGATGTGTATAAGAGACAGNNNNNNNNNN**ACGA**TTGGGTGGAGTCACATTTCTCAGATC
TCR Constant Alpha	Reverse Transcription	/5Phos/GGGCTCGGAGATGTGTATAAGAGACAGNNNNNNNNNN**GAAG**CACAGCAGGTTCTGGGTTCTG
TCR Constant Beta	Reverse Transcription	/5Phos/GGGCTCGGAGATGTGTATAAGAGACAGNNNNNNNNNN**GAAG**TTGGGTGGAGTCACATTTCTCAGATC
TCR Constant Alpha	Reverse Transcription	/5Phos/GGGCTCGGAGATGTGTATAAGAGACAGNNNNNNNNNN**TTGG**CACAGCAGGTTCTGGGTTCTG
TCR Constant Beta	Reverse Transcription	/5Phos/GGGCTCGGAGATGTGTATAAGAGACAGNNNNNNNNNN**TTGG**TTGGGTGGAGTCACATTTCTCAGATC
TCR Constant Alpha	Reverse Transcription	/5Phos/GGGCTCGGAGATGTGTATAAGAGACAGNNNNNNNNNN**AGTG**CACAGCAGGTTCTGGGTTCTG
TCR Constant Beta	Reverse Transcription	/5Phos/GGGCTCGGAGATGTGTATAAGAGACAGNNNNNNNNNN**AGTG**TTGGGTGGAGTCACATTTCTCAGATC

Description:

Barcoded RT oligos (8 different barcode pairs for alpha/beta in **bold**). Oligos anneal to the 5' end of TCR alpha and TCR beta constant regions

Round1_081	/5Phos/GTGTGCTGTCTCGT	TACACATCTCCGAGCCCACGAGACAGCACACTCT
Round1_082	/5Phos/CATTGCCGTCTCGT	TACACATCTCCGAGCCCACGAGACGGCAATGTCT
Round1_083	/5Phos/CATGTGAGTCTCGT	TACACATCTCCGAGCCCACGAGACTCACATGTCT
Round1_084	/5Phos/TGGTAACGTCTCGT	TACACATCTCCGAGCCCACGAGACGTTACCATCT
Round1_085	/5Phos/ATGGAACGTCTCGT	TACACATCTCCGAGCCCACGAGACGTTCCATTCT
Round1_086	/5Phos/AACGACAGTCTCGT	TACACATCTCCGAGCCCACGAGACTGTCGTTTCT
Round1_087	/5Phos/GTTAACCGTCTCGT	TACACATCTCCGAGCCCACGAGACGGTTAACTCT
Round1_088	/5Phos/GAACTGGGTCTCGT	TACACATCTCCGAGCCCACGAGACCCAGTTCTCT
Round1_089	/5Phos/CCGATAAGTCTCGT	TACACATCTCCGAGCCCACGAGACTTATCGGTCT
Round1_090	/5Phos/AGCGAAGGTCTCGT	TACACATCTCCGAGCCCACGAGACCTTCGCTTCT
Round1_091	/5Phos/GAGACGTGTCTCGT	TACACATCTCCGAGCCCACGAGACACGTCTCTCT
Round1_092	/5Phos/AGGCACAGTCTCGT	TACACATCTCCGAGCCCACGAGACTGTGCCTTCT
Round1_093	/5Phos/AATCGGAGTCTCGT	TACACATCTCCGAGCCCACGAGACTCCGATTTCT
Round1_094	/5Phos/GGCTCAAGTCTCGT	TACACATCTCCGAGCCCACGAGACTTGAGCCTCT
Round1_095	/5Phos/CAGTCAGGTCTCGT	TACACATCTCCGAGCCCACGAGACCTGACTGTCT
Round1_096	/5Phos/TGCTGGAGTCTCGT	TACACATCTCCGAGCCCACGAGACTCCAGCATCT
Round1_097	/5Phos/AACACAGGTCTCGT	TACACATCTCCGAGCCCACGAGACCTGTGTTTCT
Round1_098	/5Phos/AACGTTCGTCTCGT	TACACATCTCCGAGCCCACGAGACGAACGTTTCT
Round1_099	/5Phos/AACTTCGGTCTCGT	TACACATCTCCGAGCCCACGAGACCGAAGTTTCT
Round1_100	/5Phos/AAGCAAGGTCTCGT	TACACATCTCCGAGCCCACGAGACCTTGCTTTCT
Round1_101	/5Phos/ACACTCTGTCTCGT	TACACATCTCCGAGCCCACGAGACAGAGTGTTCT
Round1_102	/5Phos/ACAGATGGTCTCGT	TACACATCTCCGAGCCCACGAGACCATCTGTTCT
Round1_103	/5Phos/ACATGAGGTCTCGT	TACACATCTCCGAGCCCACGAGACCTCATGTTCT
Round1_104	/5Phos/ACGCGATGTCTCGT	TACACATCTCCGAGCCCACGAGACATCGCGTTCT
Round1_105	/5Phos/ACGTCACGTCTCGT	TACACATCTCCGAGCCCACGAGACGTGACGTTCT
Round1_106	/5Phos/ACTAACGGTCTCGT	TACACATCTCCGAGCCCACGAGACCGTTAGTTCT
Round1_107	/5Phos/ACTAGGCGTCTCGT	TACACATCTCCGAGCCCACGAGACGCCTAGTTCT
Round1_108	/5Phos/ACTTCCAGTCTCGT	TACACATCTCCGAGCCCACGAGACTGGAAGTTCT
Round1_109	/5Phos/AGAACGGGTCTCGT	TACACATCTCCGAGCCCACGAGACCCGTTCTTCT
Round1_110	/5Phos/AGAGCCTGTCTCGT	TACACATCTCCGAGCCCACGAGACAGGCTCTTCT
Round1_111	/5Phos/AGCCATCGTCTCGT	TACACATCTCCGAGCCCACGAGACGATGGCTTCT
Round1_112	/5Phos/AGCTCTGGTCTCGT	TACACATCTCCGAGCCCACGAGACCAGAGCTTCT
Round1_113	/5Phos/AGGACAAGTCTCGT	TACACATCTCCGAGCCCACGAGACTTGTCCTTCT
Round1_114	/5Phos/AGGTTAGGTCTCGT	TACACATCTCCGAGCCCACGAGACCTAACCTTCT
Round1_115	/5Phos/AGTCCATGTCTCGT	TACACATCTCCGAGCCCACGAGACATGGACTTCT
Round1_116	/5Phos/AGTGTCCGTCTCGT	TACACATCTCCGAGCCCACGAGACGGACACTTCT
Round1_117	/5Phos/ATACGGCGTCTCGT	TACACATCTCCGAGCCCACGAGACGCCGTATTCT
Round1_118	/5Phos/ATCCTGGGTCTCGT	TACACATCTCCGAGCCCACGAGACCCAGGATTCT
Round1_119	/5Phos/ATCTAGCGTCTCGT	TACACATCTCCGAGCCCACGAGACGCTAGATTCT
Round1_120	/5Phos/CAACCGTGTCTCGT	TACACATCTCCGAGCCCACGAGACACGGTTGTCT
Round1_121	/5Phos/CAACTCAGTCTCGT	TACACATCTCCGAGCCCACGAGACTGAGTTGTCT
Round1_122	/5Phos/CACATACGTCTCGT	TACACATCTCCGAGCCCACGAGACGTATGTGTCT
Round1_123	/5Phos/CAGAAGAGTCTCGT	TACACATCTCCGAGCCCACGAGACTCTTCTGTCT
Round1_124	/5Phos/CAGGACTGTCTCGT	TACACATCTCCGAGCCCACGAGACAGTCCTGTCT
Round1_125	/5Phos/CCAGACAGTCTCGT	TACACATCTCCGAGCCCACGAGACTGTCTGGTCT
Round1_126	/5Phos/CCTAAGTGTCTCGT	TACACATCTCCGAGCCCACGAGACACTTAGGTCT
Round1_127	/5Phos/CGAATCGGTCTCGT	TACACATCTCCGAGCCCACGAGACCGATTCGTCT
Round1_128	/5Phos/CGAGTATGTCTCGT	TACACATCTCCGAGCCCACGAGACATACTCGTCT
Round1_129	/5Phos/CGATCTTGTCTCGT	TACACATCTCCGAGCCCACGAGACAAGATCGTCT
Round1_130	/5Phos/CGTACACGTCTCGT	TACACATCTCCGAGCCCACGAGACGTGTACGTCT
Round1_131	/5Phos/CGTTAAGGTCTCGT	TACACATCTCCGAGCCCACGAGACCTTAACGTCT
Round1_132	/5Phos/CGTTCGAGTCTCGT	TACACATCTCCGAGCCCACGAGACTCGAACGTCT
Round1_133	/5Phos/CTACTTCGTCTCGT	TACACATCTCCGAGCCCACGAGACGAAGTAGTCT
Round1_134	/5Phos/CTAGGACGTCTCGT	TACACATCTCCGAGCCCACGAGACGTCCTAGTCT
Round1_135	/5Phos/CTATCCGGTCTCGT	TACACATCTCCGAGCCCACGAGACCGGATAGTCT
Round1_136	/5Phos/CTCATTGGTCTCGT	TACACATCTCCGAGCCCACGAGACCAATGAGTCT
Round1_137	/5Phos/CTCTTCAGTCTCGT	TACACATCTCCGAGCCCACGAGACTGAAGAGTCT
Round1_138	/5Phos/CTGATGCGTCTCGT	TACACATCTCCGAGCCCACGAGACGCATCAGTCT
Round1_139	/5Phos/CTGGTTAGTCTCGT	TACACATCTCCGAGCCCACGAGACTAACCAGTCT
Round1_140	/5Phos/CTTCTCGGTCTCGT	TACACATCTCCGAGCCCACGAGACCGAGAAGTCT
Round1_141	/5Phos/CTTGCATGTCTCGT	TACACATCTCCGAGCCCACGAGACATGCAAGTCT
Round1_142	/5Phos/GAACCAAGTCTCGT	TACACATCTCCGAGCCCACGAGACTTGGTTCTCT
Round1_143	/5Phos/GACCTCTGTCTCGT	TACACATCTCCGAGCCCACGAGACAGAGGTCTCT
Round1_144	/5Phos/GAGGATCGTCTCGT	TACACATCTCCGAGCCCACGAGACGATCCTCTCT
Round1_145	/5Phos/GATGGTAGTCTCGT	TACACATCTCCGAGCCCACGAGACTACCATCTCT
Round1_146	/5Phos/GCAAGCTGTCTCGT	TACACATCTCCGAGCCCACGAGACAGCTTGCTCT
Round1_147	/5Phos/GCATTGTGTCTCGT	TACACATCTCCGAGCCCACGAGACACAATGCTCT
Round1_148	/5Phos/GCCATAGGTCTCGT	TACACATCTCCGAGCCCACGAGACCTATGGCTCT
Round1_149	/5Phos/GCCTAGAGTCTCGT	TACACATCTCCGAGCCCACGAGACTCTAGGCTCT
Round1_150	/5Phos/GCTCTGAGTCTCGT	TACACATCTCCGAGCCCACGAGACTCAGAGCTCT
Round1_151	/5Phos/GGAGTTGGTCTCGT	TACACATCTCCGAGCCCACGAGACCAACTCCTCT
Round1_152	/5Phos/GGATGACGTCTCGT	TACACATCTCCGAGCCCACGAGACGTCATCCTCT
Round1_153	/5Phos/GGCGATAGTCTCGT	TACACATCTCCGAGCCCACGAGACTATCGCCTCT
Round1_154	/5Phos/GGTCCTAGTCTCGT	TACACATCTCCGAGCCCACGAGACTAGGACCTCT
Round1_155	/5Phos/GTACCTGGTCTCGT	TACACATCTCCGAGCCCACGAGACCAGGTACTCT
Round1_156	/5Phos/GTCATGTGTCTCGT	TACACATCTCCGAGCCCACGAGACACATGACTCT
Round1_157	/5Phos/GTGCAGAGTCTCGT	TACACATCTCCGAGCCCACGAGACTCTGCACTCT
Round1_158	/5Phos/GTTGCTCGTCTCGT	TACACATCTCCGAGCCCACGAGACGAGCAACTCT
Round1_159	/5Phos/TACGAACGTCTCGT	TACACATCTCCGAGCCCACGAGACGTTCGTATCT
Round1_160	/5Phos/TAGCTACGTCTCGT	TACACATCTCCGAGCCCACGAGACGTAGCTATCT
Round1_161	/5Phos/TATCGCTGTCTCGT	TACACATCTCCGAGCCCACGAGACAGCGATATCT
Round1_162	/5Phos/TCAACAGGTCTCGT	TACACATCTCCGAGCCCACGAGACCTGTTGATCT
Round1_163	/5Phos/TCATTCGGTCTCGT	TACACATCTCCGAGCCCACGAGACCGAATGATCT
Round1_164	/5Phos/TCCTTGCGTCTCGT	TACACATCTCCGAGCCCACGAGACGCAAGGATCT
Round1_165	/5Phos/TCGACTAGTCTCGT	TACACATCTCCGAGCCCACGAGACTAGTCGATCT
Round1_166	/5Phos/TCGAGACGTCTCGT	TACACATCTCCGAGCCCACGAGACGTCTCGATCT

Blocking Oligo (Blocks the RT overhang before Pooling of cells)

Target	Protocol Step	Sequence
RT-oligo overhang	Barcode Ligation	GGGCTCGGAGATGTGTA

Round 1 Barcoding Oligos

Name	Bottom Strand	Top Strand
Round1_001	/5Phos/GGTTAGCGTCTCGT	TACACATCTCCGAGCCCACGAGACGCTAACCTCT
Round1_002	/5Phos/CACGGAAGTCTCGT	TACACATCTCCGAGCCCACGAGACTTCCGTGTCT
Round1_003	/5Phos/GGACAAGGTCTCGT	TACACATCTCCGAGCCCACGAGACCTTGTCCTCT
Round1_004	/5Phos/TGGAGCTGTCTCGT	TACACATCTCCGAGCCCACGAGACAGCTCCATCT
Round1_005	/5Phos/TCCGTAAGTCTCGT	TACACATCTCCGAGCCCACGAGACTTACGGATCT
Round1_006	/5Phos/GATAAGGGTCTCGT	TACACATCTCCGAGCCCACGAGACCCTTATCTCT
Round1_007	/5Phos/TGAGCAAGTCTCGT	TACACATCTCCGAGCCCACGAGACTTGCTCATCT
Round1_008	/5Phos/ATAGCAGGTCTCGT	TACACATCTCCGAGCCCACGAGACCTGCTATTCT
Round1_009	/5Phos/GATCGACGTCTCGT	TACACATCTCCGAGCCCACGAGACGTCGATCTCT
Round1_010	/5Phos/GGAACATGTCTCGT	TACACATCTCCGAGCCCACGAGACATGTTCCTCT
Round1_011	/5Phos/GTAACGAGTCTCGT	TACACATCTCCGAGCCCACGAGACTCGTTACTCT
Round1_012	/5Phos/TCTCGTGGTCTCGT	TACACATCTCCGAGCCCACGAGACCACGAGATCT
Round1_013	/5Phos/AGTGGAAGTCTCGT	TACACATCTCCGAGCCCACGAGACTTCCACTTCT
Round1_014	/5Phos/GATCACAGTCTCGT	TACACATCTCCGAGCCCACGAGACTGTGATCTCT
Round1_015	/5Phos/TTCGGTAGTCTCGT	TACACATCTCCGAGCCCACGAGACTACCGAATCT
Round1_016	/5Phos/GCCGAATGTCTCGT	TACACATCTCCGAGCCCACGAGACATTCGGCTCT
Round1_017	/5Phos/TAGTGGCGTCTCGT	TACACATCTCCGAGCCCACGAGACGCCACTATCT
Round1_018	/5Phos/GAGTTGAGTCTCGT	TACACATCTCCGAGCCCACGAGACTCAACTCTCT
Round1_019	/5Phos/CTTACGGGTCTCGT	TACACATCTCCGAGCCCACGAGACCCGTAAGTCT
Round1_020	/5Phos/AGAAGCCGTCTCGT	TACACATCTCCGAGCCCACGAGACGGCTTCTTCT
Round1_021	/5Phos/GGTTCCTGTCTCGT	TACACATCTCCGAGCCCACGAGACAGGAACCTCT
Round1_022	/5Phos/GCAGGAAGTCTCGT	TACACATCTCCGAGCCCACGAGACTTCCTGCTCT
Round1_023	/5Phos/GTGCTATGTCTCGT	TACACATCTCCGAGCCCACGAGACATAGCACTCT
Round1_024	/5Phos/GTGGCAAGTCTCGT	TACACATCTCCGAGCCCACGAGACTTGCCACTCT
Round1_025	/5Phos/CGACAGAGTCTCGT	TACACATCTCCGAGCCCACGAGACTCTGTCGTCT
Round1_026	/5Phos/AGCTACTGTCTCGT	TACACATCTCCGAGCCCACGAGACAGTAGCTTCT
Round1_027	/5Phos/ACCATCCGTCTCGT	TACACATCTCCGAGCCCACGAGACGGATGGTTCT
Round1_028	/5Phos/ATGCCTAGTCTCGT	TACACATCTCCGAGCCCACGAGACTAGGCATTCT
Round1_029	/5Phos/GTCGTACGTCTCGT	TACACATCTCCGAGCCCACGAGACGTACGACTCT
Round1_030	/5Phos/TACGCCTGTCTCGT	TACACATCTCCGAGCCCACGAGACAGGCGTATCT
Round1_031	/5Phos/CTAAGGTGTCTCGT	TACACATCTCCGAGCCCACGAGACACCTTAGTCT
Round1_032	/5Phos/TACGTGGGTCTCGT	TACACATCTCCGAGCCCACGAGACCCACGTATCT
Round1_033	/5Phos/CTGACTTGTCTCGT	TACACATCTCCGAGCCCACGAGACAAGTCAGTCT
Round1_034	/5Phos/CGCAATTGTCTCGT	TACACATCTCCGAGCCCACGAGACAATTGCGTCT
Round1_035	/5Phos/GTAGACTGTCTCGT	TACACATCTCCGAGCCCACGAGACAGTCTACTCT
Round1_036	/5Phos/TCCTGCTGTCTCGT	TACACATCTCCGAGCCCACGAGACAGCAGGATCT
Round1_037	/5Phos/TTGCCAGGTCTCGT	TACACATCTCCGAGCCCACGAGACCTGGCAATCT
Round1_038	/5Phos/TTCAGGCGTCTCGT	TACACATCTCCGAGCCCACGAGACGCCTGAATCT
Round1_039	/5Phos/AACAGGTGTCTCGT	TACACATCTCCGAGCCCACGAGACACCTGTTTCT
Round1_040	/5Phos/TTATGCCGTCTCGT	TACACATCTCCGAGCCCACGAGACGGCATAATCT
Round1_041	/5Phos/CGGTATAGTCTCGT	TACACATCTCCGAGCCCACGAGACTATACCGTCT
Round1_042	/5Phos/TTGCATCGTCTCGT	TACACATCTCCGAGCCCACGAGACGATGCAATCT
Round1_043	/5Phos/CATACCTGTCTCGT	TACACATCTCCGAGCCCACGAGACAGGTATGTCT
Round1_044	/5Phos/ATGGTGTGTCTCGT	TACACATCTCCGAGCCCACGAGACACACCATTCT
Round1_045	/5Phos/GCTTATGGTCTCGT	TACACATCTCCGAGCCCACGAGACCATAAGCTCT
Round1_046	/5Phos/TAATCGGGTCTCGT	TACACATCTCCGAGCCCACGAGACCCGATTATCT
Round1_047	/5Phos/GTATAGGGTCTCGT	TACACATCTCCGAGCCCACGAGACCCTATACTCT
Round1_048	/5Phos/CCTTCTCGTCTCGT	TACACATCTCCGAGCCCACGAGACGAGAAGGTCT
Round1_049	/5Phos/CCACTAGGTCTCGT	TACACATCTCCGAGCCCACGAGACCTAGTGGTCT
Round1_050	/5Phos/AATGAGCGTCTCGT	TACACATCTCCGAGCCCACGAGACGCTCATTTCT
Round1_051	/5Phos/GTGATCGGTCTCGT	TACACATCTCCGAGCCCACGAGACCGATCACTCT
Round1_052	/5Phos/ACCAGAAGTCTCGT	TACACATCTCCGAGCCCACGAGACTTCTGGTTCT
Round1_053	/5Phos/TGACTGTGTCTCGT	TACACATCTCCGAGCCCACGAGACACAGTCATCT
Round1_054	/5Phos/TGGTCCAGTCTCGT	TACACATCTCCGAGCCCACGAGACTGGACCATCT
Round1_055	/5Phos/CCGAATCGTCTCGT	TACACATCTCCGAGCCCACGAGACGATTCGGTCT
Round1_056	/5Phos/ACACCGAGTCTCGT	TACACATCTCCGAGCCCACGAGACTCGGTGTTCT
Round1_057	/5Phos/TGTGGTTGTCTCGT	TACACATCTCCGAGCCCACGAGACAACCACATCT
Round1_058	/5Phos/TCAAGGAGTCTCGT	TACACATCTCCGAGCCCACGAGACTCCTTGATCT
Round1_059	/5Phos/GGTAGGAGTCTCGT	TACACATCTCCGAGCCCACGAGACTCCTACCTCT
Round1_060	/5Phos/GAAGAGAGTCTCGT	TACACATCTCCGAGCCCACGAGACTCTCTTCTCT
Round1_061	/5Phos/ATGTCGGGTCTCGT	TACACATCTCCGAGCCCACGAGACCCGACATTCT
Round1_062	/5Phos/TATACGCGTCTCGT	TACACATCTCCGAGCCCACGAGACGCGTATATCT
Round1_063	/5Phos/GCCTCTTGTCTCGT	TACACATCTCCGAGCCCACGAGACAAGAGGCTCT
Round1_064	/5Phos/TGTGAGAGTCTCGT	TACACATCTCCGAGCCCACGAGACTCTCACATCT
Round1_065	/5Phos/AACCGTGGTCTCGT	TACACATCTCCGAGCCCACGAGACCACGGTTTCT
Round1_066	/5Phos/CAGCGTAGTCTCGT	TACACATCTCCGAGCCCACGAGACTACGCTGTCT
Round1_067	/5Phos/TCGTAGTGTCTCGT	TACACATCTCCGAGCCCACGAGACACTACGATCT
Round1_068	/5Phos/ATCGGATGTCTCGT	TACACATCTCCGAGCCCACGAGACATCCGATTCT
Round1_069	/5Phos/GGAATGCGTCTCGT	TACACATCTCCGAGCCCACGAGACGCATTCCTCT
Round1_070	/5Phos/AATGGCGGTCTCGT	TACACATCTCCGAGCCCACGAGACCGCCATTTCT
Round1_071	/5Phos/CTGTGAAGTCTCGT	TACACATCTCCGAGCCCACGAGACTTCACAGTCT
Round1_072	/5Phos/CGAAGAAGTCTCGT	TACACATCTCCGAGCCCACGAGACTTCTTCGTCT
Round1_073	/5Phos/TCTCCACGTCTCGT	TACACATCTCCGAGCCCACGAGACGTGGAGATCT
Round1_074	/5Phos/CCTCGAAGTCTCGT	TACACATCTCCGAGCCCACGAGACTTCGAGGTCT
Round1_075	/5Phos/AGGAATGGTCTCGT	TACACATCTCCGAGCCCACGAGACCATTCCTTCT
Round1_076	/5Phos/CTCACAAGTCTCGT	TACACATCTCCGAGCCCACGAGACTTGTGAGTCT
Round1_077	/5Phos/ATGAGGAGTCTCGT	TACACATCTCCGAGCCCACGAGACTCCTCATTCT
Round1_078	/5Phos/CTGTACCGTCTCGT	TACACATCTCCGAGCCCACGAGACGGTACAGTCT
Round1_079	/5Phos/TGCACGTGTCTCGT	TACACATCTCCGAGCCCACGAGACACGTGCATCT
Round1_080	/5Phos/CCTGAACGTCTCGT	TACACATCTCCGAGCCCACGAGACGTTCAGGTCT

Round1_167	/5Phos/TCGGAAGGTCTCGT	TACACATCTCCGAGCCCACGAGACCTTCCGATCT
Round1_168	/5Phos/TCGGTTCGTCTCGT	TACACATCTCCGAGCCCACGAGACGAACCGATCT
Round1_169	/5Phos/TCTTACCGTCTCGT	TACACATCTCCGAGCCCACGAGACGGTAAGATCT
Round1_170	/5Phos/TGAGACGGTCTCGT	TACACATCTCCGAGCCCACGAGACCGTCTCATCT
Round1_171	/5Phos/TGCAACCGTCTCGT	TACACATCTCCGAGCCCACGAGACGGTTGCATCT
Round1_172	/5Phos/TGCAGAGGTCTCGT	TACACATCTCCGAGCCCACGAGACCTCTGCATCT
Round1_173	/5Phos/TGGATGAGTCTCGT	TACACATCTCCGAGCCCACGAGACTCATCCATCT
Round1_174	/5Phos/TGGCGAAGTCTCGT	TACACATCTCCGAGCCCACGAGACTTCGCCATCT
Round1_175	/5Phos/TGTCTAGGTCTCGT	TACACATCTCCGAGCCCACGAGACCTAGACATCT
Round1_176	/5Phos/TTAGAGCGTCTCGT	TACACATCTCCGAGCCCACGAGACGCTCTAATCT
Round1_177	/5Phos/TTGAAGGGTCTCGT	TACACATCTCCGAGCCCACGAGACCCTTCAATCT
Round1_178	/5Phos/TTGCGGTGTCTCGT	TACACATCTCCGAGCCCACGAGACACCGCAATCT
Round1_179	/5Phos/CTCCGTTGTCTCGT	TACACATCTCCGAGCCCACGAGACAACGGAGTCT
Round1_180	/5Phos/AGCAAGAGTCTCGT	TACACATCTCCGAGCCCACGAGACTCTTGCTTCT
Round1_181	/5Phos/GAGAGAAGTCTCGT	TACACATCTCCGAGCCCACGAGACTTCTCTCTCT
Round1_182	/5Phos/GCTTGATGTCTCGT	TACACATCTCCGAGCCCACGAGACATCAAGCTCT
Round1_183	/5Phos/ATTGCGAGTCTCGT	TACACATCTCCGAGCCCACGAGACTCGCAATTCT
Round1_184	/5Phos/GACACTAGTCTCGT	TACACATCTCCGAGCCCACGAGACTAGTGTCTCT
Round1_185	/5Phos/AAGATGGGTCTCGT	TACACATCTCCGAGCCCACGAGACCCATCTTTCT
Round1_186	/5Phos/GAGGTAGGTCTCGT	TACACATCTCCGAGCCCACGAGACCTACCTCTCT
Round1_187	/5Phos/CCATCAAGTCTCGT	TACACATCTCCGAGCCCACGAGACTTGATGGTCT
Round1_188	/5Phos/ACGCTTGGTCTCGT	TACACATCTCCGAGCCCACGAGACCAAGCGTTCT
Round1_189	/5Phos/ATTCGAGGTCTCGT	TACACATCTCCGAGCCCACGAGACCTCGAATTCT
Round1_190	/5Phos/TGACCTCGTCTCGT	TACACATCTCCGAGCCCACGAGACGAGGTCATCT
Round1_191	/5Phos/ACGGAGAGTCTCGT	TACACATCTCCGAGCCCACGAGACTCTCCGTTCT
Round1_192	/5Phos/AAGGCTGGTCTCGT	TACACATCTCCGAGCCCACGAGACCAGCCTTTCT

Description:

#Round 1 barcode oligos
#Each barcode consists of one bottom strand oligo + it's matching top strand oligo which together will form the duplex
(rev. comp. part for most of the sequence, leaving some single stranded overhangs used for ligation)
#Round 1 oligos need to be phosphorylated in order to ligate the round 2 barcodes
#Round 1 barcodes are positioned in bases 1-7 of index 1, the actual barcode are the first seven bases of the oligo sequence

Round 2 Barcoding Oligos		
Name	Bottom Strand	Top Strand
Round2_001	CAAGCAGAAGACGGCATACGAGATTCTGGCAAGA	TGCCAGAATCTCGTATGCCGTCTTCTGCTTG
Round2_002	CAAGCAGAAGACGGCATACGAGATGAACGTTAGA	AACGTTCATCTCGTATGCCGTCTTCTGCTTG
Round2_003	CAAGCAGAAGACGGCATACGAGATGAATCTCAGA	GAGATTCATCTCGTATGCCGTCTTCTGCTTG
Round2_004	CAAGCAGAAGACGGCATACGAGATAGCAAGAAGA	TCTTGCTATCTCGTATGCCGTCTTCTGCTTG
Round2_005	CAAGCAGAAGACGGCATACGAGATACGCTTGAGA	CAAGCGTATCTCGTATGCCGTCTTCTGCTTG
Round2_006	CAAGCAGAAGACGGCATACGAGATGACTAAGAGA	CTTAGTCATCTCGTATGCCGTCTTCTGCTTG
Round2_007	CAAGCAGAAGACGGCATACGAGATTCACAGGAGA	CCTGTGAATCTCGTATGCCGTCTTCTGCTTG
Round2_008	CAAGCAGAAGACGGCATACGAGATGTTCCGTAGA	ACGGAACATCTCGTATGCCGTCTTCTGCTTG
Round2_009	CAAGCAGAAGACGGCATACGAGATGGTGTGTAGA	ACACACCATCTCGTATGCCGTCTTCTGCTTG
Round2_010	CAAGCAGAAGACGGCATACGAGATTCAGCGTAGA	ACGCTGAATCTCGTATGCCGTCTTCTGCTTG
Round2_011	CAAGCAGAAGACGGCATACGAGATTAGAGTGAGA	CACTCTAATCTCGTATGCCGTCTTCTGCTTG
Round2_012	CAAGCAGAAGACGGCATACGAGATCCAAGTGAGA	CACTTGGATCTCGTATGCCGTCTTCTGCTTG
Round2_013	CAAGCAGAAGACGGCATACGAGATAAGTGCAAGA	TGCACTTATCTCGTATGCCGTCTTCTGCTTG
Round2_014	CAAGCAGAAGACGGCATACGAGATTAAGGTCAGA	GACCTTAATCTCGTATGCCGTCTTCTGCTTG
Round2_015	CAAGCAGAAGACGGCATACGAGATATGCTCCAGA	GGAGCATATCTCGTATGCCGTCTTCTGCTTG
Round2_016	CAAGCAGAAGACGGCATACGAGATCTCCAAGAGA	CTTGGAGATCTCGTATGCCGTCTTCTGCTTG
Round2_017	CAAGCAGAAGACGGCATACGAGATAAGATGGAGA	CCATCTTATCTCGTATGCCGTCTTCTGCTTG
Round2_018	CAAGCAGAAGACGGCATACGAGATAGCCTAAAGA	TTAGGCTATCTCGTATGCCGTCTTCTGCTTG
Round2_019	CAAGCAGAAGACGGCATACGAGATGGATACAAGA	TGTATCCATCTCGTATGCCGTCTTCTGCTTG
Round2_020	CAAGCAGAAGACGGCATACGAGATGTTGAAGAGA	CTTCAACATCTCGTATGCCGTCTTCTGCTTG
Round2_021	CAAGCAGAAGACGGCATACGAGATCGCTGATAGA	ATCAGCGATCTCGTATGCCGTCTTCTGCTTG
Round2_022	CAAGCAGAAGACGGCATACGAGATTACAGCAAGA	TGCTGTAATCTCGTATGCCGTCTTCTGCTTG
Round2_023	CAAGCAGAAGACGGCATACGAGATCGAGATCAGA	GATCTCGATCTCGTATGCCGTCTTCTGCTTG
Round2_024	CAAGCAGAAGACGGCATACGAGATACACAACAGA	GTTGTGTATCTCGTATGCCGTCTTCTGCTTG
Round2_025	CAAGCAGAAGACGGCATACGAGATTTCTCACAGA	GTGAGAAATCTCGTATGCCGTCTTCTGCTTG
Round2_026	CAAGCAGAAGACGGCATACGAGATGCGTGTAAGA	TACACGCATCTCGTATGCCGTCTTCTGCTTG
Round2_027	CAAGCAGAAGACGGCATACGAGATACGGAGAAGA	TCTCCGTATCTCGTATGCCGTCTTCTGCTTG
Round2_028	CAAGCAGAAGACGGCATACGAGATCTAGTGGAGA	CCACTAGATCTCGTATGCCGTCTTCTGCTTG
Round2_029	CAAGCAGAAGACGGCATACGAGATATTGCGAAGA	TCGCAATATCTCGTATGCCGTCTTCTGCTTG
Round2_030	CAAGCAGAAGACGGCATACGAGATTTGGACAAGA	TGTCCAAATCTCGTATGCCGTCTTCTGCTTG
Round2_031	CAAGCAGAAGACGGCATACGAGATATTCGAGAGA	CTCGAATATCTCGTATGCCGTCTTCTGCTTG
Round2_032	CAAGCAGAAGACGGCATACGAGATAACTGACAGA	GTCAGTTATCTCGTATGCCGTCTTCTGCTTG
Round2_033	CAAGCAGAAGACGGCATACGAGATAGTCAGGAGA	CCTGACTATCTCGTATGCCGTCTTCTGCTTG
Round2_034	CAAGCAGAAGACGGCATACGAGATACGACCTAGA	AGGTCGTATCTCGTATGCCGTCTTCTGCTTG
Round2_035	CAAGCAGAAGACGGCATACGAGATTGACCTCAGA	GAGGTCAATCTCGTATGCCGTCTTCTGCTTG
Round2_036	CAAGCAGAAGACGGCATACGAGATCCTGTCTAGA	AGACAGGATCTCGTATGCCGTCTTCTGCTTG
Round2_037	CAAGCAGAAGACGGCATACGAGATTGTTGCGAGA	CGCAACAATCTCGTATGCCGTCTTCTGCTTG
Round2_038	CAAGCAGAAGACGGCATACGAGATCGGTTGTAGA	ACAACCGATCTCGTATGCCGTCTTCTGCTTG
Round2_039	CAAGCAGAAGACGGCATACGAGATCAAGAAGAGA	CTTCTTGATCTCGTATGCCGTCTTCTGCTTG
Round2_040	CAAGCAGAAGACGGCATACGAGATGCTATTCAGA	GAATAGCATCTCGTATGCCGTCTTCTGCTTG
Round2_041	CAAGCAGAAGACGGCATACGAGATTAGGCGAAGA	TCGCCTAATCTCGTATGCCGTCTTCTGCTTG
Round2_042	CAAGCAGAAGACGGCATACGAGATGTTGTCAAGA	TGACAACATCTCGTATGCCGTCTTCTGCTTG
Round2_043	CAAGCAGAAGACGGCATACGAGATAATCCTCAGA	GAGGATTATCTCGTATGCCGTCTTCTGCTTG
Round2_044	CAAGCAGAAGACGGCATACGAGATTAGTACGAGA	CGTACTAATCTCGTATGCCGTCTTCTGCTTG
Round2_045	CAAGCAGAAGACGGCATACGAGATACCGCTAAGA	TAGCGGTATCTCGTATGCCGTCTTCTGCTTG
Round2_046	CAAGCAGAAGACGGCATACGAGATCATAGAGAGA	CTCTATGATCTCGTATGCCGTCTTCTGCTTG
Round2_047	CAAGCAGAAGACGGCATACGAGATCTTGGTGAGA	CACCAAGATCTCGTATGCCGTCTTCTGCTTG
Round2_048	CAAGCAGAAGACGGCATACGAGATATACACGAGA	CGTGTATATCTCGTATGCCGTCTTCTGCTTG
Round2_049	CAAGCAGAAGACGGCATACGAGATCACAACGAGA	CGTTGTGATCTCGTATGCCGTCTTCTGCTTG
Round2_050	CAAGCAGAAGACGGCATACGAGATATAGGCAAGA	TGCCTATATCTCGTATGCCGTCTTCTGCTTG

Round2_051	CAAGCAGAAGACGGCATACGAGATAGACGTAAGA	TACGTCTATCTCGTATGCCGTCTTCTGCTTG
Round2_052	CAAGCAGAAGACGGCATACGAGATTTCCACTAGA	AGTGGAAATCTCGTATGCCGTCTTCTGCTTG
Round2_053	CAAGCAGAAGACGGCATACGAGATTATGCAGAGA	CTGCATAATCTCGTATGCCGTCTTCTGCTTG
Round2_054	CAAGCAGAAGACGGCATACGAGATAGATGGTAGA	ACCATCTATCTCGTATGCCGTCTTCTGCTTG
Round2_055	CAAGCAGAAGACGGCATACGAGATCTTCAGCAGA	GCTGAAGATCTCGTATGCCGTCTTCTGCTTG
Round2_056	CAAGCAGAAGACGGCATACGAGATCTCCGTTAGA	AACGGAGATCTCGTATGCCGTCTTCTGCTTG
Round2_057	CAAGCAGAAGACGGCATACGAGATGTCTGTGAGA	CACAGACATCTCGTATGCCGTCTTCTGCTTG
Round2_058	CAAGCAGAAGACGGCATACGAGATCCATCAAAGA	TTGATGGATCTCGTATGCCGTCTTCTGCTTG
Round2_059	CAAGCAGAAGACGGCATACGAGATGAGGTAGAGA	CTACCTCATCTCGTATGCCGTCTTCTGCTTG
Round2_060	CAAGCAGAAGACGGCATACGAGATTGTACTGAGA	CAGTACAATCTCGTATGCCGTCTTCTGCTTG
Round2_061	CAAGCAGAAGACGGCATACGAGATAGAGTGAAGA	TCACTCTATCTCGTATGCCGTCTTCTGCTTG
Round2_062	CAAGCAGAAGACGGCATACGAGATTAACACCAGA	GGTGTTAATCTCGTATGCCGTCTTCTGCTTG
Round2_063	CAAGCAGAAGACGGCATACGAGATATCAGCGAGA	CGCTGATATCTCGTATGCCGTCTTCTGCTTG
Round2_064	CAAGCAGAAGACGGCATACGAGATAAGAACCAGA	GGTTCTTATCTCGTATGCCGTCTTCTGCTTG
Round2_065	CAAGCAGAAGACGGCATACGAGATAAGGCTGAGA	CAGCCTTATCTCGTATGCCGTCTTCTGCTTG
Round2_066	CAAGCAGAAGACGGCATACGAGATCTCTCGTAGA	ACGAGAGATCTCGTATGCCGTCTTCTGCTTG
Round2_067	CAAGCAGAAGACGGCATACGAGATGAAGTCCAGA	GGACTTCATCTCGTATGCCGTCTTCTGCTTG
Round2_068	CAAGCAGAAGACGGCATACGAGATAGGTGTCAGA	GACACCTATCTCGTATGCCGTCTTCTGCTTG
Round2_069	CAAGCAGAAGACGGCATACGAGATGCACATAAGA	TATGTGCATCTCGTATGCCGTCTTCTGCTTG
Round2_070	CAAGCAGAAGACGGCATACGAGATCTCGAGAAGA	TCTCGAGATCTCGTATGCCGTCTTCTGCTTG
Round2_071	CAAGCAGAAGACGGCATACGAGATCGTAACAAGA	TGTTACGATCTCGTATGCCGTCTTCTGCTTG
Round2_072	CAAGCAGAAGACGGCATACGAGATGTAAGAGAGA	CTCTTACATCTCGTATGCCGTCTTCTGCTTG
Round2_073	CAAGCAGAAGACGGCATACGAGATAACTCGAAGA	TCGAGTTATCTCGTATGCCGTCTTCTGCTTG
Round2_074	CAAGCAGAAGACGGCATACGAGATGAGAGAAAGA	TTCTCTCATCTCGTATGCCGTCTTCTGCTTG
Round2_075	CAAGCAGAAGACGGCATACGAGATACAACTCAGA	GAGTTGTATCTCGTATGCCGTCTTCTGCTTG
Round2_076	CAAGCAGAAGACGGCATACGAGATCGGCAATAGA	ATTGCCGATCTCGTATGCCGTCTTCTGCTTG
Round2_077	CAAGCAGAAGACGGCATACGAGATCAAGCTAAGA	TAGCTTGATCTCGTATGCCGTCTTCTGCTTG
Round2_078	CAAGCAGAAGACGGCATACGAGATGAATGCGAGA	CGCATTCATCTCGTATGCCGTCTTCTGCTTG
Round2_079	CAAGCAGAAGACGGCATACGAGATTCGCTCAAGA	TGAGCGAATCTCGTATGCCGTCTTCTGCTTG
Round2_080	CAAGCAGAAGACGGCATACGAGATTCTATGGAGA	CCATAGAATCTCGTATGCCGTCTTCTGCTTG
Round2_081	CAAGCAGAAGACGGCATACGAGATCCATAGCAGA	GCTATGGATCTCGTATGCCGTCTTCTGCTTG
Round2_082	CAAGCAGAAGACGGCATACGAGATGCTACAAAGA	TTGTAGCATCTCGTATGCCGTCTTCTGCTTG
Round2_083	CAAGCAGAAGACGGCATACGAGATGTCCGAAAGA	TTCGGACATCTCGTATGCCGTCTTCTGCTTG
Round2_084	CAAGCAGAAGACGGCATACGAGATTCCAATGAGA	CATTGGAATCTCGTATGCCGTCTTCTGCTTG
Round2_085	CAAGCAGAAGACGGCATACGAGATCACTATCAGA	GATAGTGATCTCGTATGCCGTCTTCTGCTTG
Round2_086	CAAGCAGAAGACGGCATACGAGATCAATGGAAGA	TCCATTGATCTCGTATGCCGTCTTCTGCTTG
Round2_087	CAAGCAGAAGACGGCATACGAGATTACCAGAAGA	TCTGGTAATCTCGTATGCCGTCTTCTGCTTG
Round2_088	CAAGCAGAAGACGGCATACGAGATGCGAACAAGA	TGTTCGCATCTCGTATGCCGTCTTCTGCTTG
Round2_089	CAAGCAGAAGACGGCATACGAGATTAACGAGAGA	CTCGTTAATCTCGTATGCCGTCTTCTGCTTG
Round2_090	CAAGCAGAAGACGGCATACGAGATGCTTGATAGA	ATCAAGCATCTCGTATGCCGTCTTCTGCTTG
Round2_091	CAAGCAGAAGACGGCATACGAGATTAGCCTTAGA	AAGGCTAATCTCGTATGCCGTCTTCTGCTTG
Round2_092	CAAGCAGAAGACGGCATACGAGATGTGAGTCAGA	GACTCACATCTCGTATGCCGTCTTCTGCTTG
Round2_093	CAAGCAGAAGACGGCATACGAGATACTGTAGAGA	CTACAGTATCTCGTATGCCGTCTTCTGCTTG
Round2_094	CAAGCAGAAGACGGCATACGAGATCATCATGAGA	CATGATGATCTCGTATGCCGTCTTCTGCTTG
Round2_095	CAAGCAGAAGACGGCATACGAGATGACACTAAGA	TAGTGTCATCTCGTATGCCGTCTTCTGCTTG
Round2_096	CAAGCAGAAGACGGCATACGAGATGGCATCAAGA	TGATGCCATCTCGTATGCCGTCTTCTGCTTG
Round2_097	CAAGCAGAAGACGGCATACGAGATAGGACAAAGA	TTGTCCTATCTCGTATGCCGTCTTCTGCTTG
Round2_098	CAAGCAGAAGACGGCATACGAGATGTCGTACAGA	GTACGACATCTCGTATGCCGTCTTCTGCTTG
Round2_099	CAAGCAGAAGACGGCATACGAGATGAGACGTAGA	ACGTCTCATCTCGTATGCCGTCTTCTGCTTG
Round2_100	CAAGCAGAAGACGGCATACGAGATTAGTGGCAGA	GCCACTAATCTCGTATGCCGTCTTCTGCTTG
Round2_101	CAAGCAGAAGACGGCATACGAGATGTGGCAAAGA	TTGCCACATCTCGTATGCCGTCTTCTGCTTG
Round2_102	CAAGCAGAAGACGGCATACGAGATTTGCATCAGA	GATGCAAATCTCGTATGCCGTCTTCTGCTTG
Round2_103	CAAGCAGAAGACGGCATACGAGATCAGAAGAAGA	TCTTCTGATCTCGTATGCCGTCTTCTGCTTG
Round2_104	CAAGCAGAAGACGGCATACGAGATAGAGCCTAGA	AGGCTCTATCTCGTATGCCGTCTTCTGCTTG
Round2_105	CAAGCAGAAGACGGCATACGAGATGTACCTGAGA	CAGGTACATCTCGTATGCCGTCTTCTGCTTG
Round2_106	CAAGCAGAAGACGGCATACGAGATTCCTTGCAGA	GCAAGGAATCTCGTATGCCGTCTTCTGCTTG
Round2_107	CAAGCAGAAGACGGCATACGAGATCGATCTTAGA	AAGATCGATCTCGTATGCCGTCTTCTGCTTG
Round2_108	CAAGCAGAAGACGGCATACGAGATCACGGAAAGA	TTCCGTGATCTCGTATGCCGTCTTCTGCTTG
Round2_109	CAAGCAGAAGACGGCATACGAGATTGCACGTAGA	ACGTGCAATCTCGTATGCCGTCTTCTGCTTG
Round2_110	CAAGCAGAAGACGGCATACGAGATAGGTTAGAGA	CTAACCTATCTCGTATGCCGTCTTCTGCTTG
Round2_111	CAAGCAGAAGACGGCATACGAGATCGCAATTAGA	AATTGCGATCTCGTATGCCGTCTTCTGCTTG
Round2_112	CAAGCAGAAGACGGCATACGAGATCAGTCAGAGA	CTGACTGATCTCGTATGCCGTCTTCTGCTTG
Round2_113	CAAGCAGAAGACGGCATACGAGATAGTGGAAAGA	TTCCACTATCTCGTATGCCGTCTTCTGCTTG
Round2_114	CAAGCAGAAGACGGCATACGAGATAACACAGAGA	CTGTGTTATCTCGTATGCCGTCTTCTGCTTG
Round2_115	CAAGCAGAAGACGGCATACGAGATCGAATCGAGA	CGATTCGATCTCGTATGCCGTCTTCTGCTTG
Round2_116	CAAGCAGAAGACGGCATACGAGATTGGCGAAAGA	TTCGCCAATCTCGTATGCCGTCTTCTGCTTG
Round2_117	CAAGCAGAAGACGGCATACGAGATATGGAACAGA	GTTCCATATCTCGTATGCCGTCTTCTGCTTG
Round2_118	CAAGCAGAAGACGGCATACGAGATCCGATAAAGA	TTATCGGATCTCGTATGCCGTCTTCTGCTTG
Round2_119	CAAGCAGAAGACGGCATACGAGATGTAGACTAGA	AGTCTACATCTCGTATGCCGTCTTCTGCTTG
Round2_120	CAAGCAGAAGACGGCATACGAGATGAGGATCAGA	GATCCTCATCTCGTATGCCGTCTTCTGCTTG
Round2_121	CAAGCAGAAGACGGCATACGAGATGCATTGTAGA	ACAATGCATCTCGTATGCCGTCTTCTGCTTG
Round2_122	CAAGCAGAAGACGGCATACGAGATCCGAATCAGA	GATTCGGATCTCGTATGCCGTCTTCTGCTTG
Round2_123	CAAGCAGAAGACGGCATACGAGATACCATCCAGA	GGATGGTATCTCGTATGCCGTCTTCTGCTTG
Round2_124	CAAGCAGAAGACGGCATACGAGATACTAACGAGA	CGTTAGTATCTCGTATGCCGTCTTCTGCTTG
Round2_125	CAAGCAGAAGACGGCATACGAGATACTAGGCAGA	GCCTAGTATCTCGTATGCCGTCTTCTGCTTG
Round2_126	CAAGCAGAAGACGGCATACGAGATTCGAGACAGA	GTCTCGAATCTCGTATGCCGTCTTCTGCTTG
Round2_127	CAAGCAGAAGACGGCATACGAGATATCCTGGAGA	CCAGGATATCTCGTATGCCGTCTTCTGCTTG
Round2_128	CAAGCAGAAGACGGCATACGAGATAGCGAAGAGA	CTTCGCTATCTCGTATGCCGTCTTCTGCTTG
Round2_129	CAAGCAGAAGACGGCATACGAGATGTTGCTCAGA	GAGCAACATCTCGTATGCCGTCTTCTGCTTG
Round2_130	CAAGCAGAAGACGGCATACGAGATCATTGCCAGA	GGCAATGATCTCGTATGCCGTCTTCTGCTTG
Round2_131	CAAGCAGAAGACGGCATACGAGATGCTCTGAAGA	TCAGAGCATCTCGTATGCCGTCTTCTGCTTG
Round2_132	CAAGCAGAAGACGGCATACGAGATCACATACAGA	GTATGTGATCTCGTATGCCGTCTTCTGCTTG
Round2_133	CAAGCAGAAGACGGCATACGAGATCCACTAGAGA	CTAGTGGATCTCGTATGCCGTCTTCTGCTTG
Round2_134	CAAGCAGAAGACGGCATACGAGATTCCGTAAAGA	TTACGGAATCTCGTATGCCGTCTTCTGCTTG
Round2_135	CAAGCAGAAGACGGCATACGAGATCCTTCTCAGA	GAGAAGGATCTCGTATGCCGTCTTCTGCTTG
Round2_136	CAAGCAGAAGACGGCATACGAGATGTCATGTAGA	ACATGACATCTCGTATGCCGTCTTCTGCTTG

Round2_137	CAAGCAGAAGACGGCATACGAGATTTGCGGTAGA	ACCGCAAATCTCGTATGCCGTCTTCTGCTTG
Round2_138	CAAGCAGAAGACGGCATACGAGATGGTAGGAAGA	TCCTACCATCTCGTATGCCGTCTTCTGCTTG
Round2_139	CAAGCAGAAGACGGCATACGAGATGGAGTTGAGA	CAACTCCATCTCGTATGCCGTCTTCTGCTTG
Round2_140	CAAGCAGAAGACGGCATACGAGATCTGTGAAAGA	TTCACAGATCTCGTATGCCGTCTTCTGCTTG
Round2_141	CAAGCAGAAGACGGCATACGAGATTGCTGGAAGA	TCCAGCAATCTCGTATGCCGTCTTCTGCTTG
Round2_142	CAAGCAGAAGACGGCATACGAGATACACCGAAGA	TCGGTGTATCTCGTATGCCGTCTTCTGCTTG
Round2_143	CAAGCAGAAGACGGCATACGAGATCGACAGAAGA	TCTGTCGATCTCGTATGCCGTCTTCTGCTTG
Round2_144	CAAGCAGAAGACGGCATACGAGATCTTGCATAGA	ATGCAAGATCTCGTATGCCGTCTTCTGCTTG
Round2_145	CAAGCAGAAGACGGCATACGAGATCCTAAGTAGA	ACTTAGGATCTCGTATGCCGTCTTCTGCTTG
Round2_146	CAAGCAGAAGACGGCATACGAGATTCTCCACAGA	GTGGAGAATCTCGTATGCCGTCTTCTGCTTG
Round2_147	CAAGCAGAAGACGGCATACGAGATTGACTGTAGA	ACAGTCAATCTCGTATGCCGTCTTCTGCTTG
Round2_148	CAAGCAGAAGACGGCATACGAGATCGTTCGAAGA	TCGAACGATCTCGTATGCCGTCTTCTGCTTG
Round2_149	CAAGCAGAAGACGGCATACGAGATTGTGAGAAGA	TCTCACAATCTCGTATGCCGTCTTCTGCTTG
Round2_150	CAAGCAGAAGACGGCATACGAGATCGTACACAGA	GTGTACGATCTCGTATGCCGTCTTCTGCTTG
Round2_151	CAAGCAGAAGACGGCATACGAGATTGTGGTTAGA	AACCACAATCTCGTATGCCGTCTTCTGCTTG
Round2_152	CAAGCAGAAGACGGCATACGAGATATCTAGCAGA	GCTAGATATCTCGTATGCCGTCTTCTGCTTG
Round2_153	CAAGCAGAAGACGGCATACGAGATGTAACGAAGA	TCGTTACATCTCGTATGCCGTCTTCTGCTTG
Round2_154	CAAGCAGAAGACGGCATACGAGATCAGCGTAAGA	TACGCTGATCTCGTATGCCGTCTTCTGCTTG
Round2_155	CAAGCAGAAGACGGCATACGAGATGTATAGGAGA	CCTATACATCTCGTATGCCGTCTTCTGCTTG
Round2_156	CAAGCAGAAGACGGCATACGAGATCTAAGGTAGA	ACCTTAGATCTCGTATGCCGTCTTCTGCTTG
Round2_157	CAAGCAGAAGACGGCATACGAGATCGGTATAAGA	TATACCGATCTCGTATGCCGTCTTCTGCTTG
Round2_158	CAAGCAGAAGACGGCATACGAGATACACTCTAGA	AGAGTGTATCTCGTATGCCGTCTTCTGCTTG
Round2_159	CAAGCAGAAGACGGCATACGAGATGCCATAGAGA	CTATGGCATCTCGTATGCCGTCTTCTGCTTG
Round2_160	CAAGCAGAAGACGGCATACGAGATAGAACGGAGA	CCGTTCTATCTCGTATGCCGTCTTCTGCTTG
Round2_161	CAAGCAGAAGACGGCATACGAGATTACGAACAGA	GTTCGTAATCTCGTATGCCGTCTTCTGCTTG
Round2_162	CAAGCAGAAGACGGCATACGAGATGTGCAGAAGA	TCTGCACATCTCGTATGCCGTCTTCTGCTTG
Round2_163	CAAGCAGAAGACGGCATACGAGATAGCTCTGAGA	CAGAGCTATCTCGTATGCCGTCTTCTGCTTG
Round2_164	CAAGCAGAAGACGGCATACGAGATGGTTCCTAGA	AGGAACCATCTCGTATGCCGTCTTCTGCTTG
Round2_165	CAAGCAGAAGACGGCATACGAGATCCTCGAAAGA	TTCGAGGATCTCGTATGCCGTCTTCTGCTTG
Round2_166	CAAGCAGAAGACGGCATACGAGATGATCACAAGA	TGTGATCATCTCGTATGCCGTCTTCTGCTTG
Round2_167	CAAGCAGAAGACGGCATACGAGATCGAGTATAGA	ATACTCGATCTCGTATGCCGTCTTCTGCTTG
Round2_168	CAAGCAGAAGACGGCATACGAGATCTGGTTAAGA	TAACCAGATCTCGTATGCCGTCTTCTGCTTG
Round2_169	CAAGCAGAAGACGGCATACGAGATGATAAGGAGA	CCTTATCATCTCGTATGCCGTCTTCTGCTTG
Round2_170	CAAGCAGAAGACGGCATACGAGATGCTTATGAGA	CATAAGCATCTCGTATGCCGTCTTCTGCTTG
Round2_171	CAAGCAGAAGACGGCATACGAGATCTAGGACAGA	GTCCTAGATCTCGTATGCCGTCTTCTGCTTG
Round2_172	CAAGCAGAAGACGGCATACGAGATACATGAGAGA	CTCATGTATCTCGTATGCCGTCTTCTGCTTG
Round2_173	CAAGCAGAAGACGGCATACGAGATATGTCGGAGA	CCGACATATCTCGTATGCCGTCTTCTGCTTG
Round2_174	CAAGCAGAAGACGGCATACGAGATTACGTGGAGA	CCACGTAATCTCGTATGCCGTCTTCTGCTTG
Round2_175	CAAGCAGAAGACGGCATACGAGATACGCGATAGA	ATCGCGTATCTCGTATGCCGTCTTCTGCTTG
Round2_176	CAAGCAGAAGACGGCATACGAGATATCGGATAGA	ATCCGATATCTCGTATGCCGTCTTCTGCTTG
Round2_177	CAAGCAGAAGACGGCATACGAGATAACAGGTAGA	ACCTGTTATCTCGTATGCCGTCTTCTGCTTG
Round2_178	CAAGCAGAAGACGGCATACGAGATTCGGTTCAGA	GAACCGAATCTCGTATGCCGTCTTCTGCTTG
Round2_179	CAAGCAGAAGACGGCATACGAGATCTACTTCAGA	GAAGTAGATCTCGTATGCCGTCTTCTGCTTG
Round2_180	CAAGCAGAAGACGGCATACGAGATCTGATGCAGA	GCATCAGATCTCGTATGCCGTCTTCTGCTTG
Round2_181	CAAGCAGAAGACGGCATACGAGATTCTCGTGAGA	CACGAGAATCTCGTATGCCGTCTTCTGCTTG
Round2_182	CAAGCAGAAGACGGCATACGAGATTGCAACCAGA	GGTTGCAATCTCGTATGCCGTCTTCTGCTTG
Round2_183	CAAGCAGAAGACGGCATACGAGATTGAGCAAAGA	TTGCTCAATCTCGTATGCCGTCTTCTGCTTG
Round2_184	CAAGCAGAAGACGGCATACGAGATTGAGACGAGA	CGTCTCAATCTCGTATGCCGTCTTCTGCTTG
Round2_185	CAAGCAGAAGACGGCATACGAGATTGCAGAGAGA	CTCTGCAATCTCGTATGCCGTCTTCTGCTTG
Round2_186	CAAGCAGAAGACGGCATACGAGATAGGCACAAGA	TGTGCCTATCTCGTATGCCGTCTTCTGCTTG
Round2_187	CAAGCAGAAGACGGCATACGAGATAGTGTCCAGA	GGACACTATCTCGTATGCCGTCTTCTGCTTG
Round2_188	CAAGCAGAAGACGGCATACGAGATCAACCGTAGA	ACGGTTGATCTCGTATGCCGTCTTCTGCTTG
Round2_189	CAAGCAGAAGACGGCATACGAGATGTGTGCTAGA	AGCACACATCTCGTATGCCGTCTTCTGCTTG
Round2_190	CAAGCAGAAGACGGCATACGAGATCAGGACTAGA	AGTCCTGATCTCGTATGCCGTCTTCTGCTTG
Round2_191	CAAGCAGAAGACGGCATACGAGATACTTCCAAGA	TGGAAGTATCTCGTATGCCGTCTTCTGCTTG
Round2_192	CAAGCAGAAGACGGCATACGAGATATAGCAGAGA	CTGCTATATCTCGTATGCCGTCTTCTGCTTG

Description

#Round 2 barcode oligos

#Each barcode consists of one bottom strand oligo + it's matching top strand oligo which together will form the duplex
 (rev. comp. part for most of the sequence, leaving some single stranded overhangs used for ligation)

#Round 2 barcodes are positioned in bases 11-17 of index 1, the actual barcode are the first seven bases of the oligo sequence

#Bases 8-10 in Index1 consist of the linker sequence 'TCT'

i7-Tru-Seq-long primer	Index PCR Reverse Primer	CAAGCAGAAGACGGCATACGAGAT

Barcoded Nextera Sequencing Primers for Index PCR (384 Primers used to barcode sub-libraries)		
Name	**Protocol Step**	**Sequence**
VS_Nextera_i5101	Index PCR Forward Primer	AATGATACGGCGACCACCGAGATCTACACAACACGGTTCGTCGGCAGCGTC
VS_Nextera_i5102	Index PCR Forward Primer	AATGATACGGCGACCACCGAGATCTACACAACAGGCATCGTCGGCAGCGTC
VS_Nextera_i5103	Index PCR Forward Primer	AATGATACGGCGACCACCGAGATCTACACAACATCGCTCGTCGGCAGCGTC
VS_Nextera_i5104	Index PCR Forward Primer	AATGATACGGCGACCACCGAGATCTACACAACCATCGTCGTCGGCAGCGTC
VS_Nextera_i5105	Index PCR Forward Primer	AATGATACGGCGACCACCGAGATCTACACAACCGAACTCGTCGGCAGCGTC
VS_Nextera_i5106	Index PCR Forward Primer	AATGATACGGCGACCACCGAGATCTACACAACGACTCTCGTCGGCAGCGTC
VS_Nextera_i5107	Index PCR Forward Primer	AATGATACGGCGACCACCGAGATCTACACAACGCATGTCGTCGGCAGCGTC
VS_Nextera_i5108	Index PCR Forward Primer	AATGATACGGCGACCACCGAGATCTACACAACGCCATTCGTCGGCAGCGTC
VS_Nextera_i5109	Index PCR Forward Primer	AATGATACGGCGACCACCGAGATCTACACAACGCTGATCGTCGGCAGCGTC
VS_Nextera_i5110	Index PCR Forward Primer	AATGATACGGCGACCACCGAGATCTACACAACGGAGTTCGTCGGCAGCGTC
VS_Nextera_i5111	Index PCR Forward Primer	AATGATACGGCGACCACCGAGATCTACACAACTCAGCTCGTCGGCAGCGTC
VS_Nextera_i5112	Index PCR Forward Primer	AATGATACGGCGACCACCGAGATCTACACAACTTGCGTCGTCGGCAGCGTC
VS_Nextera_i5113	Index PCR Forward Primer	AATGATACGGCGACCACCGAGATCTACACAAGAAGCGTCGTCGGCAGCGTC
VS_Nextera_i5114	Index PCR Forward Primer	AATGATACGGCGACCACCGAGATCTACACAAGCCAGTTCGTCGGCAGCGTC
VS_Nextera_i5115	Index PCR Forward Primer	AATGATACGGCGACCACCGAGATCTACACAAGCCTTCTCGTCGGCAGCGTC
VS_Nextera_i5116	Index PCR Forward Primer	AATGATACGGCGACCACCGAGATCTACACAAGCTCAGTCGTCGGCAGCGTC
VS_Nextera_i5117	Index PCR Forward Primer	AATGATACGGCGACCACCGAGATCTACACAAGCTGCATCGTCGGCAGCGTC

VS_Nextera_i5118	Index PCR Forward Primer	AATGATACGGCGACCACCGAGATCTACACAAGGAACCTCGTCGGCAGCGTC
VS_Nextera_i5119	Index PCR Forward Primer	AATGATACGGCGACCACCGAGATCTACACAAGGCTAGTCGTCGGCAGCGTC
VS_Nextera_i5120	Index PCR Forward Primer	AATGATACGGCGACCACCGAGATCTACACAAGGTCGATCGTCGGCAGCGTC
VS_Nextera_i5121	Index PCR Forward Primer	AATGATACGGCGACCACCGAGATCTACACAAGTACGCTCGTCGGCAGCGTC
VS_Nextera_i5122	Index PCR Forward Primer	AATGATACGGCGACCACCGAGATCTACACAAGTCACGTCGTCGGCAGCGTC
VS_Nextera_i5123	Index PCR Forward Primer	AATGATACGGCGACCACCGAGATCTACACAAGTCGGATCGTCGGCAGCGTC
VS_Nextera_i5124	Index PCR Forward Primer	AATGATACGGCGACCACCGAGATCTACACAAGTGCCATCGTCGGCAGCGTC
VS_Nextera_i5125	Index PCR Forward Primer	AATGATACGGCGACCACCGAGATCTACACAATCCGCTTCGTCGGCAGCGTC
VS_Nextera_i5126	Index PCR Forward Primer	AATGATACGGCGACCACCGAGATCTACACAATCGTGGTCGTCGGCAGCGTC
VS_Nextera_i5127	Index PCR Forward Primer	AATGATACGGCGACCACCGAGATCTACACAATGACGGTCGTCGGCAGCGTC
VS_Nextera_i5128	Index PCR Forward Primer	AATGATACGGCGACCACCGAGATCTACACAATGCGTCTCGTCGGCAGCGTC
VS_Nextera_i5129	Index PCR Forward Primer	AATGATACGGCGACCACCGAGATCTACACAATGGCCTTCGTCGGCAGCGTC
VS_Nextera_i5130	Index PCR Forward Primer	AATGATACGGCGACCACCGAGATCTACACACAACTGGTCGTCGGCAGCGTC
VS_Nextera_i5131	Index PCR Forward Primer	AATGATACGGCGACCACCGAGATCTACACACAAGCGTTCGTCGGCAGCGTC
VS_Nextera_i5132	Index PCR Forward Primer	AATGATACGGCGACCACCGAGATCTACACACAAGGACTCGTCGGCAGCGTC
VS_Nextera_i5133	Index PCR Forward Primer	AATGATACGGCGACCACCGAGATCTACACACAATGCGTCGTCGGCAGCGTC
VS_Nextera_i5134	Index PCR Forward Primer	AATGATACGGCGACCACCGAGATCTACACACACAGGTTCGTCGGCAGCGTC
VS_Nextera_i5135	Index PCR Forward Primer	AATGATACGGCGACCACCGAGATCTACACACACTAGCTCGTCGGCAGCGTC
VS_Nextera_i5136	Index PCR Forward Primer	AATGATACGGCGACCACCGAGATCTACACACACTCCTTCGTCGGCAGCGTC
VS_Nextera_i5137	Index PCR Forward Primer	AATGATACGGCGACCACCGAGATCTACACACAGACACTCGTCGGCAGCGTC
VS_Nextera_i5138	Index PCR Forward Primer	AATGATACGGCGACCACCGAGATCTACACACAGCACATCGTCGGCAGCGTC
VS_Nextera_i5139	Index PCR Forward Primer	AATGATACGGCGACCACCGAGATCTACACACAGCCTTTCGTCGGCAGCGTC
VS_Nextera_i5140	Index PCR Forward Primer	AATGATACGGCGACCACCGAGATCTACACACAGGATGTCGTCGGCAGCGTC
VS_Nextera_i5141	Index PCR Forward Primer	AATGATACGGCGACCACCGAGATCTACACACATGCTCTCGTCGGCAGCGTC
VS_Nextera_i5142	Index PCR Forward Primer	AATGATACGGCGACCACCGAGATCTACACACCAACCTTCGTCGGCAGCGTC
VS_Nextera_i5143	Index PCR Forward Primer	AATGATACGGCGACCACCGAGATCTACACACCAATGCTCGTCGGCAGCGTC
VS_Nextera_i5144	Index PCR Forward Primer	AATGATACGGCGACCACCGAGATCTACACACCACAAGTCGTCGGCAGCGTC
VS_Nextera_i5145	Index PCR Forward Primer	AATGATACGGCGACCACCGAGATCTACACACCAGCAATCGTCGGCAGCGTC
VS_Nextera_i5146	Index PCR Forward Primer	AATGATACGGCGACCACCGAGATCTACACACCAGGTTTCGTCGGCAGCGTC
VS_Nextera_i5147	Index PCR Forward Primer	AATGATACGGCGACCACCGAGATCTACACACCATGGATCGTCGGCAGCGTC
VS_Nextera_i5148	Index PCR Forward Primer	AATGATACGGCGACCACCGAGATCTACACACCGAAGATCGTCGGCAGCGTC
VS_Nextera_i5149	Index PCR Forward Primer	AATGATACGGCGACCACCGAGATCTACACACCGATAGTCGTCGGCAGCGTC
VS_Nextera_i5150	Index PCR Forward Primer	AATGATACGGCGACCACCGAGATCTACACACCTAGCATCGTCGGCAGCGTC
VS_Nextera_i5151	Index PCR Forward Primer	AATGATACGGCGACCACCGAGATCTACACACCTGACTTCGTCGGCAGCGTC
VS_Nextera_i5152	Index PCR Forward Primer	AATGATACGGCGACCACCGAGATCTACACACCTTCGTTCGTCGGCAGCGTC
VS_Nextera_i5153	Index PCR Forward Primer	AATGATACGGCGACCACCGAGATCTACACACCTTGACTCGTCGGCAGCGTC
VS_Nextera_i5154	Index PCR Forward Primer	AATGATACGGCGACCACCGAGATCTACACACGCAATCTCGTCGGCAGCGTC
VS_Nextera_i5155	Index PCR Forward Primer	AATGATACGGCGACCACCGAGATCTACACACGGAGAATCGTCGGCAGCGTC
VS_Nextera_i5156	Index PCR Forward Primer	AATGATACGGCGACCACCGAGATCTACACACGGTAGTTCGTCGGCAGCGTC
VS_Nextera_i5157	Index PCR Forward Primer	AATGATACGGCGACCACCGAGATCTACACACGTATGGTCGTCGGCAGCGTC
VS_Nextera_i5158	Index PCR Forward Primer	AATGATACGGCGACCACCGAGATCTACACACGTGAACTCGTCGGCAGCGTC
VS_Nextera_i5159	Index PCR Forward Primer	AATGATACGGCGACCACCGAGATCTACACACGTTGTGTCGTCGGCAGCGTC
VS_Nextera_i5160	Index PCR Forward Primer	AATGATACGGCGACCACCGAGATCTACACACTACCACTCGTCGGCAGCGTC
VS_Nextera_i5161	Index PCR Forward Primer	AATGATACGGCGACCACCGAGATCTACACACTCACCATCGTCGGCAGCGTC
VS_Nextera_i5162	Index PCR Forward Primer	AATGATACGGCGACCACCGAGATCTACACACTCAGACTCGTCGGCAGCGTC
VS_Nextera_i5163	Index PCR Forward Primer	AATGATACGGCGACCACCGAGATCTACACACTCCAGATCGTCGGCAGCGTC
VS_Nextera_i5164	Index PCR Forward Primer	AATGATACGGCGACCACCGAGATCTACACACTCCTTGTCGTCGGCAGCGTC
VS_Nextera_i5165	Index PCR Forward Primer	AATGATACGGCGACCACCGAGATCTACACACTCGAAGTCGTCGGCAGCGTC
VS_Nextera_i5166	Index PCR Forward Primer	AATGATACGGCGACCACCGAGATCTACACACTCGGTATCGTCGGCAGCGTC
VS_Nextera_i5167	Index PCR Forward Primer	AATGATACGGCGACCACCGAGATCTACACACTGAACGTCGTCGGCAGCGTC
VS_Nextera_i5168	Index PCR Forward Primer	AATGATACGGCGACCACCGAGATCTACACACTGCGATTCGTCGGCAGCGTC
VS_Nextera_i5169	Index PCR Forward Primer	AATGATACGGCGACCACCGAGATCTACACACTGGTGTTCGTCGGCAGCGTC
VS_Nextera_i5170	Index PCR Forward Primer	AATGATACGGCGACCACCGAGATCTACACACTGTCAGTCGTCGGCAGCGTC
VS_Nextera_i5171	Index PCR Forward Primer	AATGATACGGCGACCACCGAGATCTACACACTGTGCATCGTCGGCAGCGTC
VS_Nextera_i5172	Index PCR Forward Primer	AATGATACGGCGACCACCGAGATCTACACACTTCACCTCGTCGGCAGCGTC
VS_Nextera_i5173	Index PCR Forward Primer	AATGATACGGCGACCACCGAGATCTACACACTTGTCGTCGTCGGCAGCGTC
VS_Nextera_i5174	Index PCR Forward Primer	AATGATACGGCGACCACCGAGATCTACACAGAACGGATCGTCGGCAGCGTC
VS_Nextera_i5175	Index PCR Forward Primer	AATGATACGGCGACCACCGAGATCTACACAGAAGGTGTCGTCGGCAGCGTC
VS_Nextera_i5176	Index PCR Forward Primer	AATGATACGGCGACCACCGAGATCTACACAGAAGTCCTCGTCGGCAGCGTC
VS_Nextera_i5177	Index PCR Forward Primer	AATGATACGGCGACCACCGAGATCTACACAGAATCGGTCGTCGGCAGCGTC
VS_Nextera_i5178	Index PCR Forward Primer	AATGATACGGCGACCACCGAGATCTACACAGACACAGTCGTCGGCAGCGTC
VS_Nextera_i5179	Index PCR Forward Primer	AATGATACGGCGACCACCGAGATCTACACAGACATGCTCGTCGGCAGCGTC
VS_Nextera_i5180	Index PCR Forward Primer	AATGATACGGCGACCACCGAGATCTACACAGAGACCATCGTCGGCAGCGTC
VS_Nextera_i5181	Index PCR Forward Primer	AATGATACGGCGACCACCGAGATCTACACAGAGCTACTCGTCGGCAGCGTC
VS_Nextera_i5182	Index PCR Forward Primer	AATGATACGGCGACCACCGAGATCTACACAGAGTACGTCGTCGGCAGCGTC
VS_Nextera_i5183	Index PCR Forward Primer	AATGATACGGCGACCACCGAGATCTACACAGATCCTGTCGTCGGCAGCGTC
VS_Nextera_i5184	Index PCR Forward Primer	AATGATACGGCGACCACCGAGATCTACACAGATCGCTTCGTCGGCAGCGTC
VS_Nextera_i5185	Index PCR Forward Primer	AATGATACGGCGACCACCGAGATCTACACAGATGAGGTCGTCGGCAGCGTC
VS_Nextera_i5186	Index PCR Forward Primer	AATGATACGGCGACCACCGAGATCTACACAGCACACATCGTCGGCAGCGTC
VS_Nextera_i5187	Index PCR Forward Primer	AATGATACGGCGACCACCGAGATCTACACAGCATGAGTCGTCGGCAGCGTC
VS_Nextera_i5188	Index PCR Forward Primer	AATGATACGGCGACCACCGAGATCTACACAGCCAATGTCGTCGGCAGCGTC
VS_Nextera_i5189	Index PCR Forward Primer	AATGATACGGCGACCACCGAGATCTACACAGCCAGAATCGTCGGCAGCGTC
VS_Nextera_i5190	Index PCR Forward Primer	AATGATACGGCGACCACCGAGATCTACACAGCCTCTTTCGTCGGCAGCGTC
VS_Nextera_i5191	Index PCR Forward Primer	AATGATACGGCGACCACCGAGATCTACACAGCGAACTTCGTCGGCAGCGTC
VS_Nextera_i5192	Index PCR Forward Primer	AATGATACGGCGACCACCGAGATCTACACAGCGGTATTCGTCGGCAGCGTC
VS_Nextera_i5193	Index PCR Forward Primer	AATGATACGGCGACCACCGAGATCTACACAGCGTAACTCGTCGGCAGCGTC
VS_Nextera_i5194	Index PCR Forward Primer	AATGATACGGCGACCACCGAGATCTACACAGCGTGTATCGTCGGCAGCGTC
VS_Nextera_i5195	Index PCR Forward Primer	AATGATACGGCGACCACCGAGATCTACACAGCTACACTCGTCGGCAGCGTC
VS_Nextera_i5196	Index PCR Forward Primer	AATGATACGGCGACCACCGAGATCTACACAGCTCTAGTCGTCGGCAGCGTC
VS_Nextera_i5197	Index PCR Forward Primer	AATGATACGGCGACCACCGAGATCTACACAGCTGTTCTCGTCGGCAGCGTC
VS_Nextera_i5198	Index PCR Forward Primer	AATGATACGGCGACCACCGAGATCTACACAGGAACTGTCGTCGGCAGCGTC
VS_Nextera_i5199	Index PCR Forward Primer	AATGATACGGCGACCACCGAGATCTACACAGGACATCTCGTCGGCAGCGTC
VS_Nextera_i5200	Index PCR Forward Primer	AATGATACGGCGACCACCGAGATCTACACAGGACCAATCGTCGGCAGCGTC
VS_Nextera_i5201	Index PCR Forward Primer	AATGATACGGCGACCACCGAGATCTACACAGGAGAAGTCGTCGGCAGCGTC
VS_Nextera_i5202	Index PCR Forward Primer	AATGATACGGCGACCACCGAGATCTACACAGGAGTGATCGTCGGCAGCGTC
VS_Nextera_i5203	Index PCR Forward Primer	AATGATACGGCGACCACCGAGATCTACACAGGATGGTTCGTCGGCAGCGTC

VS_Nextera_i5204	Index PCR Forward Primer	AATGATACGGCGACCACCGAGATCTACACAGGCAAGATCGTCGGCAGCGTC
VS_Nextera_i5205	Index PCR Forward Primer	AATGATACGGCGACCACCGAGATCTACACAGGCAGTTTCGTCGGCAGCGTC
VS_Nextera_i5206	Index PCR Forward Primer	AATGATACGGCGACCACCGAGATCTACACAGGCTACTTCGTCGGCAGCGTC
VS_Nextera_i5207	Index PCR Forward Primer	AATGATACGGCGACCACCGAGATCTACACAGGCTTACTCGTCGGCAGCGTC
VS_Nextera_i5208	Index PCR Forward Primer	AATGATACGGCGACCACCGAGATCTACACAGGTAGAGTCGTCGGCAGCGTC
VS_Nextera_i5209	Index PCR Forward Primer	AATGATACGGCGACCACCGAGATCTACACAGGTCTCATCGTCGGCAGCGTC
VS_Nextera_i5210	Index PCR Forward Primer	AATGATACGGCGACCACCGAGATCTACACAGGTGGTATCGTCGGCAGCGTC
VS_Nextera_i5211	Index PCR Forward Primer	AATGATACGGCGACCACCGAGATCTACACAGGTTAGCTCGTCGGCAGCGTC
VS_Nextera_i5212	Index PCR Forward Primer	AATGATACGGCGACCACCGAGATCTACACAGTAGAGCTCGTCGGCAGCGTC
VS_Nextera_i5213	Index PCR Forward Primer	AATGATACGGCGACCACCGAGATCTACACAGTCACTCTCGTCGGCAGCGTC
VS_Nextera_i5214	Index PCR Forward Primer	AATGATACGGCGACCACCGAGATCTACACAGTCCTGTTCGTCGGCAGCGTC
VS_Nextera_i5215	Index PCR Forward Primer	AATGATACGGCGACCACCGAGATCTACACAGTCGGATTCGTCGGCAGCGTC
VS_Nextera_i5216	Index PCR Forward Primer	AATGATACGGCGACCACCGAGATCTACACAGTGAGGATCGTCGGCAGCGTC
VS_Nextera_i5217	Index PCR Forward Primer	AATGATACGGCGACCACCGAGATCTACACAGTGCAAGTCGTCGGCAGCGTC
VS_Nextera_i5218	Index PCR Forward Primer	AATGATACGGCGACCACCGAGATCTACACAGTGGCAATCGTCGGCAGCGTC
VS_Nextera_i5219	Index PCR Forward Primer	AATGATACGGCGACCACCGAGATCTACACAGTGGTTGTCGTCGGCAGCGTC
VS_Nextera_i5220	Index PCR Forward Primer	AATGATACGGCGACCACCGAGATCTACACAGTTACCGTCGTCGGCAGCGTC
VS_Nextera_i5221	Index PCR Forward Primer	AATGATACGGCGACCACCGAGATCTACACAGTTCGACTCGTCGGCAGCGTC
VS_Nextera_i5222	Index PCR Forward Primer	AATGATACGGCGACCACCGAGATCTACACAGTTGCGTTCGTCGGCAGCGTC
VS_Nextera_i5223	Index PCR Forward Primer	AATGATACGGCGACCACCGAGATCTACACATACCAGGTCGTCGGCAGCGTC
VS_Nextera_i5224	Index PCR Forward Primer	AATGATACGGCGACCACCGAGATCTACACATACCGCATCGTCGGCAGCGTC
VS_Nextera_i5225	Index PCR Forward Primer	AATGATACGGCGACCACCGAGATCTACACATACGGTCTCGTCGGCAGCGTC
VS_Nextera_i5226	Index PCR Forward Primer	AATGATACGGCGACCACCGAGATCTACACATACGTCGTCGTCGGCAGCGTC
VS_Nextera_i5227	Index PCR Forward Primer	AATGATACGGCGACCACCGAGATCTACACATAGGCGATCGTCGGCAGCGTC
VS_Nextera_i5228	Index PCR Forward Primer	AATGATACGGCGACCACCGAGATCTACACATAGTGCCTCGTCGGCAGCGTC
VS_Nextera_i5229	Index PCR Forward Primer	AATGATACGGCGACCACCGAGATCTACACATCAGACCTCGTCGGCAGCGTC
VS_Nextera_i5230	Index PCR Forward Primer	AATGATACGGCGACCACCGAGATCTACACATCAGTGGTCGTCGGCAGCGTC
VS_Nextera_i5231	Index PCR Forward Primer	AATGATACGGCGACCACCGAGATCTACACATCCAAGCTCGTCGGCAGCGTC
VS_Nextera_i5232	Index PCR Forward Primer	AATGATACGGCGACCACCGAGATCTACACATCCTCCATCGTCGGCAGCGTC
VS_Nextera_i5233	Index PCR Forward Primer	AATGATACGGCGACCACCGAGATCTACACATCCTGTGTCGTCGGCAGCGTC
VS_Nextera_i5234	Index PCR Forward Primer	AATGATACGGCGACCACCGAGATCTACACATCGAGGTTCGTCGGCAGCGTC
VS_Nextera_i5235	Index PCR Forward Primer	AATGATACGGCGACCACCGAGATCTACACATCGGAAGTCGTCGGCAGCGTC
VS_Nextera_i5236	Index PCR Forward Primer	AATGATACGGCGACCACCGAGATCTACACATCGGCTTTCGTCGGCAGCGTC
VS_Nextera_i5237	Index PCR Forward Primer	AATGATACGGCGACCACCGAGATCTACACATCGGTCATCGTCGGCAGCGTC
VS_Nextera_i5238	Index PCR Forward Primer	AATGATACGGCGACCACCGAGATCTACACATCTACGGTCGTCGGCAGCGTC
VS_Nextera_i5239	Index PCR Forward Primer	AATGATACGGCGACCACCGAGATCTACACATGAAGGCTCGTCGGCAGCGTC
VS_Nextera_i5240	Index PCR Forward Primer	AATGATACGGCGACCACCGAGATCTACACATGACTCGTCGTCGGCAGCGTC
VS_Nextera_i5241	Index PCR Forward Primer	AATGATACGGCGACCACCGAGATCTACACATGAGCCTTCGTCGGCAGCGTC
VS_Nextera_i5242	Index PCR Forward Primer	AATGATACGGCGACCACCGAGATCTACACATGCATCCTCGTCGGCAGCGTC
VS_Nextera_i5243	Index PCR Forward Primer	AATGATACGGCGACCACCGAGATCTACACATGCCAACTCGTCGGCAGCGTC
VS_Nextera_i5244	Index PCR Forward Primer	AATGATACGGCGACCACCGAGATCTACACATGCGATGTCGTCGGCAGCGTC
VS_Nextera_i5245	Index PCR Forward Primer	AATGATACGGCGACCACCGAGATCTACACATGCGGAATCGTCGGCAGCGTC
VS_Nextera_i5246	Index PCR Forward Primer	AATGATACGGCGACCACCGAGATCTACACATGCTCGTTCGTCGGCAGCGTC
VS_Nextera_i5247	Index PCR Forward Primer	AATGATACGGCGACCACCGAGATCTACACATGGAAGGTCGTCGGCAGCGTC
VS_Nextera_i5248	Index PCR Forward Primer	AATGATACGGCGACCACCGAGATCTACACATGGCACTTCGTCGGCAGCGTC
VS_Nextera_i5249	Index PCR Forward Primer	AATGATACGGCGACCACCGAGATCTACACATGGTCACTCGTCGGCAGCGTC
VS_Nextera_i5250	Index PCR Forward Primer	AATGATACGGCGACCACCGAGATCTACACATGTCCAGTCGTCGGCAGCGTC
VS_Nextera_i5251	Index PCR Forward Primer	AATGATACGGCGACCACCGAGATCTACACATGTGTGCTCGTCGGCAGCGTC
VS_Nextera_i5252	Index PCR Forward Primer	AATGATACGGCGACCACCGAGATCTACACATTACCGGTCGTCGGCAGCGTC
VS_Nextera_i5253	Index PCR Forward Primer	AATGATACGGCGACCACCGAGATCTACACATTAGGCGTCGTCGGCAGCGTC
VS_Nextera_i5254	Index PCR Forward Primer	AATGATACGGCGACCACCGAGATCTACACATTCCGAGTCGTCGGCAGCGTC
VS_Nextera_i5255	Index PCR Forward Primer	AATGATACGGCGACCACCGAGATCTACACATTCGCACTCGTCGGCAGCGTC
VS_Nextera_i5256	Index PCR Forward Primer	AATGATACGGCGACCACCGAGATCTACACATTGCTGCTCGTCGGCAGCGTC
VS_Nextera_i5257	Index PCR Forward Primer	AATGATACGGCGACCACCGAGATCTACACCAACACACTCGTCGGCAGCGTC
VS_Nextera_i5258	Index PCR Forward Primer	AATGATACGGCGACCACCGAGATCTACACCAACCACATCGTCGGCAGCGTC
VS_Nextera_i5259	Index PCR Forward Primer	AATGATACGGCGACCACCGAGATCTACACCAACCGATTCGTCGGCAGCGTC
VS_Nextera_i5260	Index PCR Forward Primer	AATGATACGGCGACCACCGAGATCTACACCAAGAACGTCGTCGGCAGCGTC
VS_Nextera_i5261	Index PCR Forward Primer	AATGATACGGCGACCACCGAGATCTACACCAAGCGTATCGTCGGCAGCGTC
VS_Nextera_i5262	Index PCR Forward Primer	AATGATACGGCGACCACCGAGATCTACACCAAGGAACTCGTCGGCAGCGTC
VS_Nextera_i5263	Index PCR Forward Primer	AATGATACGGCGACCACCGAGATCTACACCAAGTTGGTCGTCGGCAGCGTC
VS_Nextera_i5264	Index PCR Forward Primer	AATGATACGGCGACCACCGAGATCTACACCAATACGGTCGTCGGCAGCGTC
VS_Nextera_i5265	Index PCR Forward Primer	AATGATACGGCGACCACCGAGATCTACACCAATGCCTTCGTCGGCAGCGTC
VS_Nextera_i5266	Index PCR Forward Primer	AATGATACGGCGACCACCGAGATCTACACCAATGGAGTCGTCGGCAGCGTC
VS_Nextera_i5267	Index PCR Forward Primer	AATGATACGGCGACCACCGAGATCTACACCAATTGCCTCGTCGGCAGCGTC
VS_Nextera_i5268	Index PCR Forward Primer	AATGATACGGCGACCACCGAGATCTACACCACAATGGTCGTCGGCAGCGTC
VS_Nextera_i5269	Index PCR Forward Primer	AATGATACGGCGACCACCGAGATCTACACCACACCAATCGTCGGCAGCGTC
VS_Nextera_i5270	Index PCR Forward Primer	AATGATACGGCGACCACCGAGATCTACACCACAGAAGTCGTCGGCAGCGTC
VS_Nextera_i5271	Index PCR Forward Primer	AATGATACGGCGACCACCGAGATCTACACCACCAAGATCGTCGGCAGCGTC
VS_Nextera_i5272	Index PCR Forward Primer	AATGATACGGCGACCACCGAGATCTACACCACCATTCTCGTCGGCAGCGTC
VS_Nextera_i5273	Index PCR Forward Primer	AATGATACGGCGACCACCGAGATCTACACCACCTCATTCGTCGGCAGCGTC
VS_Nextera_i5274	Index PCR Forward Primer	AATGATACGGCGACCACCGAGATCTACACCACGAGAATCGTCGGCAGCGTC
VS_Nextera_i5275	Index PCR Forward Primer	AATGATACGGCGACCACCGAGATCTACACCACTCTCATCGTCGGCAGCGTC
VS_Nextera_i5276	Index PCR Forward Primer	AATGATACGGCGACCACCGAGATCTACACCACTGGTTTCGTCGGCAGCGTC
VS_Nextera_i5277	Index PCR Forward Primer	AATGATACGGCGACCACCGAGATCTACACCAGAAGGTTCGTCGGCAGCGTC
VS_Nextera_i5278	Index PCR Forward Primer	AATGATACGGCGACCACCGAGATCTACACCAGAGAGATCGTCGGCAGCGTC
VS_Nextera_i5279	Index PCR Forward Primer	AATGATACGGCGACCACCGAGATCTACACCAGAGTTGTCGTCGGCAGCGTC
VS_Nextera_i5280	Index PCR Forward Primer	AATGATACGGCGACCACCGAGATCTACACCAGATGAGTCGTCGGCAGCGTC
VS_Nextera_i5281	Index PCR Forward Primer	AATGATACGGCGACCACCGAGATCTACACCAGATTCCTCGTCGGCAGCGTC
VS_Nextera_i5282	Index PCR Forward Primer	AATGATACGGCGACCACCGAGATCTACACCAGCCTAATCGTCGGCAGCGTC
VS_Nextera_i5283	Index PCR Forward Primer	AATGATACGGCGACCACCGAGATCTACACCAGCTAACTCGTCGGCAGCGTC
VS_Nextera_i5284	Index PCR Forward Primer	AATGATACGGCGACCACCGAGATCTACACCAGGACTATCGTCGGCAGCGTC
VS_Nextera_i5285	Index PCR Forward Primer	AATGATACGGCGACCACCGAGATCTACACCAGGTACATCGTCGGCAGCGTC
VS_Nextera_i5286	Index PCR Forward Primer	AATGATACGGCGACCACCGAGATCTACACCAGGTGTTTCGTCGGCAGCGTC
VS_Nextera_i5287	Index PCR Forward Primer	AATGATACGGCGACCACCGAGATCTACACCAGTAGCATCGTCGGCAGCGTC
VS_Nextera_i5288	Index PCR Forward Primer	AATGATACGGCGACCACCGAGATCTACACCAGTCATCTCGTCGGCAGCGTC
VS_Nextera_i5289	Index PCR Forward Primer	AATGATACGGCGACCACCGAGATCTACACCAGTCCATTCGTCGGCAGCGTC

VS_Nextera_i5290	Index PCR Forward Primer	AATGATACGGCGACCACCGAGATCTACACCAGTGTGTTCGTCGGCAGCGTC
VS_Nextera_i5291	Index PCR Forward Primer	AATGATACGGCGACCACCGAGATCTACACCAGTTAGGTCGTCGGCAGCGTC
VS_Nextera_i5292	Index PCR Forward Primer	AATGATACGGCGACCACCGAGATCTACACCATACACCTCGTCGGCAGCGTC
VS_Nextera_i5293	Index PCR Forward Primer	AATGATACGGCGACCACCGAGATCTACACCATATCGGTCGTCGGCAGCGTC
VS_Nextera_i5294	Index PCR Forward Primer	AATGATACGGCGACCACCGAGATCTACACCATCACCTTCGTCGGCAGCGTC
VS_Nextera_i5295	Index PCR Forward Primer	AATGATACGGCGACCACCGAGATCTACACCATCCAAGTCGTCGGCAGCGTC
VS_Nextera_i5296	Index PCR Forward Primer	AATGATACGGCGACCACCGAGATCTACACCATCGATCTCGTCGGCAGCGTC
VS_Nextera_i5297	Index PCR Forward Primer	AATGATACGGCGACCACCGAGATCTACACCATCGGAATCGTCGGCAGCGTC
VS_Nextera_i5298	Index PCR Forward Primer	AATGATACGGCGACCACCGAGATCTACACCATGAGTGTCGTCGGCAGCGTC
VS_Nextera_i5299	Index PCR Forward Primer	AATGATACGGCGACCACCGAGATCTACACCATGATGCTCGTCGGCAGCGTC
VS_Nextera_i5300	Index PCR Forward Primer	AATGATACGGCGACCACCGAGATCTACACCATGCAGATCGTCGGCAGCGTC
VS_Nextera_i5301	Index PCR Forward Primer	AATGATACGGCGACCACCGAGATCTACACCATGGTCATCGTCGGCAGCGTC
VS_Nextera_i5302	Index PCR Forward Primer	AATGATACGGCGACCACCGAGATCTACACCATTCTGGTCGTCGGCAGCGTC
VS_Nextera_i5303	Index PCR Forward Primer	AATGATACGGCGACCACCGAGATCTACACCATTGACGTCGTCGGCAGCGTC
VS_Nextera_i5304	Index PCR Forward Primer	AATGATACGGCGACCACCGAGATCTACACCATTGCACTCGTCGGCAGCGTC
VS_Nextera_i5305	Index PCR Forward Primer	AATGATACGGCGACCACCGAGATCTACACCCAAGGTATCGTCGGCAGCGTC
VS_Nextera_i5306	Index PCR Forward Primer	AATGATACGGCGACCACCGAGATCTACACCCAATACCTCGTCGGCAGCGTC
VS_Nextera_i5307	Index PCR Forward Primer	AATGATACGGCGACCACCGAGATCTACACCCACAATGTCGTCGGCAGCGTC
VS_Nextera_i5308	Index PCR Forward Primer	AATGATACGGCGACCACCGAGATCTACACCCACAGAATCGTCGGCAGCGTC
VS_Nextera_i5309	Index PCR Forward Primer	AATGATACGGCGACCACCGAGATCTACACCCACGAATTCGTCGGCAGCGTC
VS_Nextera_i5310	Index PCR Forward Primer	AATGATACGGCGACCACCGAGATCTACACCCAGGTAATCGTCGGCAGCGTC
VS_Nextera_i5311	Index PCR Forward Primer	AATGATACGGCGACCACCGAGATCTACACCCAGTAAGTCGTCGGCAGCGTC
VS_Nextera_i5312	Index PCR Forward Primer	AATGATACGGCGACCACCGAGATCTACACCCATAGCTTCGTCGGCAGCGTC
VS_Nextera_i5313	Index PCR Forward Primer	AATGATACGGCGACCACCGAGATCTACACCCATATGCTCGTCGGCAGCGTC
VS_Nextera_i5314	Index PCR Forward Primer	AATGATACGGCGACCACCGAGATCTACACCCATCAACTCGTCGGCAGCGTC
VS_Nextera_i5315	Index PCR Forward Primer	AATGATACGGCGACCACCGAGATCTACACCCATGACATCGTCGGCAGCGTC
VS_Nextera_i5316	Index PCR Forward Primer	AATGATACGGCGACCACCGAGATCTACACCCATTGGATCGTCGGCAGCGTC
VS_Nextera_i5317	Index PCR Forward Primer	AATGATACGGCGACCACCGAGATCTACACCCGAATACTCGTCGGCAGCGTC
VS_Nextera_i5318	Index PCR Forward Primer	AATGATACGGCGACCACCGAGATCTACACCCGACAATTCGTCGGCAGCGTC
VS_Nextera_i5319	Index PCR Forward Primer	AATGATACGGCGACCACCGAGATCTACACCCGATCAATCGTCGGCAGCGTC
VS_Nextera_i5320	Index PCR Forward Primer	AATGATACGGCGACCACCGAGATCTACACCCGATTGTTCGTCGGCAGCGTC
VS_Nextera_i5321	Index PCR Forward Primer	AATGATACGGCGACCACCGAGATCTACACCCGCATTATCGTCGGCAGCGTC
VS_Nextera_i5322	Index PCR Forward Primer	AATGATACGGCGACCACCGAGATCTACACCCGGAATTTCGTCGGCAGCGTC
VS_Nextera_i5323	Index PCR Forward Primer	AATGATACGGCGACCACCGAGATCTACACCCGTAAGATCGTCGGCAGCGTC
VS_Nextera_i5324	Index PCR Forward Primer	AATGATACGGCGACCACCGAGATCTACACCCGTTGATTCGTCGGCAGCGTC
VS_Nextera_i5325	Index PCR Forward Primer	AATGATACGGCGACCACCGAGATCTACACCCTACATGTCGTCGGCAGCGTC
VS_Nextera_i5326	Index PCR Forward Primer	AATGATACGGCGACCACCGAGATCTACACCCTACGAATCGTCGGCAGCGTC
VS_Nextera_i5327	Index PCR Forward Primer	AATGATACGGCGACCACCGAGATCTACACCCTAGAACTCGTCGGCAGCGTC
VS_Nextera_i5328	Index PCR Forward Primer	AATGATACGGCGACCACCGAGATCTACACCCTAGTGATCGTCGGCAGCGTC
VS_Nextera_i5329	Index PCR Forward Primer	AATGATACGGCGACCACCGAGATCTACACCCTCAAGTTCGTCGGCAGCGTC
VS_Nextera_i5330	Index PCR Forward Primer	AATGATACGGCGACCACCGAGATCTACACCCTCTTAGTCGTCGGCAGCGTC
VS_Nextera_i5331	Index PCR Forward Primer	AATGATACGGCGACCACCGAGATCTACACCCTGACAATCGTCGGCAGCGTC
VS_Nextera_i5332	Index PCR Forward Primer	AATGATACGGCGACCACCGAGATCTACACCCTTAGAGTCGTCGGCAGCGTC
VS_Nextera_i5333	Index PCR Forward Primer	AATGATACGGCGACCACCGAGATCTACACCCTTCCTATCGTCGGCAGCGTC
VS_Nextera_i5334	Index PCR Forward Primer	AATGATACGGCGACCACCGAGATCTACACCGAACAAGTCGTCGGCAGCGTC
VS_Nextera_i5335	Index PCR Forward Primer	AATGATACGGCGACCACCGAGATCTACACCGAAGATCTCGTCGGCAGCGTC
VS_Nextera_i5336	Index PCR Forward Primer	AATGATACGGCGACCACCGAGATCTACACCGAAGCAATCGTCGGCAGCGTC
VS_Nextera_i5337	Index PCR Forward Primer	AATGATACGGCGACCACCGAGATCTACACCGACACTTTCGTCGGCAGCGTC
VS_Nextera_i5338	Index PCR Forward Primer	AATGATACGGCGACCACCGAGATCTACACCGACGTTATCGTCGGCAGCGTC
VS_Nextera_i5339	Index PCR Forward Primer	AATGATACGGCGACCACCGAGATCTACACCGACTAGTTCGTCGGCAGCGTC
VS_Nextera_i5340	Index PCR Forward Primer	AATGATACGGCGACCACCGAGATCTACACCGAGAAGATCGTCGGCAGCGTC
VS_Nextera_i5341	Index PCR Forward Primer	AATGATACGGCGACCACCGAGATCTACACCGAGATAGTCGTCGGCAGCGTC
VS_Nextera_i5342	Index PCR Forward Primer	AATGATACGGCGACCACCGAGATCTACACCGAGTGATTCGTCGGCAGCGTC
VS_Nextera_i5343	Index PCR Forward Primer	AATGATACGGCGACCACCGAGATCTACACCGATAACCTCGTCGGCAGCGTC
VS_Nextera_i5344	Index PCR Forward Primer	AATGATACGGCGACCACCGAGATCTACACCGATAGTGTCGTCGGCAGCGTC
VS_Nextera_i5345	Index PCR Forward Primer	AATGATACGGCGACCACCGAGATCTACACCGATCGAATCGTCGGCAGCGTC
VS_Nextera_i5346	Index PCR Forward Primer	AATGATACGGCGACCACCGAGATCTACACCGATTCAGTCGTCGGCAGCGTC
VS_Nextera_i5347	Index PCR Forward Primer	AATGATACGGCGACCACCGAGATCTACACCGCAACATTCGTCGGCAGCGTC
VS_Nextera_i5348	Index PCR Forward Primer	AATGATACGGCGACCACCGAGATCTACACCGCAATCATCGTCGGCAGCGTC
VS_Nextera_i5349	Index PCR Forward Primer	AATGATACGGCGACCACCGAGATCTACACCGCTACTATCGTCGGCAGCGTC
VS_Nextera_i5350	Index PCR Forward Primer	AATGATACGGCGACCACCGAGATCTACACCGCTCAATTCGTCGGCAGCGTC
VS_Nextera_i5351	Index PCR Forward Primer	AATGATACGGCGACCACCGAGATCTACACCGCTGTAATCGTCGGCAGCGTC
VS_Nextera_i5352	Index PCR Forward Primer	AATGATACGGCGACCACCGAGATCTACACCGGAAGAATCGTCGGCAGCGTC
VS_Nextera_i5353	Index PCR Forward Primer	AATGATACGGCGACCACCGAGATCTACACCGGATATGTCGTCGGCAGCGTC
VS_Nextera_i5354	Index PCR Forward Primer	AATGATACGGCGACCACCGAGATCTACACCGGTATTCTCGTCGGCAGCGTC
VS_Nextera_i5355	Index PCR Forward Primer	AATGATACGGCGACCACCGAGATCTACACCGTACAGTTCGTCGGCAGCGTC
VS_Nextera_i5356	Index PCR Forward Primer	AATGATACGGCGACCACCGAGATCTACACCGTACTTCTCGTCGGCAGCGTC
VS_Nextera_i5357	Index PCR Forward Primer	AATGATACGGCGACCACCGAGATCTACACCGTAGACATCGTCGGCAGCGTC
VS_Nextera_i5358	Index PCR Forward Primer	AATGATACGGCGACCACCGAGATCTACACCGTAGCTTTCGTCGGCAGCGTC
VS_Nextera_i5359	Index PCR Forward Primer	AATGATACGGCGACCACCGAGATCTACACCGTAGTAGTCGTCGGCAGCGTC
VS_Nextera_i5360	Index PCR Forward Primer	AATGATACGGCGACCACCGAGATCTACACCGTCAGTATCGTCGGCAGCGTC
VS_Nextera_i5361	Index PCR Forward Primer	AATGATACGGCGACCACCGAGATCTACACCGTCATACTCGTCGGCAGCGTC
VS_Nextera_i5362	Index PCR Forward Primer	AATGATACGGCGACCACCGAGATCTACACCGTGCTAATCGTCGGCAGCGTC
VS_Nextera_i5363	Index PCR Forward Primer	AATGATACGGCGACCACCGAGATCTACACCGTGGAATTCGTCGGCAGCGTC
VS_Nextera_i5364	Index PCR Forward Primer	AATGATACGGCGACCACCGAGATCTACACCGTGTATCTCGTCGGCAGCGTC
VS_Nextera_i5365	Index PCR Forward Primer	AATGATACGGCGACCACCGAGATCTACACCGTGTTGTTCGTCGGCAGCGTC
VS_Nextera_i5366	Index PCR Forward Primer	AATGATACGGCGACCACCGAGATCTACACCTAACGACTCGTCGGCAGCGTC
VS_Nextera_i5367	Index PCR Forward Primer	AATGATACGGCGACCACCGAGATCTACACCTAAGTGCTCGTCGGCAGCGTC
VS_Nextera_i5368	Index PCR Forward Primer	AATGATACGGCGACCACCGAGATCTACACCTAATCCGTCGTCGGCAGCGTC
VS_Nextera_i5369	Index PCR Forward Primer	AATGATACGGCGACCACCGAGATCTACACCTACATGGTCGTCGGCAGCGTC
VS_Nextera_i5370	Index PCR Forward Primer	AATGATACGGCGACCACCGAGATCTACACCTACTGCTTCGTCGGCAGCGTC
VS_Nextera_i5371	Index PCR Forward Primer	AATGATACGGCGACCACCGAGATCTACACCTAGACTCTCGTCGGCAGCGTC
VS_Nextera_i5372	Index PCR Forward Primer	AATGATACGGCGACCACCGAGATCTACACCTAGAGCATCGTCGGCAGCGTC
VS_Nextera_i5373	Index PCR Forward Primer	AATGATACGGCGACCACCGAGATCTACACCTAGCTGTTCGTCGGCAGCGTC
VS_Nextera_i5374	Index PCR Forward Primer	AATGATACGGCGACCACCGAGATCTACACCTATCTCGTCGTCGGCAGCGTC
VS_Nextera_i5375	Index PCR Forward Primer	AATGATACGGCGACCACCGAGATCTACACCTATTCGCTCGTCGGCAGCGTC

VS_Nextera_i5376	Index PCR Forward Primer	AATGATACGGCGACCACCGAGATCTACACCTCAAGTGTCGTCGGCAGCGTC
VS_Nextera_i5377	Index PCR Forward Primer	AATGATACGGCGACCACCGAGATCTACACCTCACATCTCGTCGGCAGCGTC
VS_Nextera_i5378	Index PCR Forward Primer	AATGATACGGCGACCACCGAGATCTACACCTCACTAGTCGTCGGCAGCGTC
VS_Nextera_i5379	Index PCR Forward Primer	AATGATACGGCGACCACCGAGATCTACACCTCAGGAATCGTCGGCAGCGTC
VS_Nextera_i5380	Index PCR Forward Primer	AATGATACGGCGACCACCGAGATCTACACCTCAGTCTTCGTCGGCAGCGTC
VS_Nextera_i5381	Index PCR Forward Primer	AATGATACGGCGACCACCGAGATCTACACCTCTAACGTCGTCGGCAGCGTC
VS_Nextera_i5382	Index PCR Forward Primer	AATGATACGGCGACCACCGAGATCTACACCTCTCAGATCGTCGGCAGCGTC
VS_Nextera_i5383	Index PCR Forward Primer	AATGATACGGCGACCACCGAGATCTACACCTCTGCATTCGTCGGCAGCGTC
VS_Nextera_i5384	Index PCR Forward Primer	AATGATACGGCGACCACCGAGATCTACACCTGACTGATCGTCGGCAGCGTC
VS_Nextera_i5385	Index PCR Forward Primer	AATGATACGGCGACCACCGAGATCTACACCTGAGGTTTCGTCGGCAGCGTC
VS_Nextera_i5386	Index PCR Forward Primer	AATGATACGGCGACCACCGAGATCTACACCTGATAGCTCGTCGGCAGCGTC
VS_Nextera_i5387	Index PCR Forward Primer	AATGATACGGCGACCACCGAGATCTACACCTGCAACATCGTCGGCAGCGTC
VS_Nextera_i5388	Index PCR Forward Primer	AATGATACGGCGACCACCGAGATCTACACCTGTACCTTCGTCGGCAGCGTC
VS_Nextera_i5389	Index PCR Forward Primer	AATGATACGGCGACCACCGAGATCTACACCTGTCTACTCGTCGGCAGCGTC
VS_Nextera_i5390	Index PCR Forward Primer	AATGATACGGCGACCACCGAGATCTACACCTGTGAAGTCGTCGGCAGCGTC
VS_Nextera_i5391	Index PCR Forward Primer	AATGATACGGCGACCACCGAGATCTACACCTGTTCTGTCGTCGGCAGCGTC
VS_Nextera_i5392	Index PCR Forward Primer	AATGATACGGCGACCACCGAGATCTACACCTTAGAGGTCGTCGGCAGCGTC
VS_Nextera_i5393	Index PCR Forward Primer	AATGATACGGCGACCACCGAGATCTACACCTTCCACTTCGTCGGCAGCGTC
VS_Nextera_i5394	Index PCR Forward Primer	AATGATACGGCGACCACCGAGATCTACACCTTCGCTATCGTCGGCAGCGTC
VS_Nextera_i5395	Index PCR Forward Primer	AATGATACGGCGACCACCGAGATCTACACCTTCGTGTTCGTCGGCAGCGTC
VS_Nextera_i5396	Index PCR Forward Primer	AATGATACGGCGACCACCGAGATCTACACCTTCTGGATCGTCGGCAGCGTC
VS_Nextera_i5397	Index PCR Forward Primer	AATGATACGGCGACCACCGAGATCTACACCTTGACGTTCGTCGGCAGCGTC
VS_Nextera_i5398	Index PCR Forward Primer	AATGATACGGCGACCACCGAGATCTACACCTTGATCGTCGTCGGCAGCGTC
VS_Nextera_i5399	Index PCR Forward Primer	AATGATACGGCGACCACCGAGATCTACACCTTGCGTTTCGTCGGCAGCGTC
VS_Nextera_i5400	Index PCR Forward Primer	AATGATACGGCGACCACCGAGATCTACACCTTGGTTCTCGTCGGCAGCGTC
VS_Nextera_i5401	Index PCR Forward Primer	AATGATACGGCGACCACCGAGATCTACACGAACCAACTCGTCGGCAGCGTC
VS_Nextera_i5402	Index PCR Forward Primer	AATGATACGGCGACCACCGAGATCTACACGAACGGTATCGTCGGCAGCGTC
VS_Nextera_i5403	Index PCR Forward Primer	AATGATACGGCGACCACCGAGATCTACACGAACGTGTTCGTCGGCAGCGTC
VS_Nextera_i5404	Index PCR Forward Primer	AATGATACGGCGACCACCGAGATCTACACGAACTTCGTCGTCGGCAGCGTC
VS_Nextera_i5405	Index PCR Forward Primer	AATGATACGGCGACCACCGAGATCTACACGAAGACAGTCGTCGGCAGCGTC
VS_Nextera_i5406	Index PCR Forward Primer	AATGATACGGCGACCACCGAGATCTACACGAAGCTCTTCGTCGGCAGCGTC
VS_Nextera_i5407	Index PCR Forward Primer	AATGATACGGCGACCACCGAGATCTACACGAAGGACATCGTCGGCAGCGTC
VS_Nextera_i5408	Index PCR Forward Primer	AATGATACGGCGACCACCGAGATCTACACGAAGGCTTTCGTCGGCAGCGTC
VS_Nextera_i5409	Index PCR Forward Primer	AATGATACGGCGACCACCGAGATCTACACGAAGTGGATCGTCGGCAGCGTC
VS_Nextera_i5410	Index PCR Forward Primer	AATGATACGGCGACCACCGAGATCTACACGAATAGGCTCGTCGGCAGCGTC
VS_Nextera_i5411	Index PCR Forward Primer	AATGATACGGCGACCACCGAGATCTACACGAATCAGGTCGTCGGCAGCGTC
VS_Nextera_i5412	Index PCR Forward Primer	AATGATACGGCGACCACCGAGATCTACACGAATGCGATCGTCGGCAGCGTC
VS_Nextera_i5413	Index PCR Forward Primer	AATGATACGGCGACCACCGAGATCTACACGAATGTCCTCGTCGGCAGCGTC
VS_Nextera_i5414	Index PCR Forward Primer	AATGATACGGCGACCACCGAGATCTACACGACACAGATCGTCGGCAGCGTC
VS_Nextera_i5415	Index PCR Forward Primer	AATGATACGGCGACCACCGAGATCTACACGACAGGATTCGTCGGCAGCGTC
VS_Nextera_i5416	Index PCR Forward Primer	AATGATACGGCGACCACCGAGATCTACACGACATACGTCGTCGGCAGCGTC
VS_Nextera_i5417	Index PCR Forward Primer	AATGATACGGCGACCACCGAGATCTACACGACCTTGATCGTCGGCAGCGTC
VS_Nextera_i5418	Index PCR Forward Primer	AATGATACGGCGACCACCGAGATCTACACGACGATGTTCGTCGGCAGCGTC
VS_Nextera_i5419	Index PCR Forward Primer	AATGATACGGCGACCACCGAGATCTACACGACGGTAATCGTCGGCAGCGTC
VS_Nextera_i5420	Index PCR Forward Primer	AATGATACGGCGACCACCGAGATCTACACGACTAGAGTCGTCGGCAGCGTC
VS_Nextera_i5421	Index PCR Forward Primer	AATGATACGGCGACCACCGAGATCTACACGACTCACTTCGTCGGCAGCGTC
VS_Nextera_i5422	Index PCR Forward Primer	AATGATACGGCGACCACCGAGATCTACACGACTCTACTCGTCGGCAGCGTC
VS_Nextera_i5423	Index PCR Forward Primer	AATGATACGGCGACCACCGAGATCTACACGACTGATCTCGTCGGCAGCGTC
VS_Nextera_i5424	Index PCR Forward Primer	AATGATACGGCGACCACCGAGATCTACACGAGACAAGTCGTCGGCAGCGTC
VS_Nextera_i5425	Index PCR Forward Primer	AATGATACGGCGACCACCGAGATCTACACGAGAGCAATCGTCGGCAGCGTC
VS_Nextera_i5426	Index PCR Forward Primer	AATGATACGGCGACCACCGAGATCTACACGAGATTGGTCGTCGGCAGCGTC
VS_Nextera_i5427	Index PCR Forward Primer	AATGATACGGCGACCACCGAGATCTACACGAGCATCTTCGTCGGCAGCGTC
VS_Nextera_i5428	Index PCR Forward Primer	AATGATACGGCGACCACCGAGATCTACACGAGCCATATCGTCGGCAGCGTC
VS_Nextera_i5429	Index PCR Forward Primer	AATGATACGGCGACCACCGAGATCTACACGAGGAAGATCGTCGGCAGCGTC
VS_Nextera_i5430	Index PCR Forward Primer	AATGATACGGCGACCACCGAGATCTACACGAGGTATGTCGTCGGCAGCGTC
VS_Nextera_i5431	Index PCR Forward Primer	AATGATACGGCGACCACCGAGATCTACACGAGGTCATTCGTCGGCAGCGTC
VS_Nextera_i5432	Index PCR Forward Primer	AATGATACGGCGACCACCGAGATCTACACGAGTACTGTCGTCGGCAGCGTC
VS_Nextera_i5433	Index PCR Forward Primer	AATGATACGGCGACCACCGAGATCTACACGAGTCGTTTCGTCGGCAGCGTC
VS_Nextera_i5434	Index PCR Forward Primer	AATGATACGGCGACCACCGAGATCTACACGAGTGTAGTCGTCGGCAGCGTC
VS_Nextera_i5435	Index PCR Forward Primer	AATGATACGGCGACCACCGAGATCTACACGAGTTGACTCGTCGGCAGCGTC
VS_Nextera_i5436	Index PCR Forward Primer	AATGATACGGCGACCACCGAGATCTACACGATACCGTTCGTCGGCAGCGTC
VS_Nextera_i5437	Index PCR Forward Primer	AATGATACGGCGACCACCGAGATCTACACGATACGTGTCGTCGGCAGCGTC
VS_Nextera_i5438	Index PCR Forward Primer	AATGATACGGCGACCACCGAGATCTACACGATAGTGCTCGTCGGCAGCGTC
VS_Nextera_i5439	Index PCR Forward Primer	AATGATACGGCGACCACCGAGATCTACACGATCAACCTCGTCGGCAGCGTC
VS_Nextera_i5440	Index PCR Forward Primer	AATGATACGGCGACCACCGAGATCTACACGATCAGGTTCGTCGGCAGCGTC
VS_Nextera_i5441	Index PCR Forward Primer	AATGATACGGCGACCACCGAGATCTACACGATCCTCATCGTCGGCAGCGTC
VS_Nextera_i5442	Index PCR Forward Primer	AATGATACGGCGACCACCGAGATCTACACGATGACCATCGTCGGCAGCGTC
VS_Nextera_i5443	Index PCR Forward Primer	AATGATACGGCGACCACCGAGATCTACACGATGCGAATCGTCGGCAGCGTC
VS_Nextera_i5444	Index PCR Forward Primer	AATGATACGGCGACCACCGAGATCTACACGATGGAAGTCGTCGGCAGCGTC
VS_Nextera_i5445	Index PCR Forward Primer	AATGATACGGCGACCACCGAGATCTACACGATGTAGCTCGTCGGCAGCGTC
VS_Nextera_i5446	Index PCR Forward Primer	AATGATACGGCGACCACCGAGATCTACACGATGTGCTTCGTCGGCAGCGTC
VS_Nextera_i5447	Index PCR Forward Primer	AATGATACGGCGACCACCGAGATCTACACGATTCCAGTCGTCGGCAGCGTC
VS_Nextera_i5448	Index PCR Forward Primer	AATGATACGGCGACCACCGAGATCTACACGATTGGCATCGTCGGCAGCGTC
VS_Nextera_i5449	Index PCR Forward Primer	AATGATACGGCGACCACCGAGATCTACACGCAACATCTCGTCGGCAGCGTC
VS_Nextera_i5450	Index PCR Forward Primer	AATGATACGGCGACCACCGAGATCTACACGCAACCAATCGTCGGCAGCGTC
VS_Nextera_i5451	Index PCR Forward Primer	AATGATACGGCGACCACCGAGATCTACACGCAAGAAGTCGTCGGCAGCGTC
VS_Nextera_i5452	Index PCR Forward Primer	AATGATACGGCGACCACCGAGATCTACACGCAAGTCTTCGTCGGCAGCGTC
VS_Nextera_i5453	Index PCR Forward Primer	AATGATACGGCGACCACCGAGATCTACACGCACAAGATCGTCGGCAGCGTC
VS_Nextera_i5454	Index PCR Forward Primer	AATGATACGGCGACCACCGAGATCTACACGCACATAGTCGTCGGCAGCGTC
VS_Nextera_i5455	Index PCR Forward Primer	AATGATACGGCGACCACCGAGATCTACACGCACTCTATCGTCGGCAGCGTC
VS_Nextera_i5456	Index PCR Forward Primer	AATGATACGGCGACCACCGAGATCTACACGCACTGATTCGTCGGCAGCGTC
VS_Nextera_i5457	Index PCR Forward Primer	AATGATACGGCGACCACCGAGATCTACACGCAGAGTTTCGTCGGCAGCGTC
VS_Nextera_i5458	Index PCR Forward Primer	AATGATACGGCGACCACCGAGATCTACACGCAGCTTATCGTCGGCAGCGTC
VS_Nextera_i5459	Index PCR Forward Primer	AATGATACGGCGACCACCGAGATCTACACGCAGTACTTCGTCGGCAGCGTC
VS_Nextera_i5460	Index PCR Forward Primer	AATGATACGGCGACCACCGAGATCTACACGCAGTTACTCGTCGGCAGCGTC
VS_Nextera_i5461	Index PCR Forward Primer	AATGATACGGCGACCACCGAGATCTACACGCATAACGTCGTCGGCAGCGTC

VS_Nextera_i5462	Index PCR Forward Primer	AATGATACGGCGACCACCGAGATCTACACGCATGGAATCGTCGGCAGCGTC
VS_Nextera_i5463	Index PCR Forward Primer	AATGATACGGCGACCACCGAGATCTACACGCATTGTCTCGTCGGCAGCGTC
VS_Nextera_i5464	Index PCR Forward Primer	AATGATACGGCGACCACCGAGATCTACACGCCAAGAATCGTCGGCAGCGTC
VS_Nextera_i5465	Index PCR Forward Primer	AATGATACGGCGACCACCGAGATCTACACGCCAGTTATCGTCGGCAGCGTC
VS_Nextera_i5466	Index PCR Forward Primer	AATGATACGGCGACCACCGAGATCTACACGCCATAACTCGTCGGCAGCGTC
VS_Nextera_i5467	Index PCR Forward Primer	AATGATACGGCGACCACCGAGATCTACACGCCTATTGTCGTCGGCAGCGTC
VS_Nextera_i5468	Index PCR Forward Primer	AATGATACGGCGACCACCGAGATCTACACGCCTTACATCGTCGGCAGCGTC
VS_Nextera_i5469	Index PCR Forward Primer	AATGATACGGCGACCACCGAGATCTACACGCGAACATTCGTCGGCAGCGTC
VS_Nextera_i5470	Index PCR Forward Primer	AATGATACGGCGACCACCGAGATCTACACGCGAATCATCGTCGGCAGCGTC
VS_Nextera_i5471	Index PCR Forward Primer	AATGATACGGCGACCACCGAGATCTACACGCGTAGTATCGTCGGCAGCGTC
VS_Nextera_i5472	Index PCR Forward Primer	AATGATACGGCGACCACCGAGATCTACACGCGTCTAATCGTCGGCAGCGTC
VS_Nextera_i5473	Index PCR Forward Primer	AATGATACGGCGACCACCGAGATCTACACGCGTGATTTCGTCGGCAGCGTC
VS_Nextera_i5474	Index PCR Forward Primer	AATGATACGGCGACCACCGAGATCTACACGCGTTAAGTCGTCGGCAGCGTC
VS_Nextera_i5475	Index PCR Forward Primer	AATGATACGGCGACCACCGAGATCTACACGCTAACTCTCGTCGGCAGCGTC
VS_Nextera_i5476	Index PCR Forward Primer	AATGATACGGCGACCACCGAGATCTACACGCTAATGGTCGTCGGCAGCGTC
VS_Nextera_i5477	Index PCR Forward Primer	AATGATACGGCGACCACCGAGATCTACACGCTACACATCGTCGGCAGCGTC
VS_Nextera_i5478	Index PCR Forward Primer	AATGATACGGCGACCACCGAGATCTACACGCTAGAGTTCGTCGGCAGCGTC
VS_Nextera_i5479	Index PCR Forward Primer	AATGATACGGCGACCACCGAGATCTACACGCTATGAGTCGTCGGCAGCGTC
VS_Nextera_i5480	Index PCR Forward Primer	AATGATACGGCGACCACCGAGATCTACACGCTCCAATTCGTCGGCAGCGTC
VS_Nextera_i5481	Index PCR Forward Primer	AATGATACGGCGACCACCGAGATCTACACGCTCGTAATCGTCGGCAGCGTC
VS_Nextera_i5482	Index PCR Forward Primer	AATGATACGGCGACCACCGAGATCTACACGCTCTATGTCGTCGGCAGCGTC
VS_Nextera_i5483	Index PCR Forward Primer	AATGATACGGCGACCACCGAGATCTACACGCTCTTGTTCGTCGGCAGCGTC
VS_Nextera_i5484	Index PCR Forward Primer	AATGATACGGCGACCACCGAGATCTACACGCTGGATATCGTCGGCAGCGTC